



KCDC Simulation Manual - for the COMBINED detector simulations

KCDC - the KASCADE Cosmic Ray Data Centre

Open Access Solution for the
KArlsruhe Shower Core and Array Detector (KASCADE)

KIT - University of the State of Baden-Wuerttemberg
and National Research Centre of the Helmholtz Association

Authors:	Jürgen Wochele, Donghwa Kang, Doris Wochele, Andreas Haungs
Address:	Karlsruhe Institute of Technology (KIT) Institute for Astroparticle Physics (IAP) Hermann-von-Helmholtz-Platz 1 76344 Eggenstein-Leopoldshafen
Internet:	kcdc.iap.kit.edu www.kit.edu
DOI:	https://doi.org/10.17616/R3TS4P
Version:	V.02
Last update:	2022-05-04

TABLE OF CONTENTS

1	INTRODUCTION	7
1.1	KCDC - The KASCADE Cosmic Ray Data Centre	7
1.2	Why Simulations	9
2	SIMULATIONS	11
2.1	Air shower simulations using CORSIKA	13
2.1.1	QGSjet	14
2.1.2	EPOS	14
2.1.3	SIBYLL	14
2.1.4	FLUKA	14
2.2	Detector simulation with CRES	15
2.3	Data Reconstruction with KRETA	15
2.4	General Information on the Simulated Quantities	15
2.5	General Information on simulated Detector Components	16
2.6	Simulations for the LOPES Detector	17
3	RECONSTRUCTION OF SIMULATED COMBINED DATA IN KCDC	19
3.1	Energy (E)	21
3.1.1	Energy estimation	22
3.1.2	Formula for Energy Estimator	22
3.2	Number of electrons and Number of muons (Ne, Nmu)	24
3.3	Age (Age)	28
3.4	Shower Core Position (Xc, Yc)	29
3.5	Shower Direction (Ze, Az)	33
3.6	COMBINED at lower energies	36
4	RECONSTRUCTION OF SIMULATED KASCADE DATA IN KCDC	39
4.1	e/γ – Energy Deposits	40
4.1.1	Number of active e/γ -detector stations (EDepositN)	40
4.1.2	Number of e/γ -detector stations with hits	40
4.1.3	e/γ Energy Deposit for each detector station (Edeposit)	41
4.1.4	Station ID (EDepositS)	42
4.1.5	Example	44
4.2	Muon – Energy Deposits	45
4.2.1	Number of active μ-detector stations (MDepositN)	45
4.2.2	Number of e/γ -detector stations with hits	45
4.2.3	μ-Energy Deposit value for each detector station (MDeposit)	46
4.2.4	Station ID (MDepositS)	47
4.2.5	Example	48
4.3	Arrival Times	49
4.3.1	Number of detector stations with valid arrival times (ArrivalN)	49
4.3.2	Arrival Times per Station (Arrival)	50
4.3.3	Station ID (ArrivalS)	51
4.3.4	Example	52
4.4	Run Number & Event Number	53

5	RECONSTRUCTION OF SIMULATED GRANDE DATA IN KCDC.....	55
5.1	GRANDE Energy Deposits per Station (GDeposit)	55
5.1.1	Number of active GRANDE detector stations (GDepositN)	56
5.1.2	Number of active GRANDE detector stations with hits	56
5.1.3	GRANDE Energy Deposit for each detector station (GDeposit)	56
5.1.4	GRANDE Station ID (GDepositS)	57
5.1.5	Example	58
5.2	Arrival Times	59
5.2.1	Number of GRANDE detector stations with valid arrival times (GArrivalN)	59
5.2.2	Arrival Times per GRANDE Station (GArrival)	60
5.2.3	GRANDE Station ID (GArrivalS)	61
5.2.4	Example	62
6	SIMULATION DATA IN KCDC.....	63
6.1	True Primary Energy (TrEP)	64
6.2	True Primary Particle ID (TrPP)	65
6.3	True Shower Direction (TrZe, TrAz)	65
6.4	True Numbers of Electrons (TrNe)	67
6.5	True Numbers of Muons (TrNm)	68
6.6	True Numbers of Photons (TrNp)	69
6.7	True Numbers of Hadrons (TrNh)	70
6.8	True Shower Core Position (TrXc, TrYc)	71
7	SIMULATION DATA ANALYSIS HELPS.....	73
7.1	Cuts.....	73
7.1.1	Quality Cuts for simulated COMBINED Showers	73
7.2	Expert's Advices	74
7.3	Calculation of KASCADE Detector Station Locations from ID.....	75
7.4	Calculation of GRANDE Detector Station Locations from ID.....	75
8	SIMULATION DATA SETS	77
8.1	COMBINED Simulation Data Sets.....	78
8.1.1	QGSjet-II-04 & FLUKA 2012.2.14_32	78
8.1.2	EPOS LHC & FLUKA 2011.2b.4_32	79
8.1.3	SIBYLL 2.3c & FLUKA 2011.2c.3_64	80
8.1.4	SIBYLL 2.3d & Fluka 2011.2x4-64.....	81
8.2	Get Root Simulations	82
9	SIMULATION DATA FORMAT	85
9.1	ROOT Files.....	85
9.2	Problems while handling the Data Files	86
9.2.1	Warning when opening root files	86
9.2.2	32-bit LINUX Systems	87
10	REFERENCE LIST.....	89
10.1	KCDC.....	89
10.2	KASCADE.....	89
10.3	KASCADE-Grande	90
10.4	COMBINED.....	90
10.5	WEB –Links	90
10.6	Simulations	90

11	GLOSSARY	91
12	APPENDIX	95
12.1	Appendix A – KASCADE Station Coordinates.....	95
12.2	Appendix B – GRANDE Station Coordinates.....	100

1 INTRODUCTION

The **KCDC Simulation Manual for the Combined Data Analysis** provides detailed explanation of data sets simulated for the KASCADE/KASCADE-Grande detectors and made publicly accessible with the KCDC Project Internet Application.

We use the name **COMBINED** as a synonym for combined data analysis of the KASCADE and the GRANDE detector systems of the KASCADE-Grande experiment. The combined analysis merges the advantages of the formerly separated KASCADE and GRANDE analyses and leads to a consistent spectrum in the energy range 10^{15} to 10^{18} eV.

The KCDC-Team is quite aware of the fact that not all details concerning air shower simulation, detector simulation and the analysis of the data can be described in this manual. Details of the KASCADE/KASCADE-Grande detector layout and the combined analysis of the measured data are published in the 'KCDC-Combined User Manual' as well available.

As the detector components and the data acquisition system are already described in detail in the 'KCDC User Manual', we kindly ask the user to get the details from there.

1.1 KCDC - THE KASCADE COSMIC RAY DATA CENTRE

KCDC is the 'KASCADE Cosmic Ray Data Centre', where via a web-based interface data of a astroparticle physics experiment have been made available for the interested public.

The KASCADE experiment, financed by public money, was a large-area detector for the measurement of high-energy cosmic rays. These charged particles (fully ionised atomic nuclei) are accelerated in active cosmic objects, propagated through the intergalactic and interstellar medium of the Universe, and reach our Earth for energies above 10^{14} eV with a rate of less than one per minute and square meter. Hitting our Atmosphere, they subsequently interact with nuclei and generate a cascade of millions of secondary particles, which partly reach the Earth surface and can be detected. This phenomenon is called an extensive air shower: EAS. With an array of particle detectors, this secondary cosmic radiation of individual EAS can be detected and the parameters of the impinging primary particle reconstructed. In a second step,

1 Introduction

the energy spectrum, elemental composition and the arrival distribution of the primary cosmic rays are investigated and by this, the astrophysical question to the origin of cosmic rays is studied. KASCADE was extended to KASCADE-Grande in 2003 to reach higher energies of primary cosmic rays where the rate decreases to less than one per day and square meter. KASCADE-Grande stopped finally the active data acquisition of all its components end of 2012 and is already decommissioned. The international collaboration of the experiment, however, continues the detailed analysis of nearly 20 years of data.

Moreover, with KCDC we provide the public the edited data, i.e. the reconstructed parameters of the primary cosmic rays measured via the detection of EAS with the KASCADE-Grande experiment, via a customized web page. The aim of this particular project is the installation and establishment of a public data centre for high-energy astroparticle physics. In the research field of astroparticle physics, such a data release is a novelty, whereas the data publication in astronomy has been established for a long time. However, due to basic differences in the measurements of cosmic-ray induced air-showers compared with astronomical data, KCDC provides the first conceptional design, how the data can be treated and processed so that they are reasonably usable outside the community of experts in the research field. Since 18.11.2013, the KCDC web portal is online and the amount of data has been extended in six major releases since then. With the release '**NABOO 2.0**', we offered as well simulation data from three major high-energy models, QGSjet, EPOS and SIBYLL with two or three different sub-models each.

With the latest release **PENTARUS 1.0**, measured data and simulations from a Combined Data Analysis of KASCADE and GRANDE data have been published.

The following chapter describes shortly the air shower simulation with CORSIKA, the KASCADE detector simulation using the cosmic ray event simulation code CRES (**Cosmic Ray Events Simulation**) and the reconstruction code KRETA (**KASCADE Reconstruction of Extensive Air showers**).

1.2 WHY SIMULATIONS

Analysing experimental data on Extensive Air Showers (EAS) requires a detailed theoretical modelling of the cascade, which develops when a high-energy primary particle enters the atmosphere. This can only be achieved by detailed Monte Carlo calculations taking into account all knowledge of high-energy strong and electromagnetic interactions.

2 SIMULATIONS

As the flux of primary cosmic ray particles in the energy range close to and above 1 PeV is very small, indirect measurements via the detection of extensive air showers induced by high energetic particles entering the atmosphere are feasible at present. Determination of spectra for individual elements or mass groups is limited by the large intrinsic fluctuations of EAS observables. Furthermore, any analysis of air shower data has to rely on EAS simulations and our limited knowledge of particle physics in the energy range of relevance. Since the primary energies of the showers are beyond the energy range of man-made accelerators and reactions relevant to shower development occur in the very forward direction not accessible in collider experiments, uncertainties in the description of hadronic interactions in shower development are unavoidable. One has, therefore, to rely on the use of phenomenological interaction models which differ in their predictions in some respect strongly, making the task of retrieving information about individual energy spectra from air shower data even more difficult.

With COMBINED we have been reconstructing energy spectra and mass composition for five elements representing different mass groups of primary cosmic ray particles, using three different high energy hadronic interaction models and thus helped the model builders to improve their simulation models. All the models used are implemented in the CORSIKA simulation package. CORSIKA (**CO**smic **R**ay event **SI**mulation for **KA**scade) has been written especially for KASCADE and extended since then to become the standard simulation package in the field of cosmic ray air shower simulations (<https://www.iap.kit.edu/corsika/>).

Simulating air showers for COMBINED is a three-step procedure:

- air shower simulation performed by CORSIKA
- detector simulation performed by CRES
- data reconstruction performed by KRETA.

Fig. 2.1. illustrates the parallel workflow of measurements and simulations.

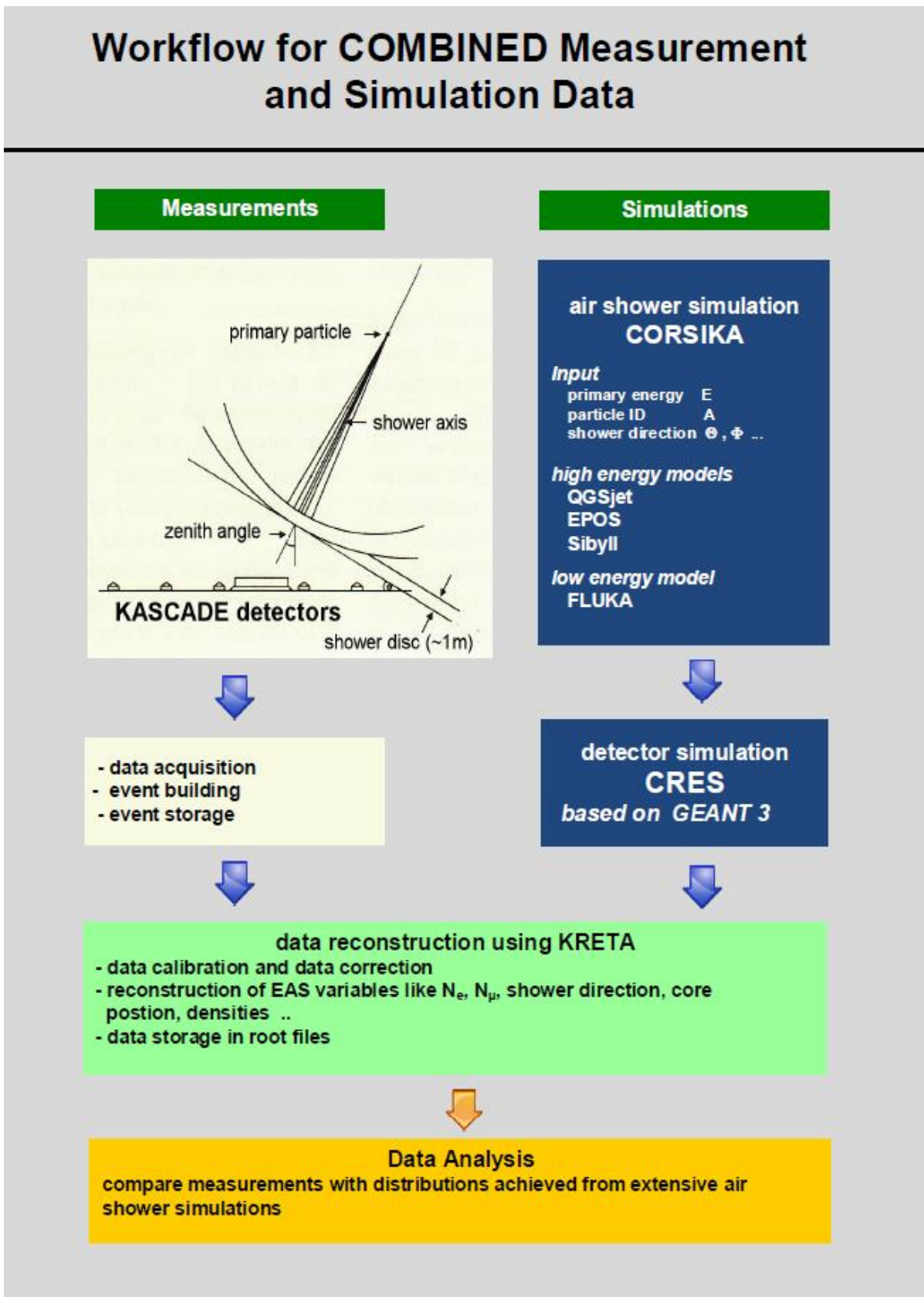


Fig. 2.1

COMBINED Data Analysis workflow for measurements and simulations

2.1 AIR SHOWER SIMULATIONS USING CORSIKA

CORSIKA (**CO**smic **R**ay event **SI**mulation for **KA**scade) is a detailed Monte Carlo program to study the evolution and properties of extensive air showers in the atmosphere. The first version 1.0 of CORSIKA dates from October 26, 1989.

Protons, light nuclei up to iron, photons, and many other particles may be treated as primaries. The particles are tracked through the atmosphere until they undergo reactions with the air nuclei or - in the case of instable secondaries – decay.

The CORSIKA program allows simulating interactions and decays of nuclei, hadrons, muons, electrons, and photons in the atmosphere up to energies of some 10^{20} eV. It gives type, energy, location, direction and arrival times of all secondary particles that are created in an air shower and pass a selected observation level.

A variety of high- and low energy hadronic interaction models is implemented. In COMBINED we were using three high-energy models from three different model families:

- QGSjet-II-04
- EPOS-LHC
- SIBYLL 2.3c

and one low energy model in different versions

- FLUKA.

The data from these six models have been made available the public via the KCDC web portal to enable the users to perform their own mass composition analysis.

For further details, please refer to the CORSIKA users guide and the references therein.

<https://web.iap.kit.edu/corsika/usersguide/usersguide.pdf>

Due to the fast improvement of computing power in recent years detailed simulations of EAS for different primaries, zenith angles and primary energies and of the detailed response of the KASCADE experiment to these events could be performed with sufficient statistical accuracy.

2 Simulations

2.1.1 QGSJET

QGSJET (Quark Gluon String model with JETs) is an extension of the QGS model, which describes hadronic interactions on the basis of exchanging supercritical Pomerons. Additionally QGSJET includes minijets to describe the hard interactions, which are important at the highest energies. The current version is QGSJET-II-04 including Pomeron loop and the cross-section is tuned to LHC data.

2.1.2 EPOS

EPOS (Energy conserving quantum mechanical multi-scattering approach, based on Partons, Off-shell remnants and Splitting parton ladders) uses the universality hypothesis to treat the high-energy interactions enabling a safe extrapolation up to higher energies, where cross sections and the particle production are calculated consistently, taking into account energy conservation in both cases.

The current version is EPOS LHC, in which LHC data are taken into account to constrain model parameters.

2.1.3 SIBYLL

SIBYLL is a program developed to simulate hadronic interactions at extreme high energies based on the QCD mini-jet model. For more than 15 years, version 2.1 of Sibyll has been one of the standard models for air shower simulation. Motivated by data of LHC and fixed-target experiments and a better understanding of the phenomenology of hadronic interactions, an improved version of this model, version 2.3, has been released in 2016. SIBYLL 2.3 internally produces charmed particles. Moreover, strange baryons and anti-baryons are accepted as projectiles. Sibyll 2.3c, is a further improvement where particle production spectra have been adjusted to match the expectation of Feynman scaling in the fragmentation region. The main change in the latest model is Sibyll 2.3d with regard to Sibyll 2.3c is in the production of π_0 in jets. In Sibyll 2.3c this production is strongly suppressed due to the interference from a component of the model intended to be active in low energy interactions only.

2.1.4 FLUKA

FLUKA (FLUctuating KAscade) is a package of routines to follow energetic particles through matter by the Monte Carlo method. In combination with CORSIKA only that part is used which

describes the **low-energy hadronic interactions**. FLUKA is used within CORSIKA to calculate the inelastic hadron cross-sections with the components of air and to perform their interaction and secondary particle production, including many details of the de-excitation of the target nucleus.

2.2 DETECTOR SIMULATION WITH CRES

CRES (Cosmic Ray Event Simulation) is a code package for the simulation of the signals/energy deposits in all detector components of KASCADE/KASCADE-Grande as response to an extensive air shower as simulated with **CORSIKA**. CRES has been developed, based on the GEANT3 package. CRES accepts simulated air shower data from CORSIKA as input and delivers simulated detector signals. The data structure of the CRES output (rawfz-files) is the same as from the KASCADE measurements, which means that both are analysed using the same reconstruction program KRETA.

CRES is written in FORTRAN 77. It uses CERN library packages and routines.

2.3 DATA RECONSTRUCTION WITH KRETA

KRETA (Kascade Reconstruction for ExTensive Air showers) reads the rawfz files from measured data and simulations and reconstructs the basic shower observables, storing all the results in the form of histograms and vectors of parameters (ntuples). Fig. 2.1 illustrates the parallel workflow of measurements and simulations.

The reconstruction procedure starts from the signals/energy-deposits in all detector components and determines physical quantities like the number of electrons, of muons, of hadrons, hadronic energies, arrival times, track directions and so on. It develops internally over three levels using an iterative process to come to the final results.

KRETA is written in FORTRAN 77. It uses CERN library packages and routines

2.4 GENERAL INFORMATION ON THE SIMULATED QUANTITIES

Unlike for measured data where we have calibration data like Air Temperature and more event information like Date and EventTime, we have here some additional information on the shower properties like true primary energy and particle ID derived directly from the air shower

2 Simulations

simulation CORSIKA or from the detector simulation CRES. From about 200 observables obtained in the analysis of the simulated data, we choose 34 to be published in KCDC. Ten of these parameters are representing the true shower information. These Values are summed up in ‘Monte Carlo Information’ described in more detail in chapter 6 while chapter 3 handles the values and data arrays reconstructed with COMBINED. Chapters 4 and 5 deal with the measured data in the detector stations of KASCADE and GRANDE like Energy Deposits and Arrival Times, which form the basis of the combined data analysis.

It was one of our main goals to publish the simulation data in a format as close as possible to the measured data published with the last release **PENTARUS I.O**, to make it as easy as possible for the users. Thus, we provide four ROOT trees in every download file:

ROOT tree	description
general	all data arrays; run- & event-number
combined	all reconstructed COMBINED quantities (E, Xc,Yc,Ze,Az,Ne,Nmu,Age)
trmc	all MC information from CORSIKA and CRES (TrEP,TRPP,TrXc,TrYc, TrZe, TrAz,TrNe,TrNg,TrNm,TrNh)
row_map	information to synchronise the trees

Presently we are only offering ROOT files, but we can provide the HDF5 files on request.

2.5 GENERAL INFORMATION ON SIMULATED DETECTOR COMPONENTS

In KASCADE, we have always simulated the response of all active detectors of the 10 components in CORSIKA and CRES storing only the resulting rawfz-files from CRES. This has been done because keeping the CORSIKA files would have been far beyond the scope of our storage capacity while in the rawfz files only the real responses of the active detectors are kept. Furthermore, we have been using one CORSIKA shower several times in CRES, thrown at different randomly chosen locations of pre-defined detector areas, different for KASCADE, GRANDE and the CALORIMETER. Comparing the time consumption for one shower for CORSIKA, CRES and KRETA, we find that the air shower simulations consume about 90% of the total time nearly independent of the energy of the primary particle. The multiple reuse of one shower is a kind of compromise. On the one hand we want to save computing time and storage space, on the

2 Simulations

other hand we have to be careful not to insert a 'bias', likely when using one air shower too many times. This effect is most important at high energies where we have only few showers simulated.

The table below shows the formerly published three detector components with their simulation areas and the number of reuses per shower. The origin of the coordinate system is the centre of the KASCADE array.

	active simulation area (with respect to the centre of KASCADE)	reused
GRANDE / COMBINED	X: -630m ... +120m ; Y: -670m ... +120m	10
KASCADE	X: -104m ... +104m ; Y: -104m ... +104m	3
CALORIMETER	X: -11.5m ... +11.5m; Y: -4.81m ... +15.19m	1

For the COMBINED analysis, only the GRANDE simulations have been used because they cover both, the GRANDE and the KASCADE detector arrays.

2.6 SIMULATIONS FOR THE LOPES DETECTOR

For the LOPES detector component presently no simulations are published via the KCDC web portal.

3 RECONSTRUCTION OF SIMULATED COMBINED DATA IN KCDC

For the COMBINED analysis, (detailed description see “*KCDC-Combined Manual*”) we published 13 quantities, of which five are data arrays. These arrays hold information on energy deposits and arrival times in each of the 252 stations of the KASCADE detectors and of the 37 stations of the GRANDE detectors. Displayed in the table below are also the two parameters Run and Event numbers usually referred to as ‘*general event parameters*’.

Quantity	Description	Unit	ID
Reconstructed Data			
Energy	first order reconstructed Energy	eV	<i>E</i>
Core Position X	location of the reconstructed shower core x-position	m	<i>Xc</i>
Core Position Y	location of the reconstructed shower core y-position	m	<i>Yc</i>
Zenith Angle	reconstructed zenith angle with respect to the vertical	° (<i>degree</i>)	<i>Ze</i>
Azimuth Angle	reconstructed azimuth angle with respect to the north	° (<i>degree</i>)	<i>Az</i>
Electron Number	reconstructed number of electrons (fit)	(<i>number of</i>)	<i>Ne</i>
Muon Number	reconstructed number of Muons (fit)	(<i>number of</i>)	<i>Nmu</i>
Age	shower shape parameter		<i>Age</i>
e/γ - energy deposits	energy deposit in MeV per KASCADE detector station [252]	(<i>MeV</i>)	<i>EDeposit</i>
μ - energy deposits	energy deposit in MeV per KASCADE detector station [192]	(<i>MeV</i>)	<i>MDeposit</i>
Arrival Times	arrival times in ns per KASCADE detector station [252]	<i>ns</i>	<i>Arrival</i>
Energy Deposits	charged energy deposit in MeV per GRANDE detector station	(<i>MeV</i>)	<i>GDeposit</i>

3 Reconstruction of Simulated COMBINED Data in KCDC

Quantity	Description	Unit	ID
Arrival Times	arrival times in ns per GRANDE detector station	(ns)	<i>GArrival</i>
General Event Parameters			
Run Number	internal simulation counting number	(number of)	<i>R</i>
Event Number	internal simulation counting number	(number of)	<i>Ev</i>

In simulations, every shower has been thrown 10 times on the KASCADE-Grande detector array, randomly distributed on an area of 750x790m² as shown in fig 3.0.1. Displayed as well are the 37 GRANDE detector stations (small black squares) and the area of the KASCADE detector array (dotted square). The solid red line encloses the active area that was used for this KCDC publication.

The plots shown in this chapter are only examples, based on this subsample of the simulated data for one model (QGSjet-II-04) and mostly for proton induced showers. So, applying user cuts in your own analysis can change these spectra drastically.

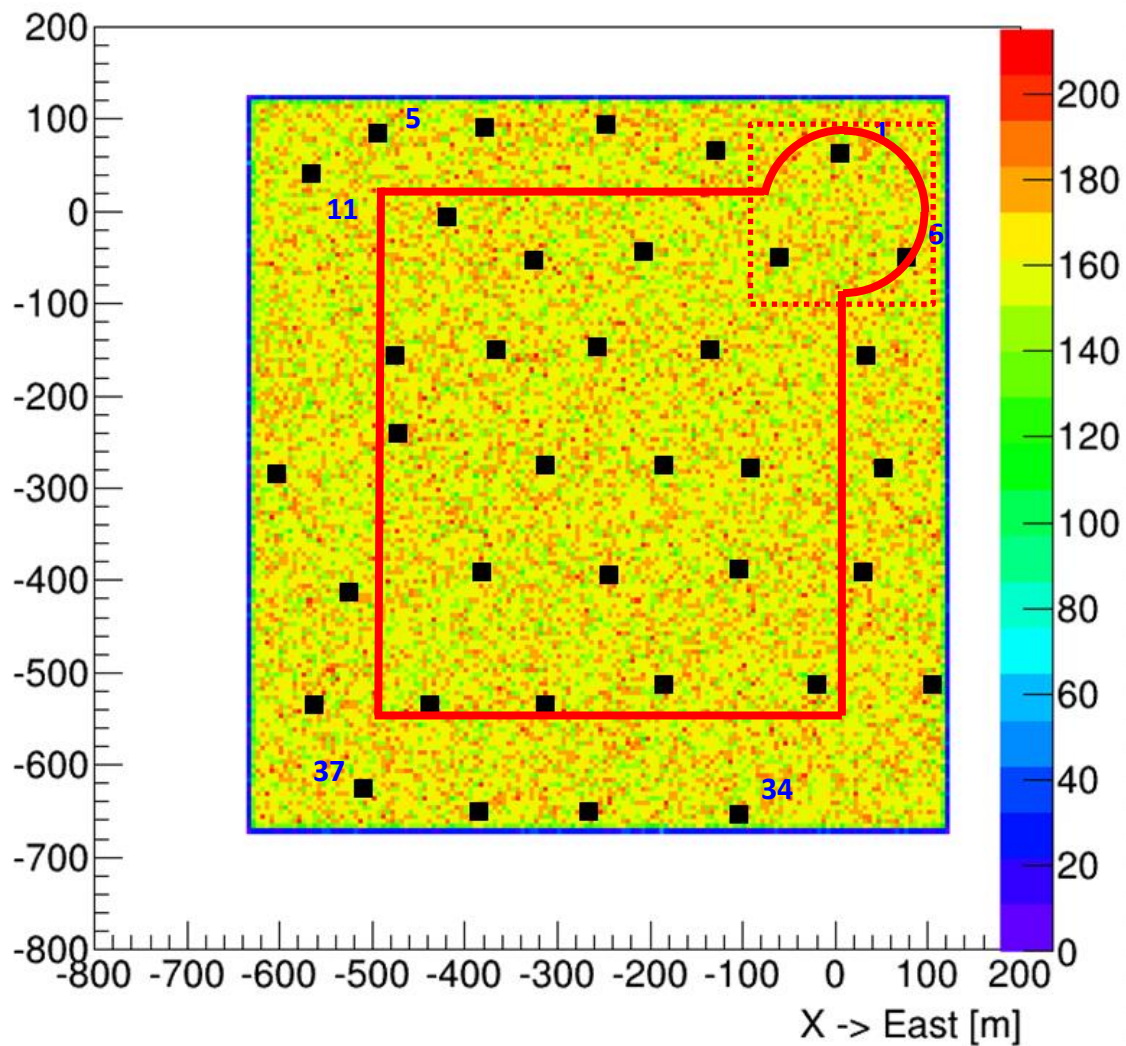


Fig. 3.0.1 *Distribution of the shower cores of all simulated showers in for the COMBINED analysis without any cuts. Shown also are the GRANDE detector stations and the KASCADE array (dotted square). The red line encloses the active area used for KCDC.*

3.1 ENERGY (E)

One of the main goals of the air shower measurement is to determine the energy spectrum of the cosmic rays. Due to uncertainties in the hadronic interactions and the large fluctuations in the shower size, this determination of energy and mass is rather challenging. In the KASCADE detector array we measured the electromagnetic and muonic components of air showers separately. In GRANDE the number of muons is derived from the KASCADE array by means of a LECF (lateral energy correction function) extrapolated to GRANDE distances. By subtracting this from the function of the charged particles measured by GRANDE, we obtain values for the electromagnetic component in GRANDE. By using both observables, we perform a

transformation matrix in order to convert the number of electrons and muons to the energy of primary particles taking into account the angle of incidence. The parameters of the formula of the energy estimator are derived from extensive air shower simulations.

3.1.1 ENERGY ESTIMATION

To get a rough energy estimation the comparison of the reconstructed data and the CORSIKA simulations have been used by applying the hadronic interaction model of **QGSjet-II-04** (Quark-Gluon-String Model, version II-4) for laboratory energies above 200GeV and the low energy model **Fluka 2011.2.14_32** for energies below. The simulations cover the energy range of $1 \cdot 10^{14}$ to $3 \cdot 10^{18}$ eV with zenith angles in the interval $0^\circ - 42^\circ$. Used in this publication are only showers with primary energie above 10^{15} eV and zenith angles below 30° (details see chapter 3.6). The spectral index in the simulations was $\gamma=-2$ to save time and disk space and then corrected for the real spectral index of the cosmic rays to $\gamma=-2.7$.

3.1.2 FORMULA FOR ENERGY ESTIMATOR

For the energy estimation in the COMBINED analysis, we choose a very simple formula:

$$\lg(E) = 1.632 + 0.8907 * \lg(N_{e^+} + N_{\mu})$$

The spectrum of the reconstructed energy of the primary particle for KASCADE based on this formula is shown in Fig. 3.1.1 (red). Displayed as well is the spectrum of the incident particles after the standard quality cuts of the COMBINED analysis have been applied i.e. the true primary energy (black). Clearly visible also is that the full efficiency of the reconstruction is reached at about $10^{15.5}$ eV.

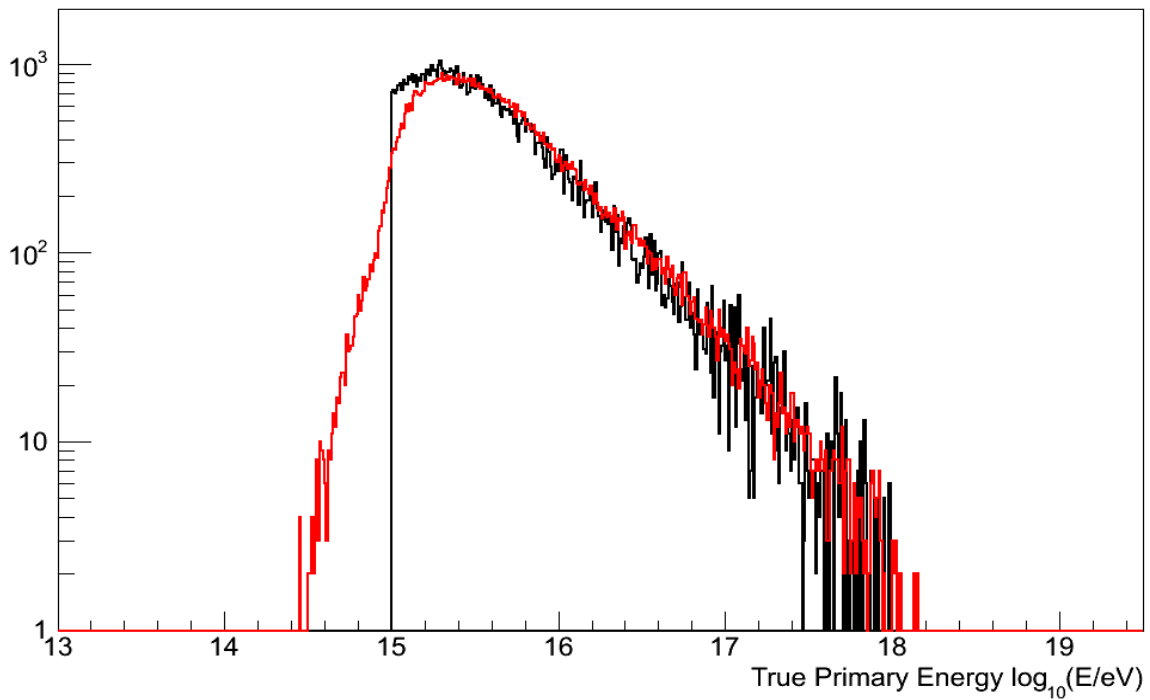


Fig. 3.1.1 *The reconstructed energy spectrum (red) and the true energy spectrum (black) in log-log scale for reconstructed protons*

Fig. 3.1.2 shows the quality of the energy reconstruction compared to the true primary energy of the incident protons. The red dashed line denotes the expected values.

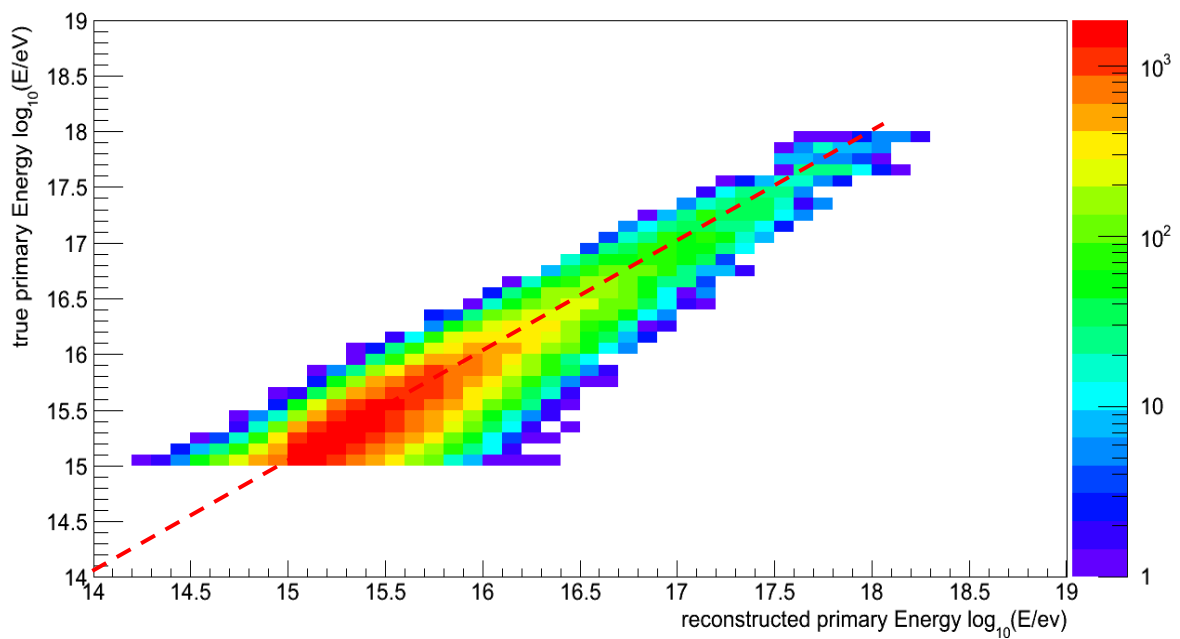


Fig. 3.1.2 *True primary energy of the incident particle vs reconstructed primary energy for proton-induced showers. The dashed red line denotes the expected value.*

3.2 NUMBER OF ELECTRONS AND NUMBER OF MUONS (N_e , N_{μ})

From the COMBINED simulations, we derive the energy deposits of charged particles and muons at ground level, as well as their arrival time. From these data, the arrival direction of the shower, its impact point on ground (shower core) and the total number of electrons and muons in the shower are reconstructed. Details see the '*KCDC-Combined Manual*'.

Fig. 3.2.1 shows the N_e spectrum of the simulated proton showers reconstructed with KRETA (red) and the true N_e spectrum (black). The quality cut is at $\lg(N_e)=3.2$ for events with their shower core inside the KASCADE detector array, and $\lg(N_e)=4.8$ when the shower core lies within the GRANDE array. This is also the reason for the event poor zone below $\lg(N_e) = 4.8$, which is only populated by events within the KASCADE array. The excellent agreement of the reconstructed number of electrons with the true number as shown in fig. 3.2.2 proves the quality of the energy calibration and the reconstruction. The dashed line denotes the expected values.

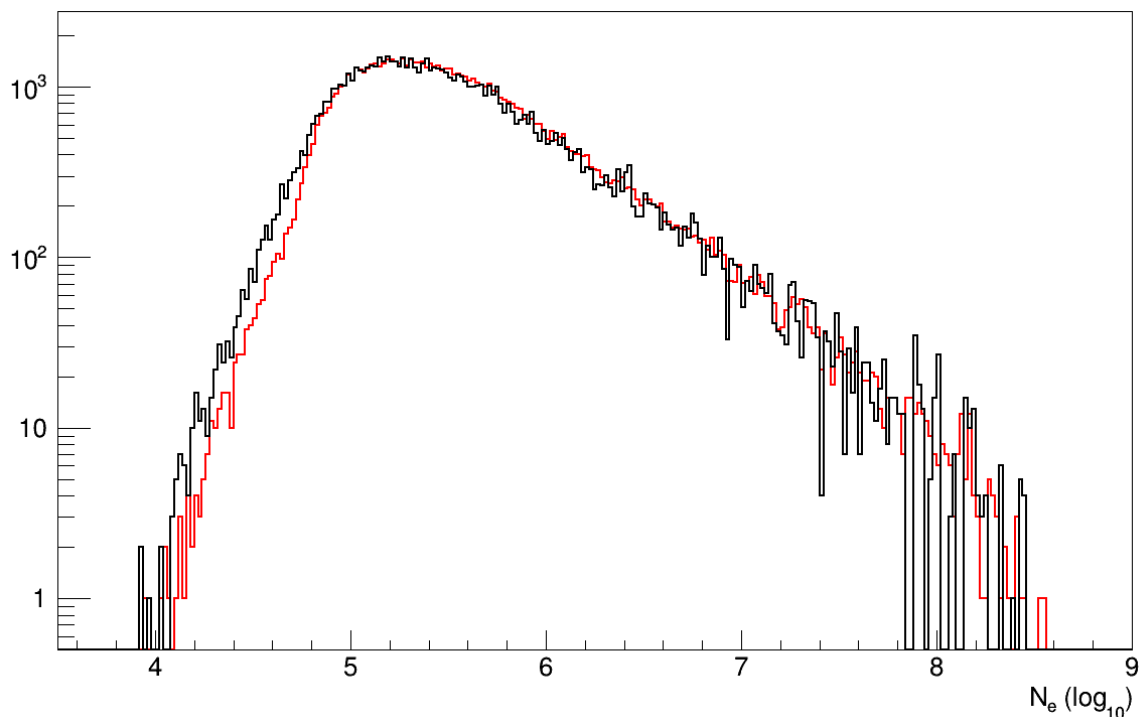


Fig. 3.2.1 *The spectrum of the reconstructed number of electrons (red) and the true numbers from CORSIKA (black)*

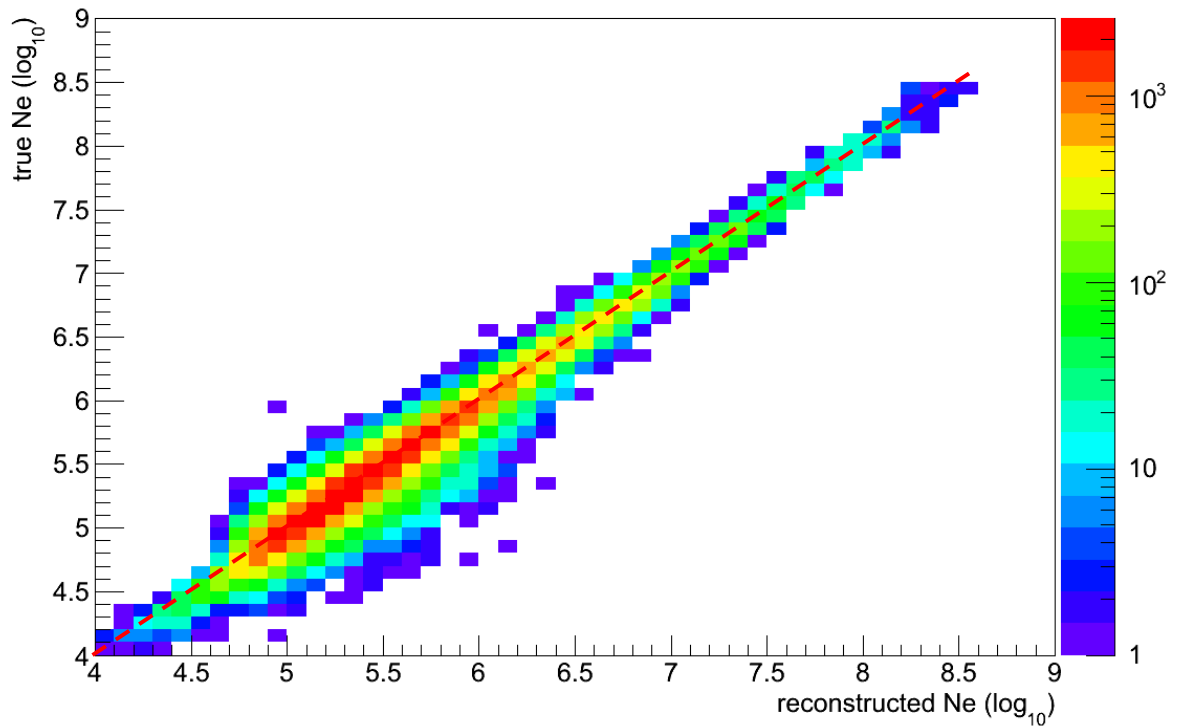


Fig. 3.2.2 *lgN_e Spectrum; true number of electrons vs lgN_e after reconstruction for proton induced showers .The dashed red line denotes the expected values.*

In fig. 3.2.3 the N_μ spectrum of the simulated proton showers reconstructed with KRETA (red) is displayed and the true N_μ spectrum (black). The quality cut is at $\lg N_\mu=3.0$ for showers with the reconstructed core position within the fiducial area. The good agreement of the reconstructed number of muons with the real number is shown in fig. 3.2.4.

3 Reconstruction of Simulated COMBINED Data in KCDC

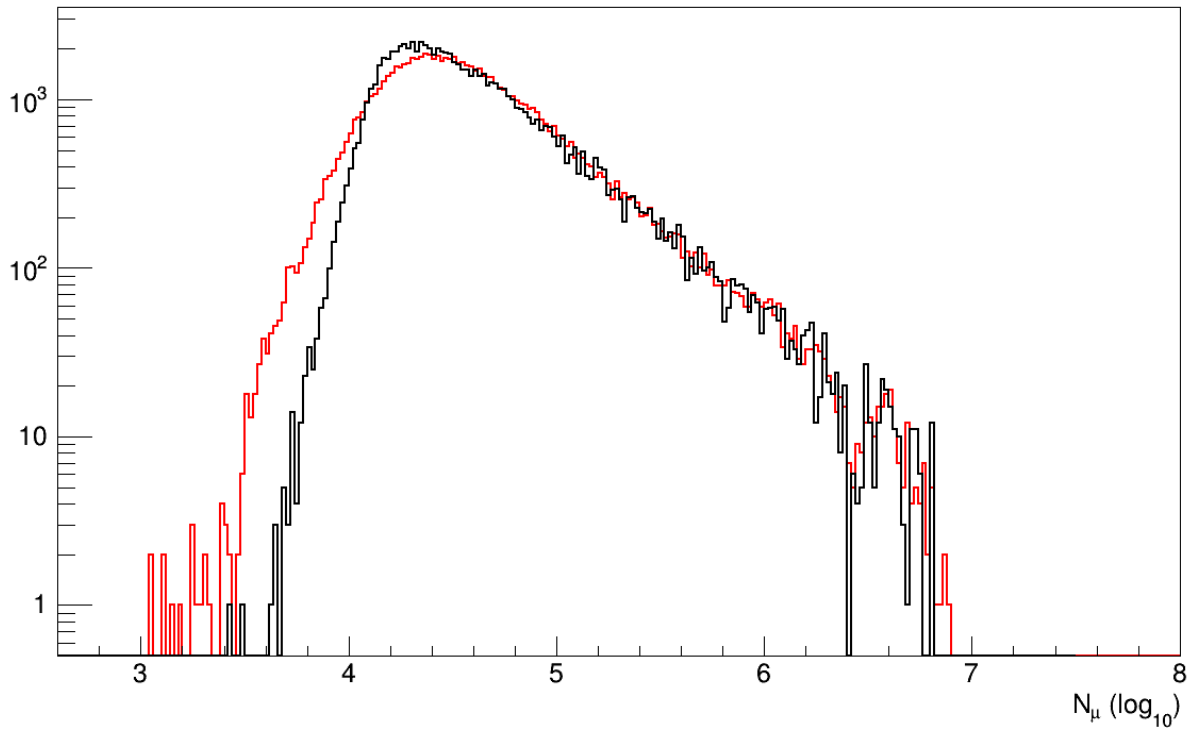


Fig. 3.2.3 *The spectrum of the reconstructed number of muons (red) and the true numbers from CORSIKA (black)*

3 Reconstruction of Simulated COMBINED Data in KCDC

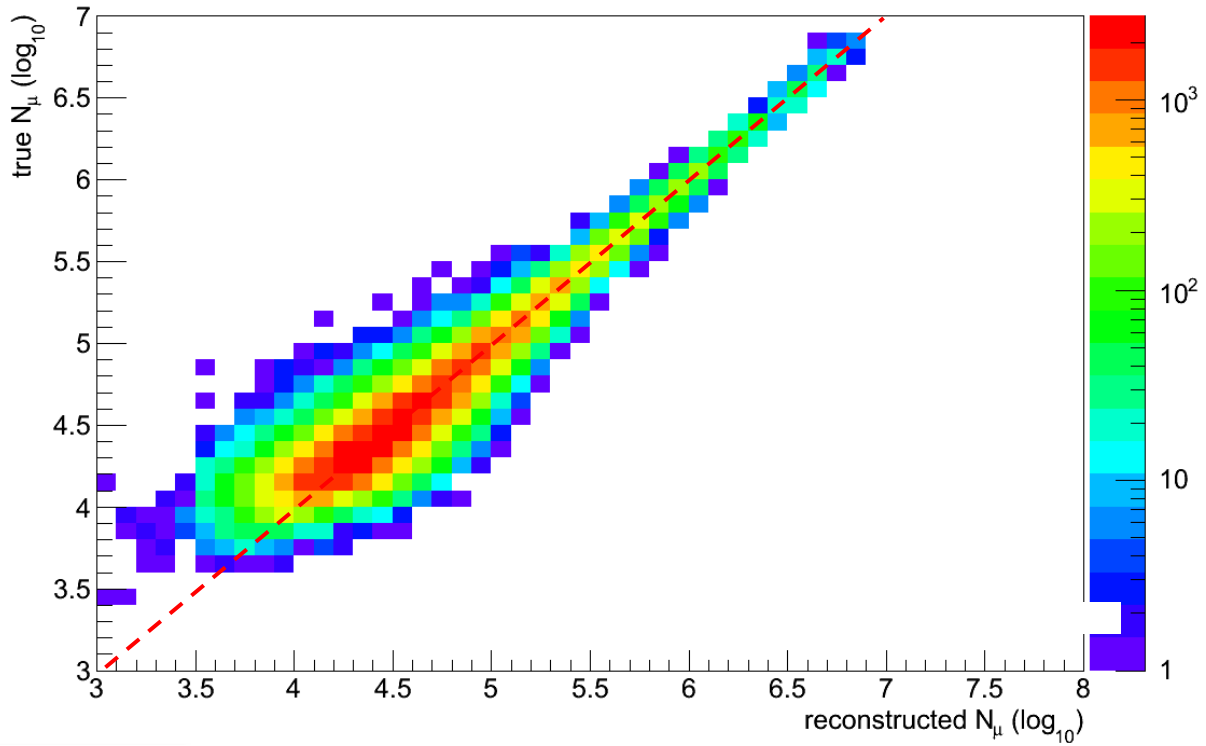


Fig. 3.2.4 *lgN_μ Spectrum; true number of muons vs lgN_μ after reconstruction for proton-induced showers. The dashed red line denotes the expected value.*

In fig. 3.2.5, the $lgN_\mu - lgN_e$ distribution from CORSIKA simulations as reconstructed by the COMBINED analysis is displayed.

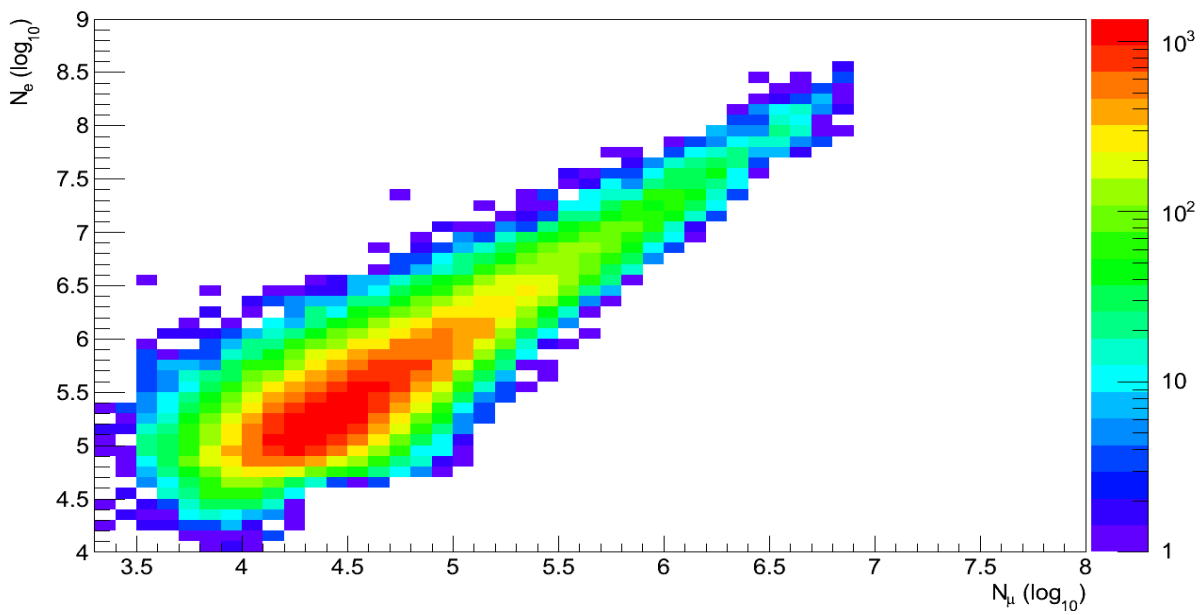


Fig. 3.2.5 *$lgN_\mu - lgN_e$ distribution measured by COMBINED*

3.3 AGE (AGE)

Contrary to variables like number of electrons N_e or number of muons N_μ , the value of the age parameter has no absolute meaning, as it depends on the choice of the lateral distribution function, which is fitted to the shower data. It may also be called **lateral shape parameter** because it describes the steepness of the lateral electron density distribution. COMBINED uses a modified NKG-function to fit the lateral shower shape. Within this function, the age parameter values are limited theoretically to a range from 0.1 to 1.6. Common shower values however range from 0.15 to 1.48. Lower values describe steeper lateral distributions.

The shape (steepness) of the lateral density distribution of a given shower depends on the energy of the primary particle, as well as on its nature. The higher the shower energy, the steeper the lateral distribution. A heavy primary particle with the same energy as a light one gives rise to a flatter lateral distribution, as the shower starts earlier in the atmosphere. When reaching ground, the shower is "older", which gives the age parameter its name. The age parameter therefore may help (in combination with number of electrons) to distinguish between primary particles of different mass.

Fig. 3.3.1 shows the distribution of the Age parameter within its valid range.

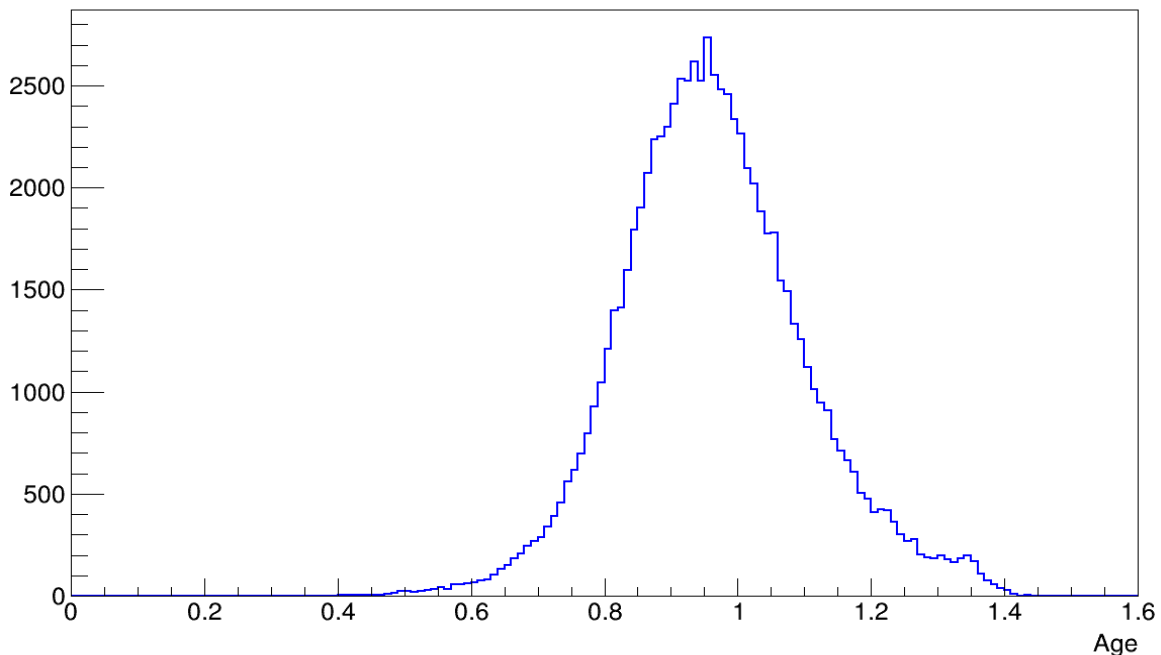


Fig. 3.3.1 *The AGE distribution from the modified NKG function for reconstructed proton showers.*

3.4 SHOWER CORE POSITION (X_C , Y_C)

The Core Position is the reconstructed location of the shower centre at KASCADE-Grande level derived from the energy deposits of each detector station of one event. The unit of the core position is [m].

For the reconstruction of the core position in the COMBINED Data Analysis basically the energy deposits in every detector station from the KASCADE and GRANDE detector arrays are used. By means of a *neural network algorithm* which combines high efficiency for the identification of the shower core with good rejection capability for showers that fall outside the fiducial volume, the core can be determined to a precision of about 1m. In addition, this method offers a simple approach to identify events with subcores.

In figs 3.4.1. and 3.4.2 the distributions of the X- and Y-core positions are shown. The sharp edge at $x=0$ m and $y=25$ mm is caused by the fiducial area cuts.

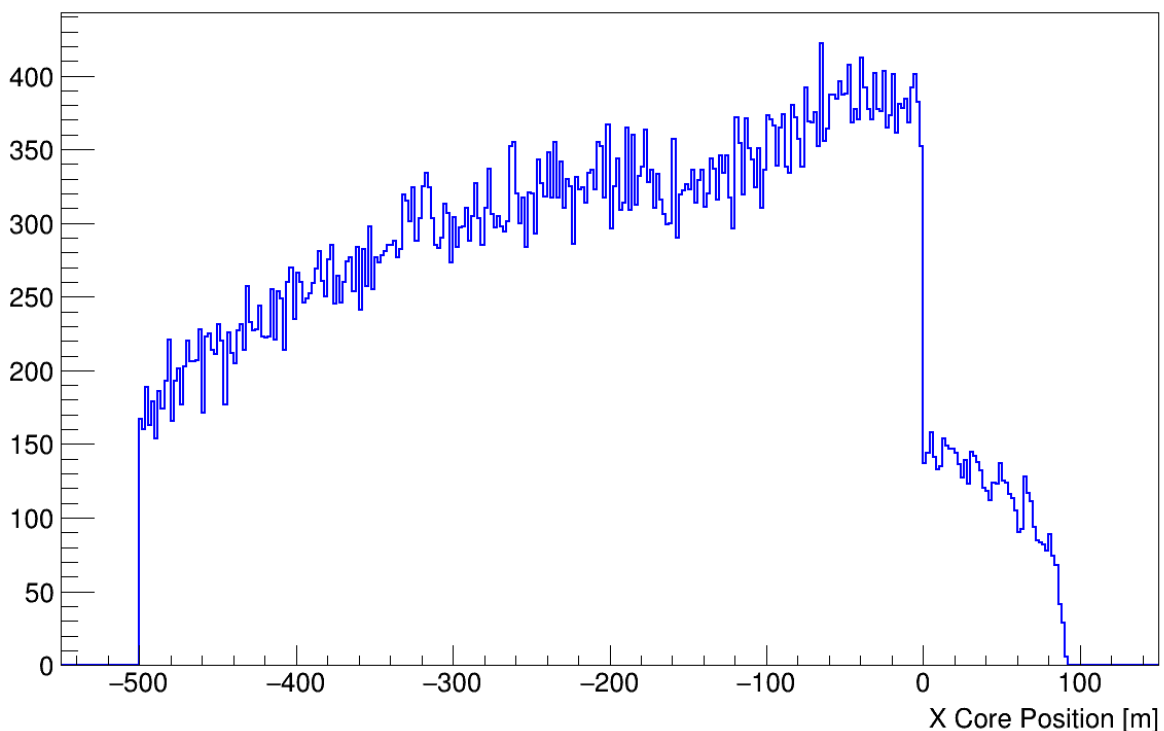


Fig. 3.4.1

X-core position of reconstructed proton showers

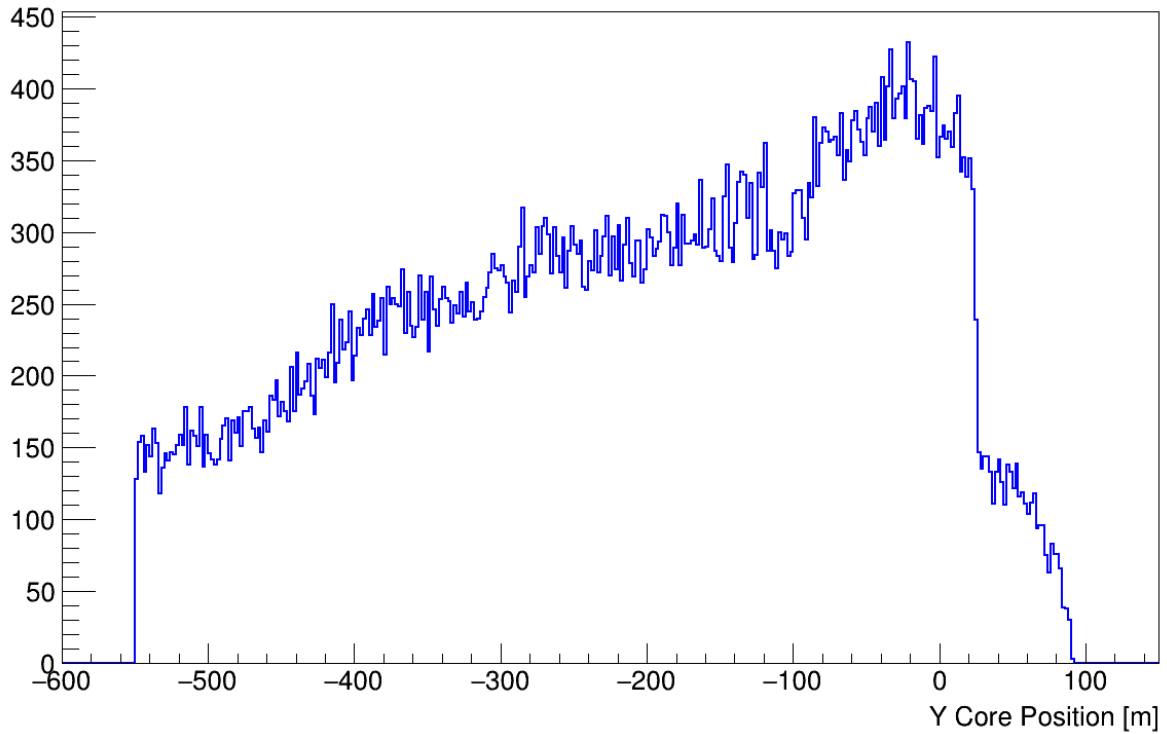


Fig. 3.4.2 *y-core position of reconstructed proton showers*

The distribution of the reconstructed shower core is plotted in the fig. 3.4.3. Extensive air showers with a core position outside the detector area have a great probability for being incorrectly reconstructed. Therefore, only showers within the fiducial area plotted are taken into account (see also fig 3.0.1).

The quality of the reconstruction is shown in figs 3.4.4 to 3.4.6. In figs. 3.4.4 & 3.4.5 the X- and Y-positions are displayed versus the true positions of the simulated shower core, while in fig. 3.4.6 the absolute deviation of the reconstructed shower core position is shown. The true core position is derived from CRES detector simulations, where the shower core is randomly distributed over a pre-defined detector area (see also fig 3.0.1).

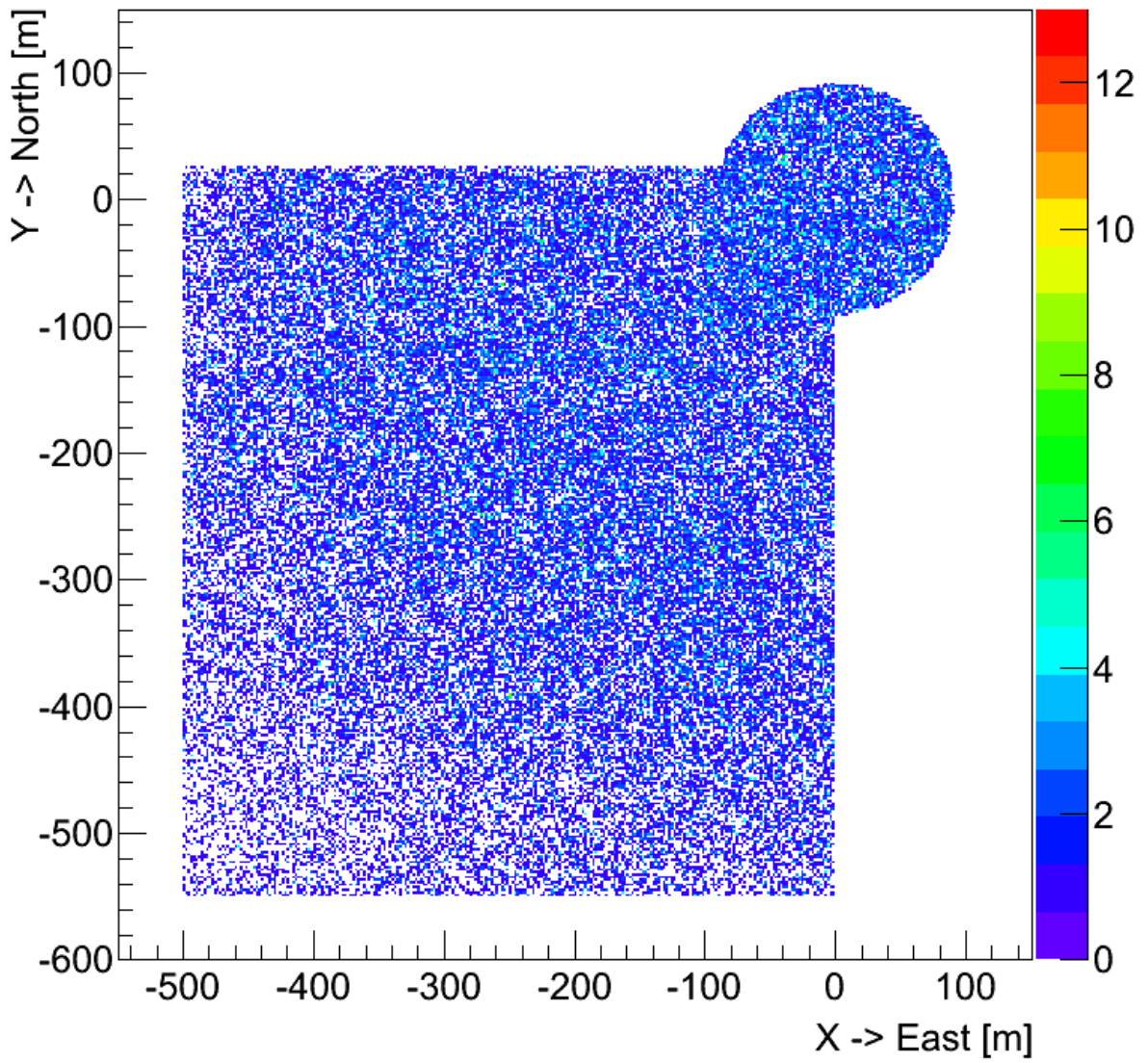


Fig. 3.4.3 *Shower core distribution for reconstructed proton showers*

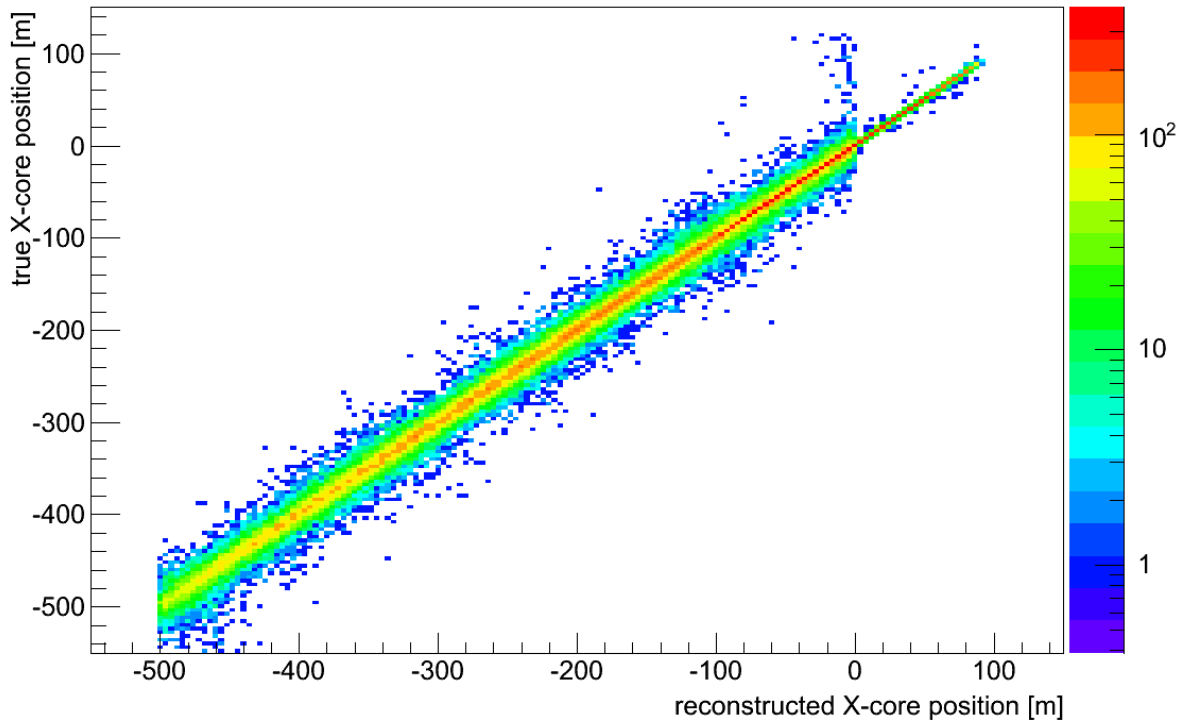


Fig. 3.4.4 *True X-shower core position vs reconstructed X-shower core position for proton induced showers*

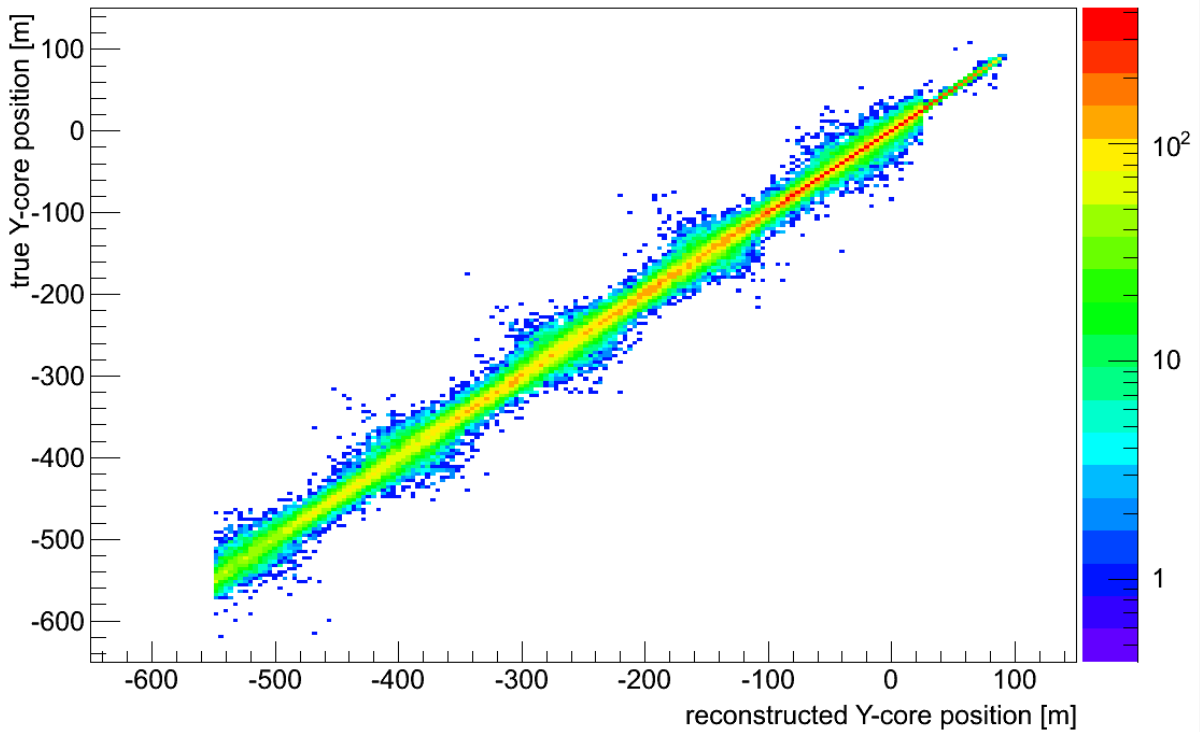


Fig. 3.4.5 *True Y-shower core position vs reconstructed Y-shower core position for proton induced showers*

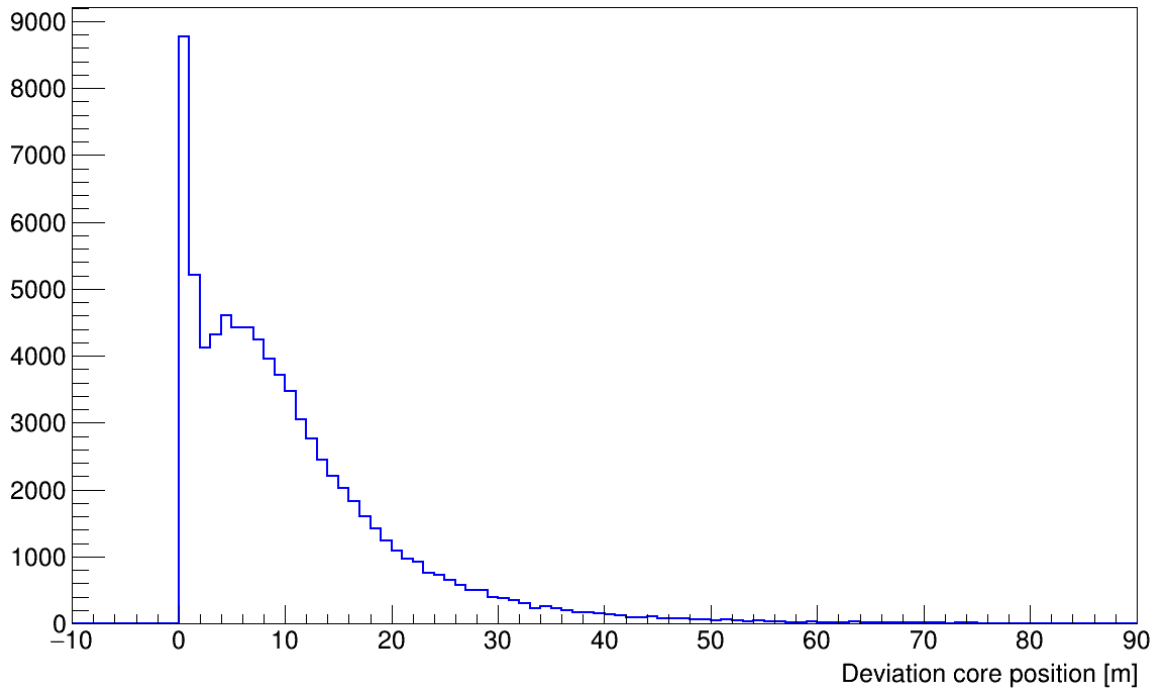


Fig. 3.4.6 *absolute deviation of the shower core position between true and reconstructed core positions*

3.5 SHOWER DIRECTION (ZE, Az)

From the COMBINED simulations, we get the arrival times and the energy deposits of air shower particles. The shower direction is determined by evaluating the arrival times of the first particle in each detector station. To increase the accuracy, the energy deposits are taken into account when the direction of the shower disk is calculated.

The angular resolution drops significantly above about $\theta > 30^\circ$, caused by the fact that the reconstruction algorithm for COMBINED has been fine-tuned to zenith angles below 30° .

In KASCADE coordinates, the zenith angle is measured against the vertical direction, which means that $\theta = 0^\circ$ is pointing upwards and 90° denotes a horizontal shower. The azimuth is defined as an angle measured clockwise starting in northern direction (90° is east). The regular orientation of the KASCADE Array has an offset of about $+15^\circ$ against the real northern direction, caused by the fact that the conditions of the location (KIT, Campus North) allows only

3 Reconstruction of Simulated COMBINED Data in KCDC

this orientation. This offset is corrected for in the data analysis. The unit of the azimuth and zenith angle is [°].

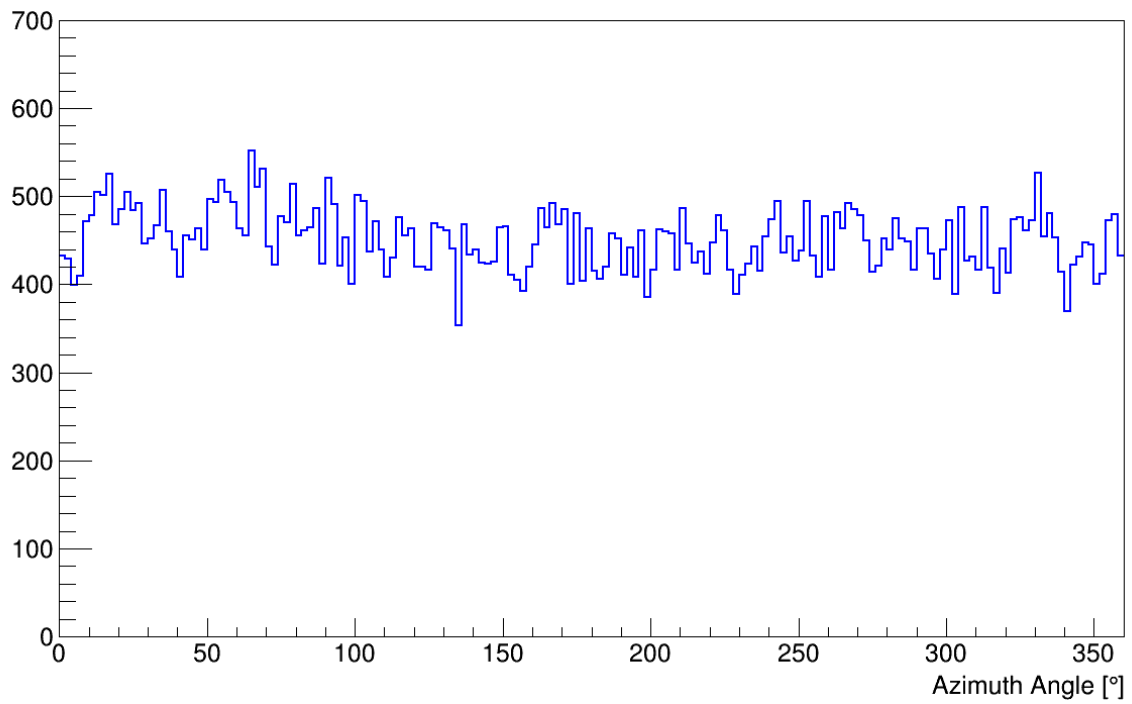


Fig. 3.5.1 *The distribution of the reconstructed azimuth angle for proton induced showers*

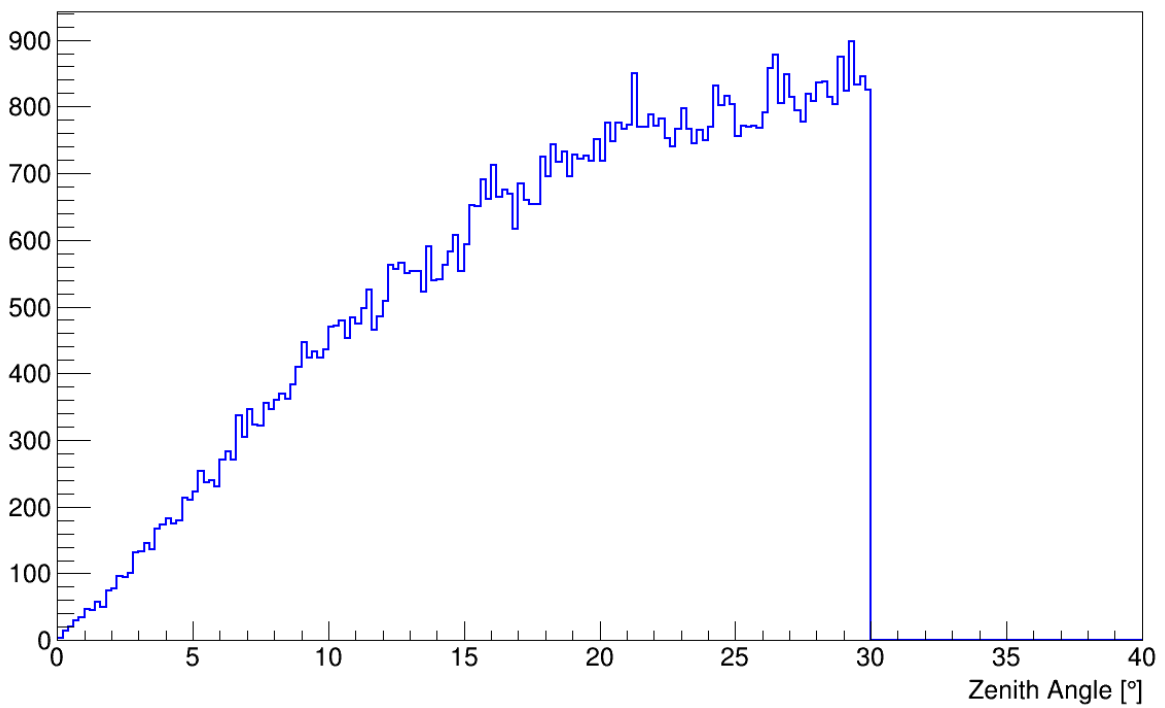


Fig. 3.5.2 *The distribution of the reconstructed zenith angle for proton induced showers*

3 Reconstruction of Simulated COMBINED Data in KCDC

In fig. 3.5.1 the distributions of the azimuth angle for simulated protons is shown. The distribution of the simulated and reconstructed zenith angle shown in fig 3.5.2.

The quality of the angular reconstruction is shown in figs 3.5.3 and 3.5.4 where Z_e - and the A_z -angles are displayed versus the true shower directions. The true angles are input parameters for the air shower simulation program CORSIKA.

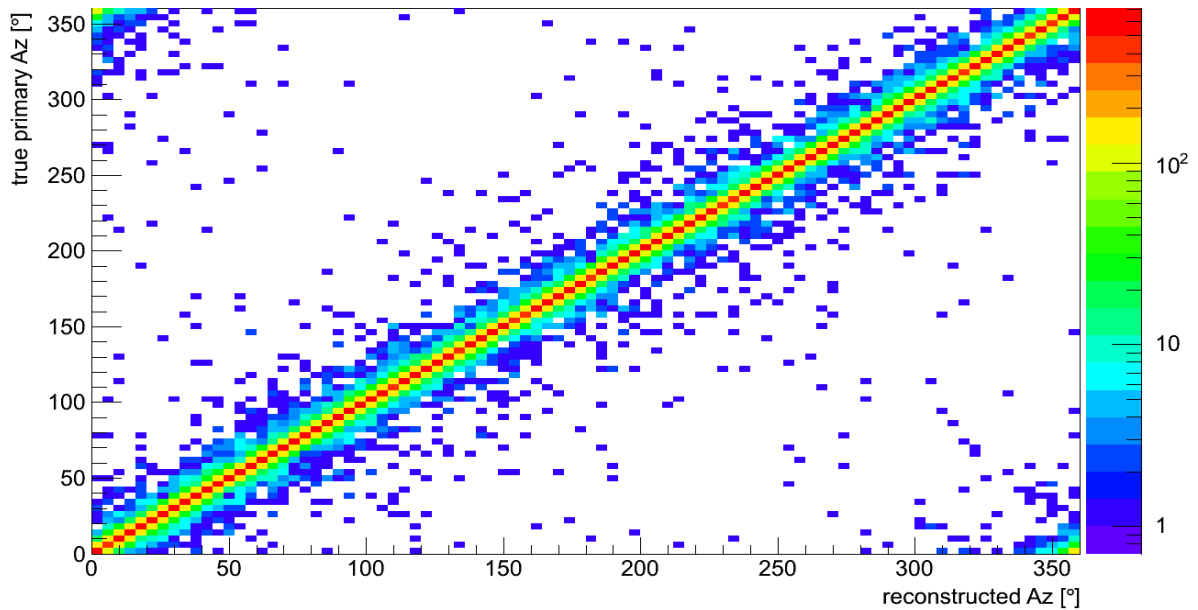


Fig. 3.5.3 *True Az angle vs reconstructed azimuth angle for proton induced showers*

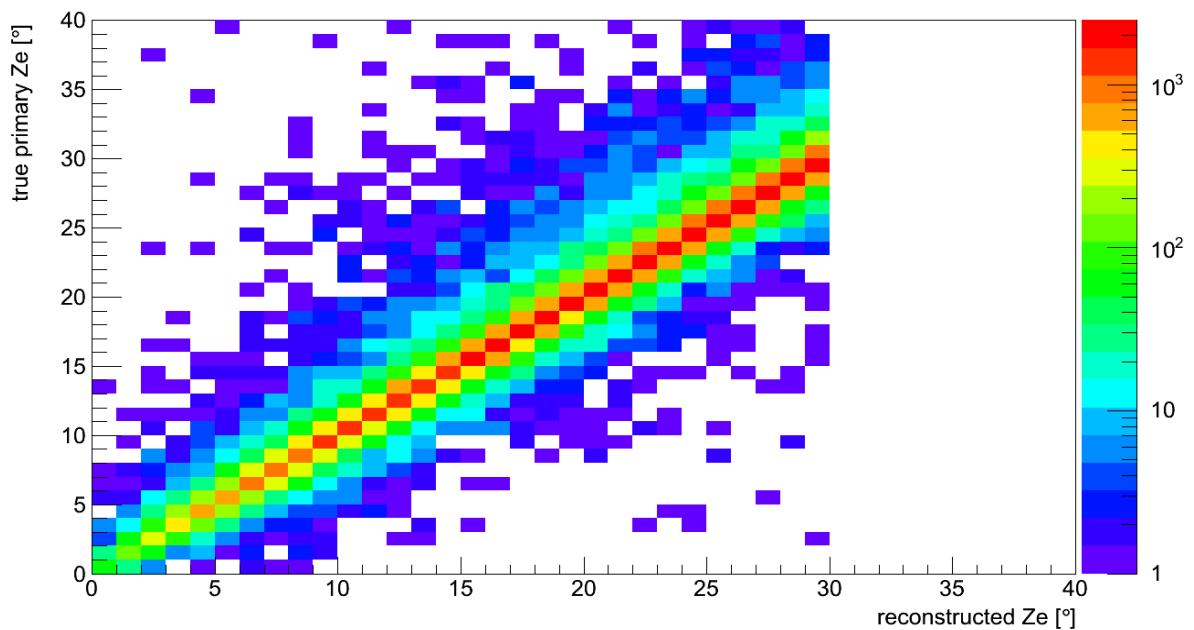


Fig. 3.5.4 *True Ze angle vs reconstructed zenith angle for proton induced showers*

3.6 COMBINED AT LOWER ENERGIES

The energy range of the simulations analyzed with the COMBINED data analysis mechanism covers only events with incident energies above 10^{15} eV. The COMBINED analysis method itself can reconstruct low energy events quite well, but only if they are near or within the KASCADE array. Fig 3.6.1 shows the shower core distribution of showers with incident energies above 10^{14} eV (left) and of energies below 10^{15} eV (right) indicating that the increase in the area of the KASCADE array (91m radius) is mainly caused by low-energy events.

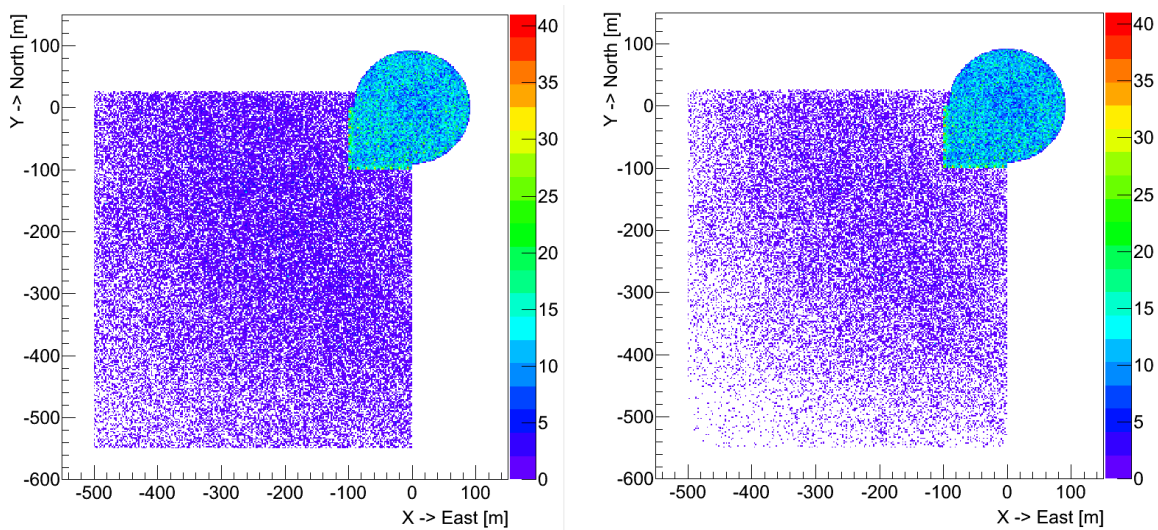


Fig. 3.6.1 *Shower core distribution for reconstructed proton showers at different primary energy ranges: left $10^{14} < E_0 < 10^{18}$ eV; right $10^{14} < E_0 < 10^{15}$ eV*

The reconstructed energy for different ranges of the primary particle are shown in fig 3.6.2. Protons with incident energies above 10^{14} eV (black envelop curve), above 10^{15} eV (red curve) and below 10^{15} eV (blue curve) are displayed.

As for low-energy events the leading reconstruction algorithm is the same as for the data already published with KCDC release **NABOO 2.0**, we decided to limit ourselves to the energy range above 10^{15} eV. Furthermore, the COMBINED analysis only reaches full efficiency around $10^{15.5}$ eV (see fig 3.1.1) where the number of events with primary energies below 10^{15} eV can be neglected.

3 Reconstruction of Simulated COMBINED Data in KCDC

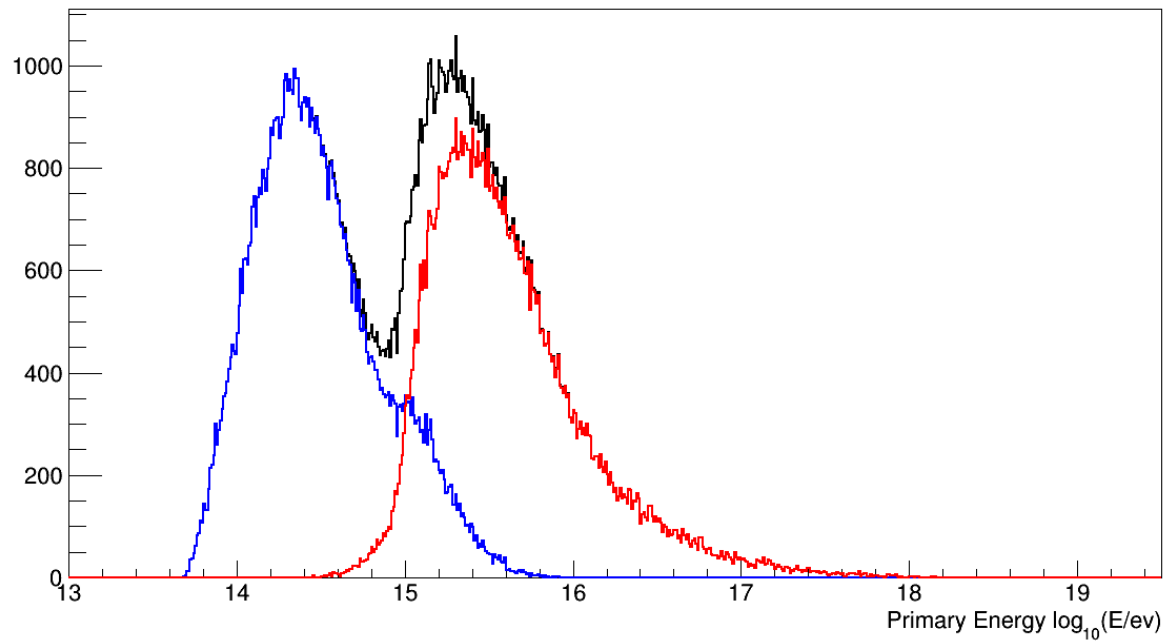


Fig. 3.6.2 *Distribution of the reconstructed energy at different primary energy ranges.*
black: $10^{14} < E_0 < 10^{18} \text{eV}$; blue $10^{14} < E_0 < 10^{15} \text{eV}$; red $10^{15} < E_0 < 10^{18} \text{eV}$

4 RECONSTRUCTION OF SIMULATED KASCADE DATA IN KCDC

With the release of the COMBINED analysis, we publish the three data arrays from KASCADE, the energy deposits of electrons and muons and the arrival times per station as given by the reconstruction program KRETA (*Kascade Reconstruction for ExTensive Air showers*).

GRANDE Quantity	Description	Unit	ID
Reconstructed Data			
e/γ - energy deposits	energy deposit in MeV / station [252]	(MeV)	<i>EDeposit</i>
μ - energy deposits	energy deposit in MeV / station [192]	(MeV)	<i>MDeposit</i>
Arrival Times	arrival Times / station [252]	ns	<i>Arrival</i>

The energy deposits of each single detector station are simulated in the e/ γ - and in the μ -detectors.

While in measurements, a detector station flagged ‘inactive’ or ‘overflow’ was excluded from the data analysis, it is different in simulations. Here we do not have any ‘inactive’ detector stations to be excluded. Stations with energy deposit overflows are excluded from the data analysis in KRETA but **included in the data sets** because they might hold valuable information depending on the analysis performed by the KCDC user.

Detector stations which had no signal above the threshold are set to $E_{\text{deposit}}=0$ MeV.

The plots shown in this chapter are only examples, mostly based on a subsample of the simulated data sets and only for one simulation model (QGSjet-II-04) with primary energies above 10^{15} eV. So, applying user cuts in your own analysis can change these spectra drastically.

4.1 e/γ – ENERGY DEPOSITS

Handling the ‘ e/γ Energy Deposits’ quantity mostly requires some additional information either on the absolute coordinates of the detector station or on the distance to the reconstructed shower core. Therefore, the quantity **EDepositS** is always supplied with the energy values. For simulations, all stations are always active which implies that the number of detector stations with valid energy deposit information (**EDepositN**) is always 252.

Thus, you will always be supplied with the following data sets:

EDepositN	number of active e/γ -detector stations with energy deposit ≥ 0
EDeposit	energy deposit per station in MeV
EDepositS	detector station ID [1...252]

4.1.1 NUMBER OF ACTIVE e/γ -DETECTOR STATIONS (EDEPOSITN)

The number of active e/γ -detector stations stored in **EDepositN** is for simulations always 252 because there is no feature implemented in the simulation dealing with inactive stations.

Note: This value is always shipped with ‘ e/γ Energy Deposit’ Quantity in the root files.

4.1.2 NUMBER OF e/γ -DETECTOR STATIONS WITH HITS

The distribution of the number of e/γ -detectors with $E_{deposit}>0$ is given in fig 4.1.1.

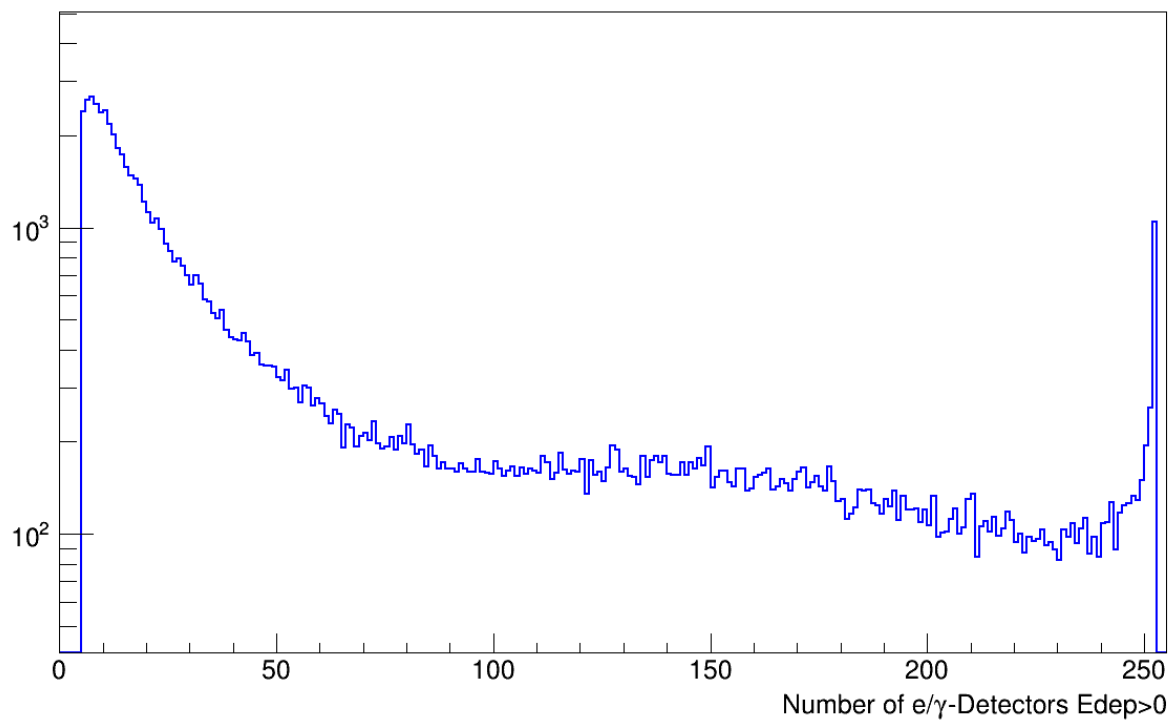


Fig. 4.1.1 *Distribution of the number of e/γ -detector stations with hits*

4.1.3 e/γ ENERGY DEPOSIT FOR EACH DETECTOR STATION (EDEPOSIT)

The Energy deposits are directly taken from the simulations for each detector station. **EDeposit** values are given in MeV. In fig 4.1.2, the energy deposits for simulated proton induced showers are plotted. The overflow cut is set to 10 GeV.

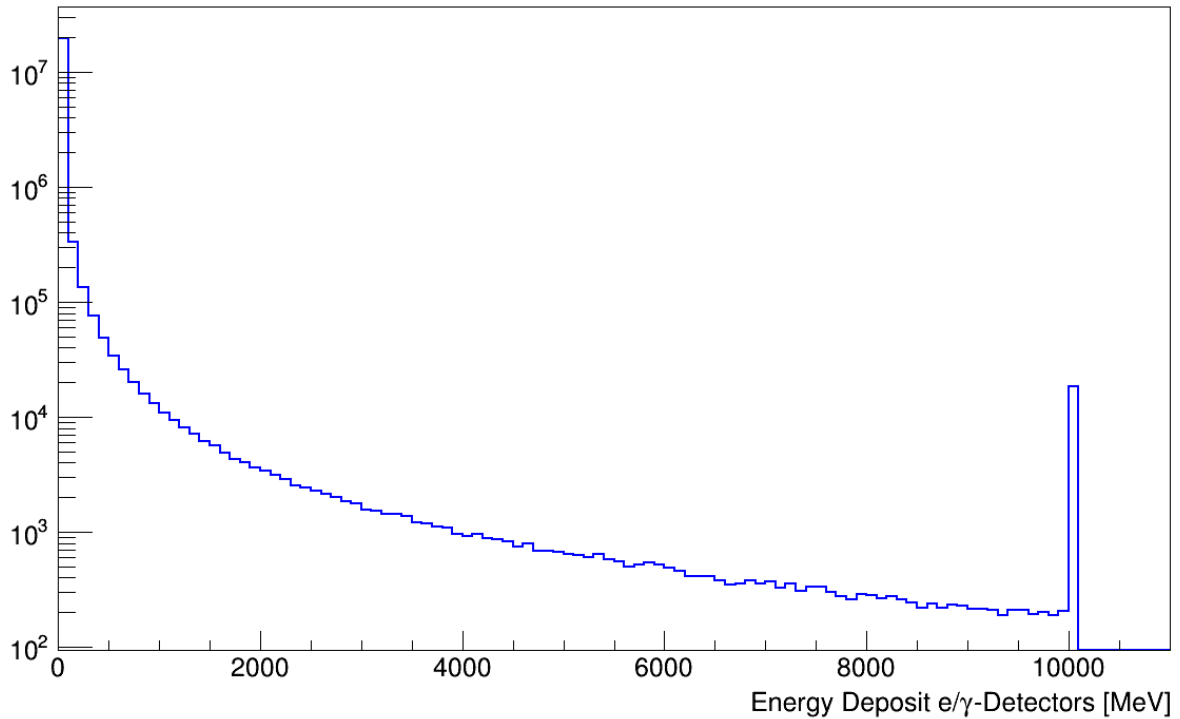


Fig. 4.1.2 *Distribution of the e/γ-Energy Deposits of all active stations*

4.1.4 STATION ID (EDEPOSITS)

The station ID holds the information of the location of the respective detector station. The transformation from the station ID to the true detector position in KASCADE coordinates of the respective Array detector station is in detail described in chapter 7.3 and Appendix A.

Fig 4.1.3 shows the distribution of station IDs of the active e/γ-detector stations. The distribution is flat for simulations because we do not include inactive stations in our detector simulations. Stations with energy deposits above 10 GeV are active too, the deposits are not taken into account for analysis but are included in the data samples.

Note: This value is always shipped with 'e/γ Energy Deposit' Quantity in the root files.

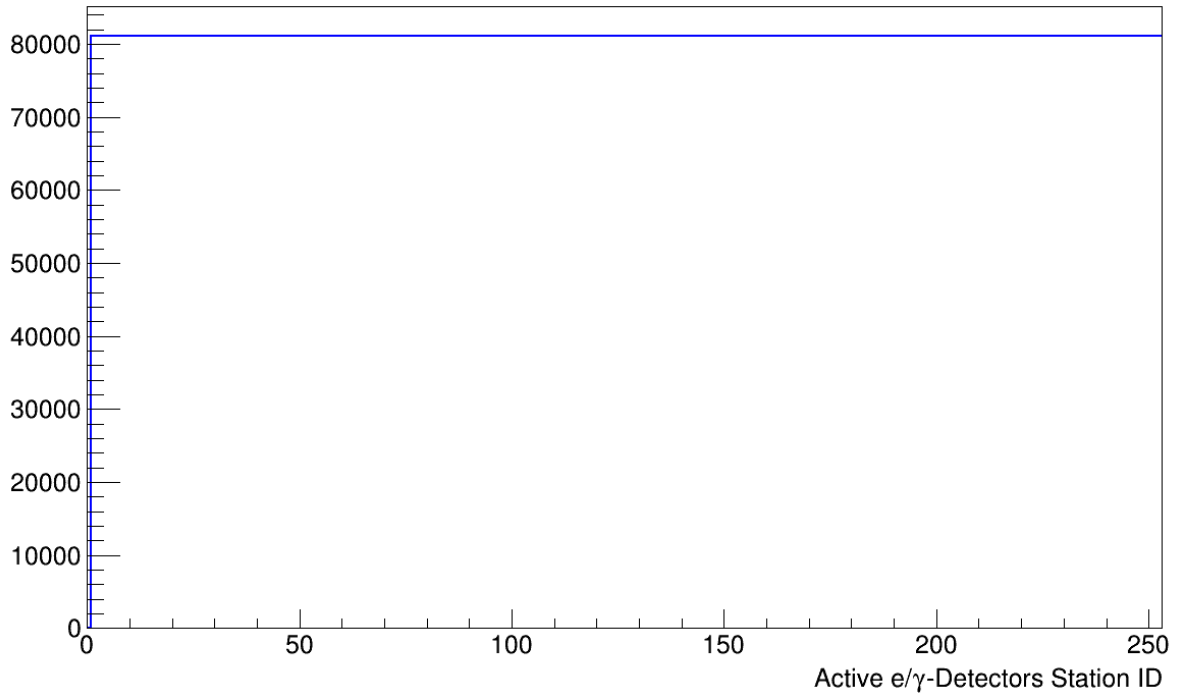


Fig. 4.1.3 *Distribution of station IDs for active e/γ-detector stations*

For further studies the effective e/γ-detector area for a given station can be derived from the station ID. As described in chapter 2 of the KCDC-Manual two different detector setups are realised in the KASCADE array. The inner 4 clusters consist of only 15 stations, (the 16th position is blocked by the Central Calorimeter) and are equipped with 4 liquid scintillator cones with an effective area of 3.14m² to measure the shower core. The outer 12 cluster have two liquid scintillation e/γ-detectors with an effective area of 1.57m² (see fig. 4.1.4). The table below shows the correlation between station ID and effective detector area.

Station ID	Area [m ²]	Area Code
1 - 80	1.57	0
81 - 110	3.14	1
111 - 142	1.57	0
143 - 172	3.14	1
173 - 252	1.57	0

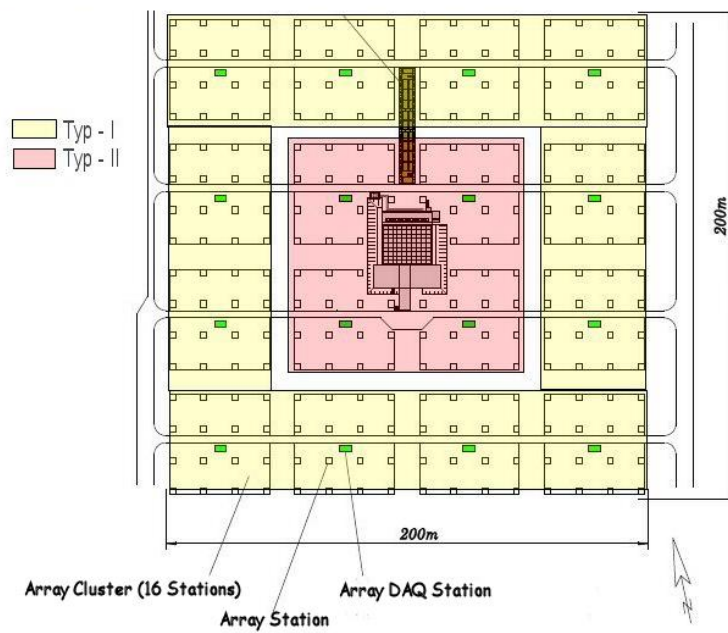


Fig. 4.1.4 *Array setup; schematic view of the KASCADE detector array*
yellow: two e/γ-detectors, 1.57m²; red: four e/γ-detectors, 3.14m² per station;

4.1.5 EXAMPLE

As an example for energy deposits in the KASCADE array the **EDeposit** distribution of two events is shown in fig. 4.1.5. The warmer the color the higher the deposited energy in the 252 e/γ-detector stations.

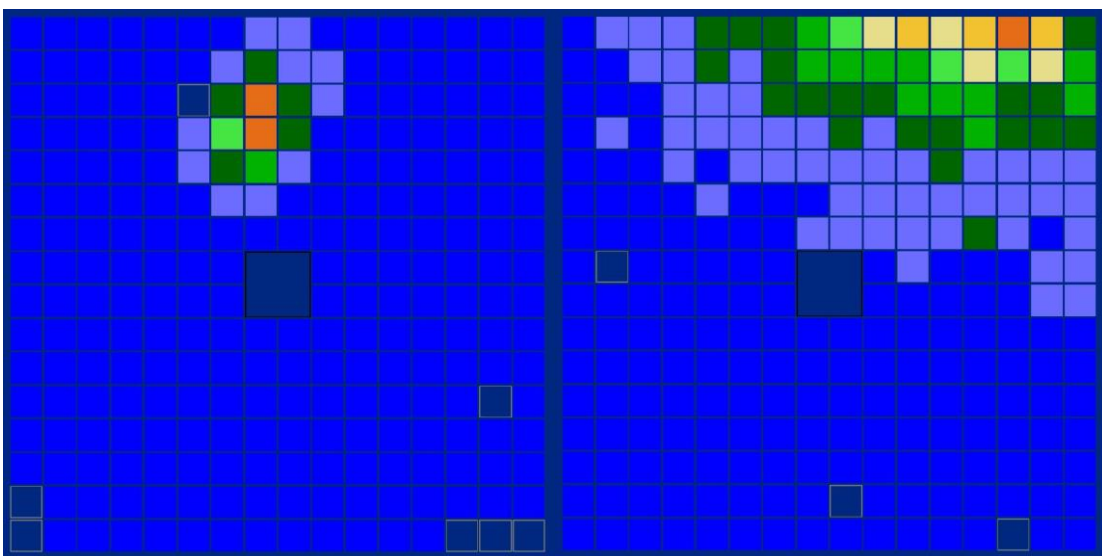


Fig. 4.1.5 *Two examples of e/γ-energy deposits in the KASCADE array*

4.2 MUON – ENERGY DEPOSITS

Handling the ‘**Muon Energy Deposits**’ quantity mostly requires some additional information either on the absolute coordinates of the detector station or on the distance to the reconstructed shower core. Therefore, the quantity **MDepositS** is always supplied with the Energy Deposit values. For simulations, all stations are always active which implies that the number of detector stations with valid energy deposit information (**MDepositN**) is always 192.

Thus, you will always be supplied with the following data sets:

MDepositN	number of active μ -detector stations with energy deposit ≥ 0
MDeposit	muon energy deposit per station in MeV
MDepositS	detector station ID [1 ... 252]

4.2.1 NUMBER OF ACTIVE μ -DETECTOR STATIONS (MDEPOSITN)

For simulations, all μ -detector stations are always active which implies that the number of stations with valid energy deposit information (**MDepositN**) is always 192. As the detector station IDs are the same as for the e/γ -energy deposits, the range of the IDs is up to 252 because the four inner cluster (64 stations) are not equipped with μ -detectors.

Note: This value is always shipped with the ‘Muon Energy Deposit’ Quantity in the root files.

4.2.2 NUMBER OF E/γ -DETECTOR STATIONS WITH HITS

The distribution of the number of μ -detectors with energy deposit $MDeposit > 0$ in this event is given in fig 4.2.1.

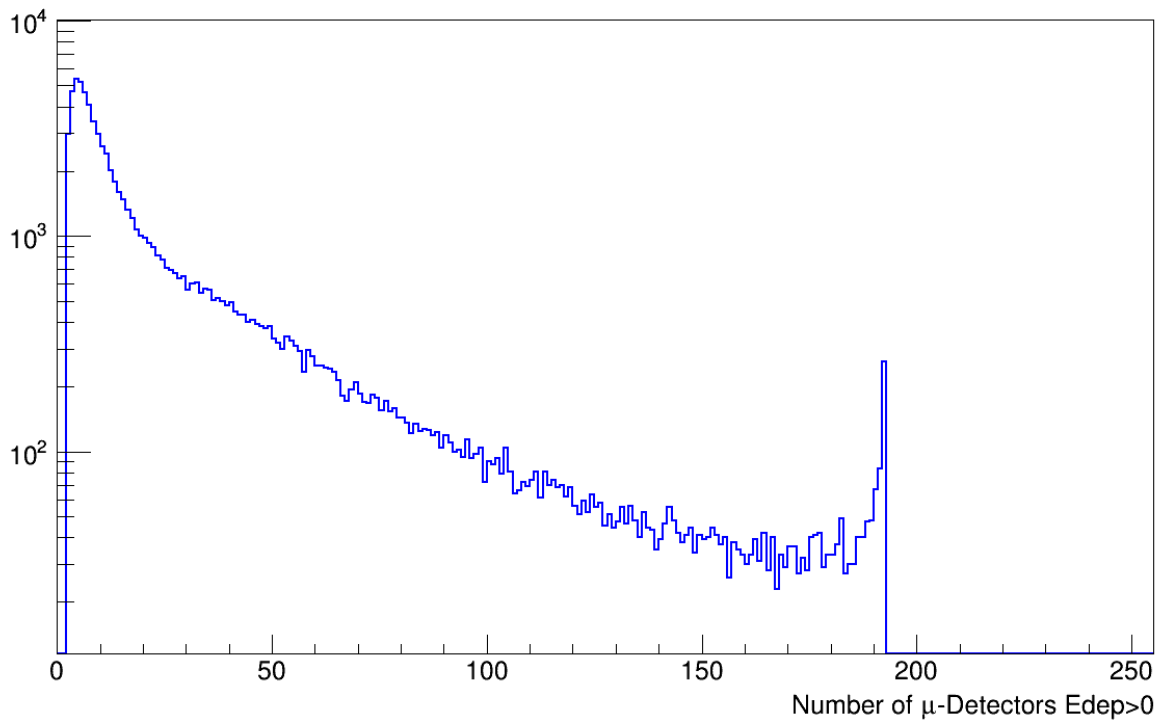


Fig. 4.2.1 *Distribution of the number of μ -detector stations with hits*

4.2.3 μ -ENERGY DEPOSIT VALUE FOR EACH DETECTOR STATION (MDEPOSIT)

The Energy deposits are directly taken from the simulations for each detector station. **MDeposit** values are given in MeV. In fig 4.2.2 the energy deposits for simulated proton induced showers are plotted. The overflow cut is set to 400 MeV.

Note: Muon energy deposits within a 40m radius around the reconstructed shower core are usually not used for data analysis because of the saturation and the punch through effects, which cannot be estimated, but is included in the simulation data sets.

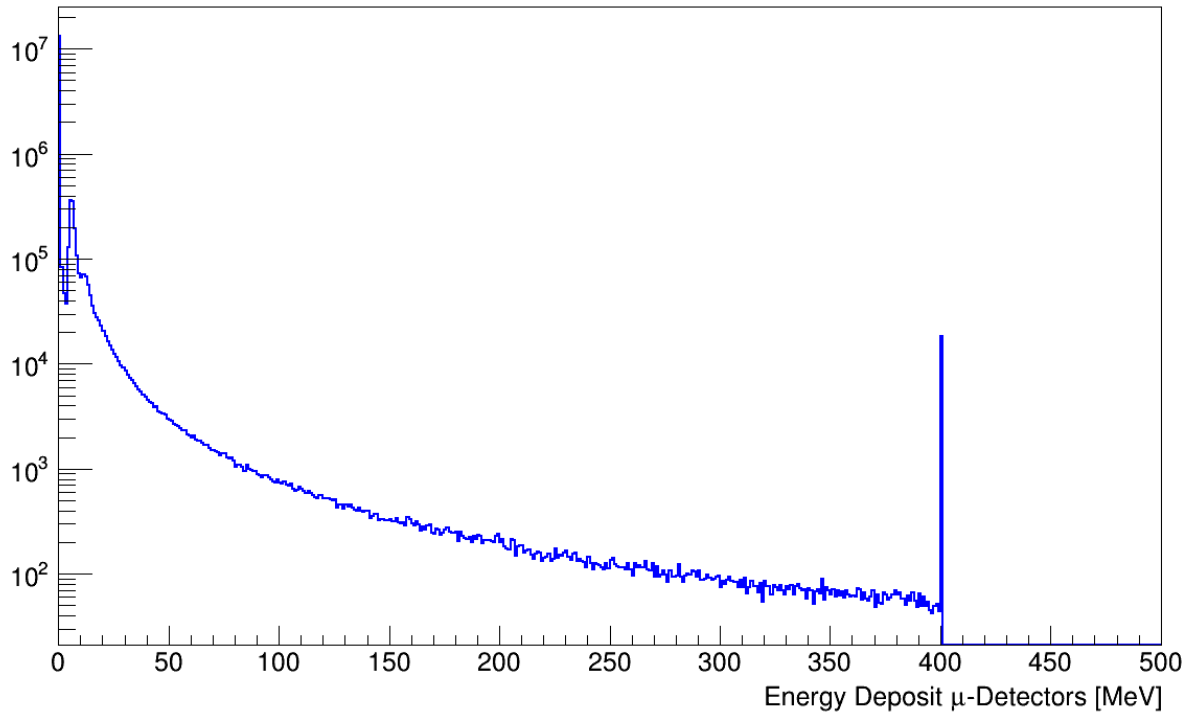


fig. 4.2.2 *Distribution of the μ -energy deposits of all active stations*

4.2.4 STATION ID (MDEPOSITS)

The *station ID* (same as for e/γ -detectors in 4.1.4) holds the information of the location of the respective detector station. The transformation from the *station ID* to the KASCADE coordinates of the respective Array detector station is in detail described in chapter 7.3 and Appendix A.

Fig 4.2.3 shows the distribution of station IDs of the active μ -detector stations. The two regions not populated represent the 4 inner array clusters, which are not equipped with μ -detectors (see KCDC-Manual, chapter 2.2). The otherwise flat distribution in the simulation is due to the fact, that there are no inactive stations in simulations. Stations with energy deposits above 400 MeV and stations within a 40m radius from the shower core are not taken into account for the analysis but are included in the data sample.

The effective μ -detector area for all 192 stations is 3.24 m² (yellow area in fig 4.1.4).

Note: This value is always shipped with the 'Muon Energy Deposit' Quantity in the root files.

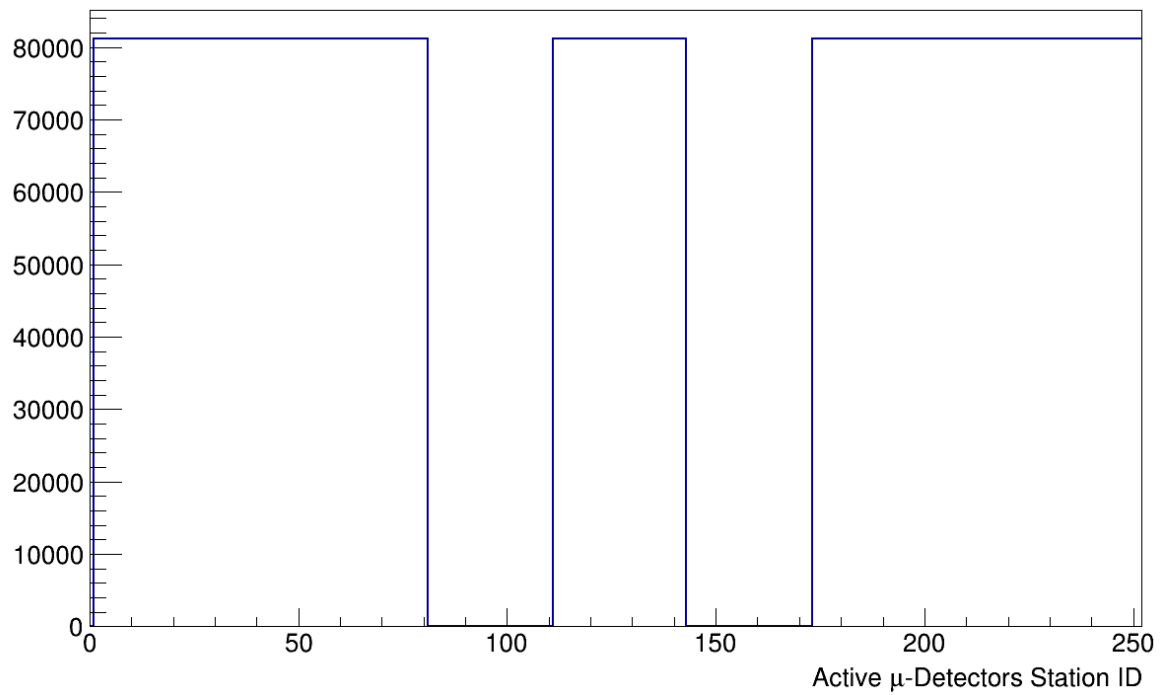


Fig. 4.2.3 *Distribution of station IDs for active μ -detector stations*

4.2.5 EXAMPLE

As an example for energy deposits in the KASCADE array the **MDeposit** distribution of two events is shown in fig. 4.2.4. The warmer the color the higher the deposited energy in the 192 μ -detector stations.

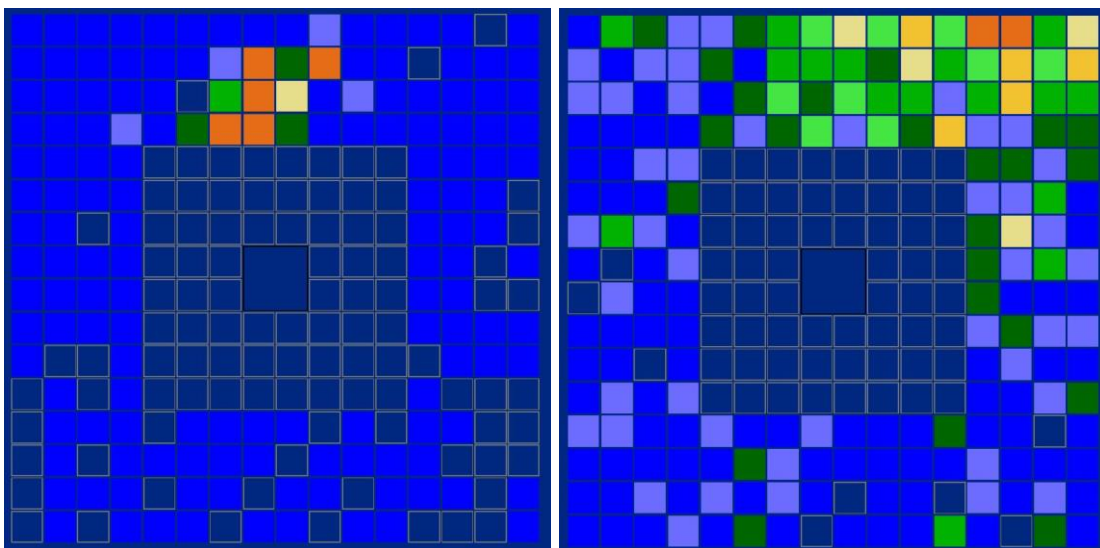


Fig. 4.2.4 *Two examples of μ -energy deposits in the KASCADE array*

4.3 ARRIVAL TIMES

In the measurement the ‘Arrival Times’ of each COMBINED detector station represents the first time stamp of each station that has been hit by a charged particle corrected for cable delays and electronic effects. Basically, the same applies in simulations but no further corrections are necessary. The first signals of each station represent the shower front and are used to determine the shower direction. The values of the arrival times are taken only from the e/γ -detectors.

A detector station that did not provide any time information was treated as ‘silent station’. Only arrival times and station IDs for non-silent stations are included in the data sets.

Handling the ‘Arrival Times’ quantity mostly requires some additional information either on the absolute coordinates of the detector station or on the distance to the reconstructed shower core. Therefore the quantity **Arrivals** is always supplied with the times values. Furthermore, the number of detector stations with valid arrival time information (**ArrivalN**) is provided as well.

Note: in chapter 7.2 are examples on how to handle the quantity ‘Arrival Times’

Thus, you will always be supplied with the following data sets:

ArrivalN	number of active e/γ -detectors for this event (0 ... 252)
Arrival	Arrival time in [ns] bins
Arrivals	detector station ID [1...252]

4.3.1 NUMBER OF DETECTOR STATIONS WITH VALID ARRIVAL TIMES (ARRIVALN)

The range of **ArrivalN** is between about 40 and 252. The distribution is shown in fig.4.3.1.

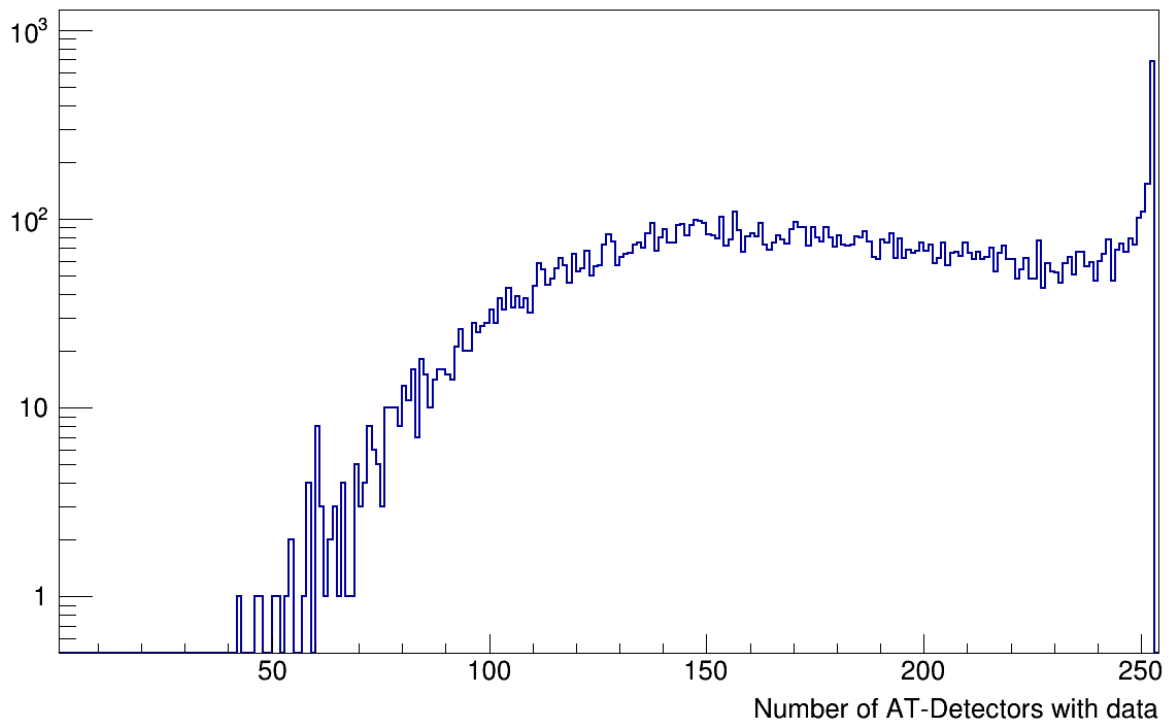


Fig. 4.3.1. *Distribution of the true number of detector stations with 'Arrival Time' information*

4.3.2 ARRIVAL TIMES PER STATION (ARRIVAL)

The arrival times are given with a resolution of 1ns/bin. Fig 4.3.2 shows the 'arrival time'–distribution. In the measurements, the values of the arrival times can as well be negative due to the fact that the reference to calculate the individual time stamps is not the first signal above a certain threshold but the time of coincidence that matches the trigger condition set in the hardware. In simulations only positive values are possible for COMBINED because the first time stamp is always taken as trigger signal at time '0 ns' or '1 ns'. This is the reason for the sharp peak at the beginning of the spectrum. At higher Energies there will be no significant change in the shape of the spectrum compared to the measurements as indicated in the red curve of fig. 4.3.2 where a cut as been applied on $N_e > 500000$.

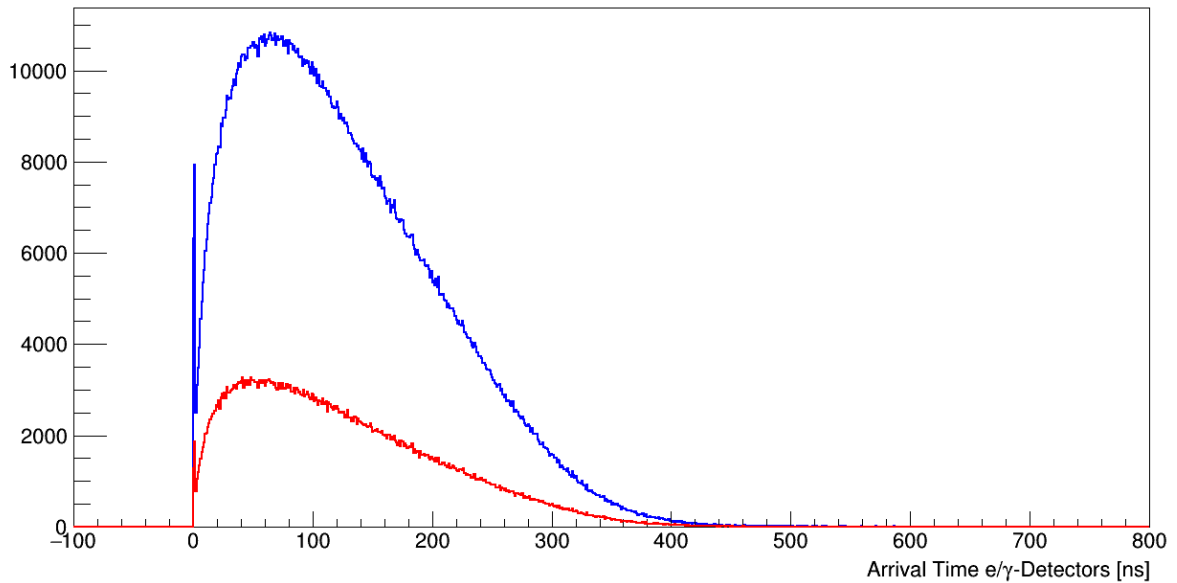


Fig. 4.3.2. *Arrival time distribution; no N_e cuts (blue); $N_e > 500000$ (red)*

4.3.3 STATION ID (ARRIVALS)

The station ID (same as in 4.1.4) holds the information of the location of the respective detector station. The transformation from the *station ID* to the KASCADE coordinates of the respective Array detector station is in detail described in chapter 7.3 and Appendix A.

Fig 4.3.3 shows the distribution of station IDs of the active e/γ -detector stations. The two regions with the higher population mark the four inner clusters, which have a detection area twice the size of the outer 12 clusters.

Note: This value is always shipped with 'Arrival Times' Quantity in the root files.

Reconstruction of Simulated KASCADE Data in KCDC

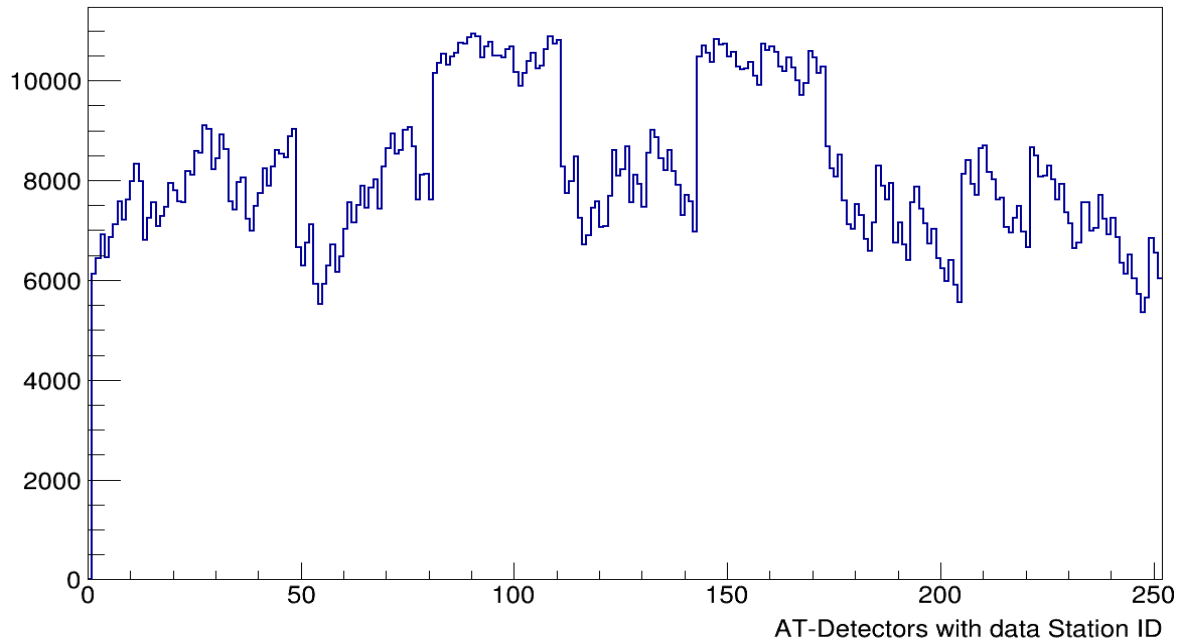


Fig.4.3.3. *Distribution of station IDs for e/ γ -detector stations with valid Arrival Times*

4.3.4 EXAMPLE

As an example for the arrival time in the KASCADE array the **Arrival** distribution of two events is shown fig 4.3.4. The warmer the color the bigger the time difference which usually corresponds to larger zenith angles. In the left example, the shower is coming roughly from $Az \sim 220^\circ$, in the right example from $Az \sim 320^\circ$.

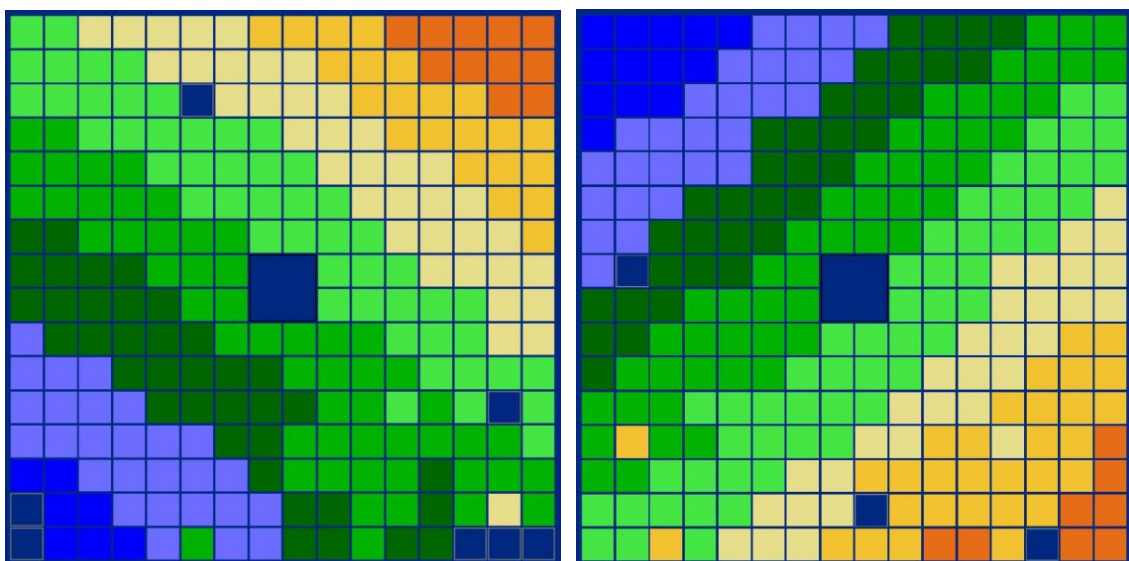


Fig. 4.3.4 *Two example of an arrival time distributions of the e/ γ -detectors in KASCADE*

4.4 RUN NUMBER & EVENT NUMBER

Run Number and **Event Number** are two parameters that characterise an event uniquely. They will always be supplied with the data sets.

While the run number is a rather random number for simulations, the Event Number starts at '1' with each run and is increased with every simulated shower.

5 RECONSTRUCTION OF SIMULATED GRANDE DATA IN KCDC

With the release of the COMBINED analysis, we publish the two data arrays from GRANDE, the energy deposits of the charged particles and the arrival times per station as given by the reconstruction program KRETA (*Kascade Reconstruction for ExTensive Air showers*).

GRANDE Quantity	Description	Unit	ID
Reconstructed Data			
Energy Deposits	charged energy deposit per GRANDE detector station	(MeV)	GDeposit
Arrival Times	Arrival Times per GRANDE detector station	(ns)	GArrival

In simulations, every shower has been thrown 10 times on GRANDE (COMBINED), randomly distributed on an area of 750x790m² as shown in fig 3.0.1.

The plots shown in this chapter are only examples, mostly based on a subsample of the simulated data sets and only for one simulation model (QGSjet-II-04). So, applying user cuts in your own analysis can change these spectra drastically.

5.1 GRANDE ENERGY DEPOSITS PER STATION (GDEPOSIT)

The energy deposits of each single detector station are simulated and reconstructed in the 37 GRANDE detectors.

Detector stations that had no signal above the threshold are as well taken into account. The energy value of these ‘silent’ stations is set to ‘0’.

Note: in chapter 7.4 are examples on how to handle the quantity ‘GRANDE Energy Deposit’

Handling the ‘**GRANDE Energy Deposits**’ quantity mostly requires some additional information either on the absolute coordinates of the detector station or on the distance to the reconstructed shower core. Therefore, the quantity **GDepositS** is always supplied with the energy values. For simulations, all stations are always active which implies that the number of detector stations with valid energy deposit information (**GDepositN**) is always 37.

Thus, you will always be supplied with the following data sets:

GDepositN	number of active GRANDE detector stations with energy deposit ≥ 0
GDeposit	energy deposit per station in MeV
GDepositS	detector station ID [1...37]

5.1.1 NUMBER OF ACTIVE GRANDE DETECTOR STATIONS (GDEPOSITN)

The number of active GRANDE detector stations stored in **GDepositN** is always 37 in simulations.

Note: This value is always shipped with ‘Grande Energy Deposit’ Quantity in the root files.

5.1.2 NUMBER OF ACTIVE GRANDE DETECTOR STATIONS WITH HITS

The distribution of the number of GRANDE detectors with $GDeposit > 0$ is given in fig 5.1.1.

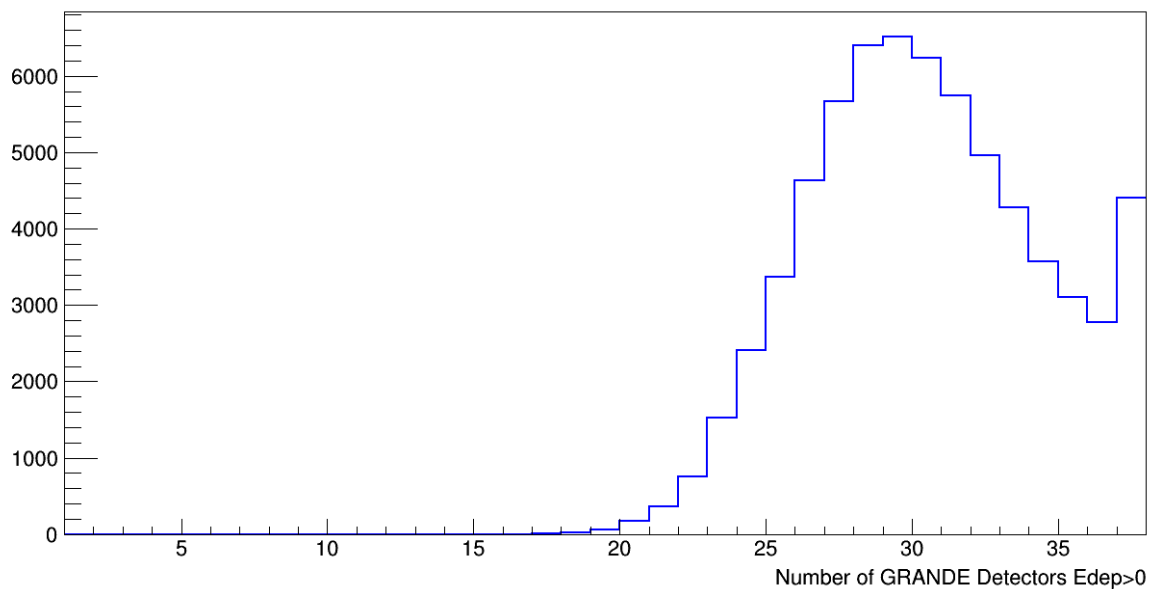


Fig. 5.1.1 *Distribution of the true number of GRANDE detector stations with hits*

5.1.3 GRANDE ENERGY DEPOSIT FOR EACH DETECTOR STATION (GDEPOSIT)

The energy deposits are directly taken from the simulations for each GRANDE detector station. **GDeposit** values are given in MeV. In fig 5.1.2, the energy deposits for simulated proton induced showers are plotted. The overflow cut is set to 90 GeV.

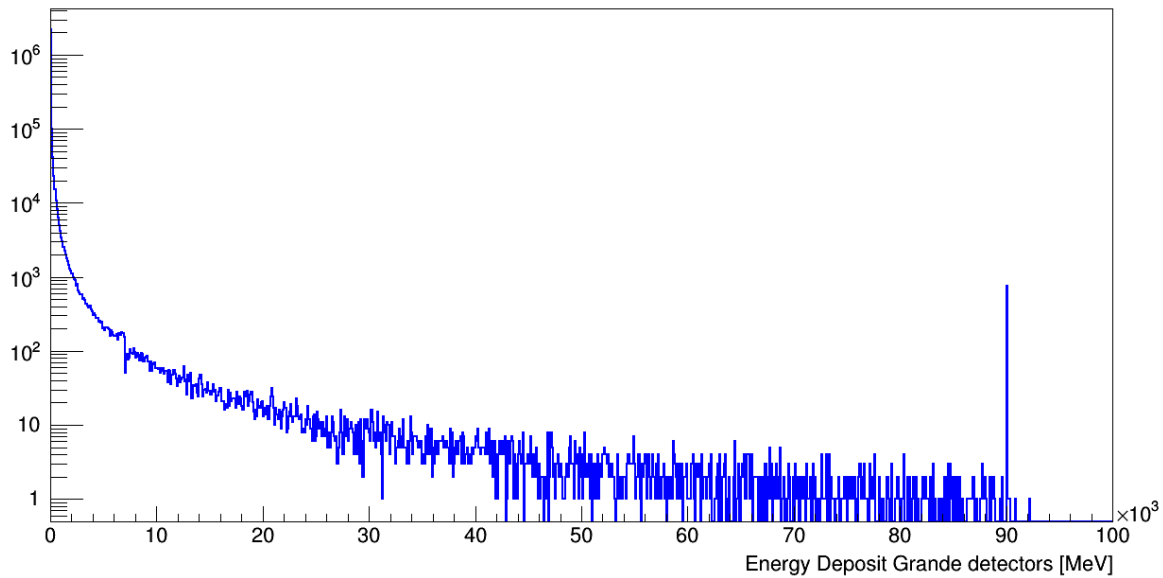


Fig. 5.1.2 *Distribution of the GRANDE Energy Deposits of all active stations*

5.1.4 GRANDE STATION ID (GDEPOSITS)

The station ID holds the information of the location of the respective detector station. The transformation from the station ID to the true detector position in KASCADE coordinates of the respective GRANDE detector station is in detail described in chapter 7.4 and Appendix B.

Fig 5.1.3 shows the distribution of station IDs of the active GRANDE detector stations. The distribution is flat for simulations because we do not include inactive stations in our detector simulations. Stations with energy deposits above 90 GeV are active too, the deposits are not taken into account for analysis but are included in the data samples.

Note: This value is always shipped with 'Grande Energy Deposit' Quantity in the root files.

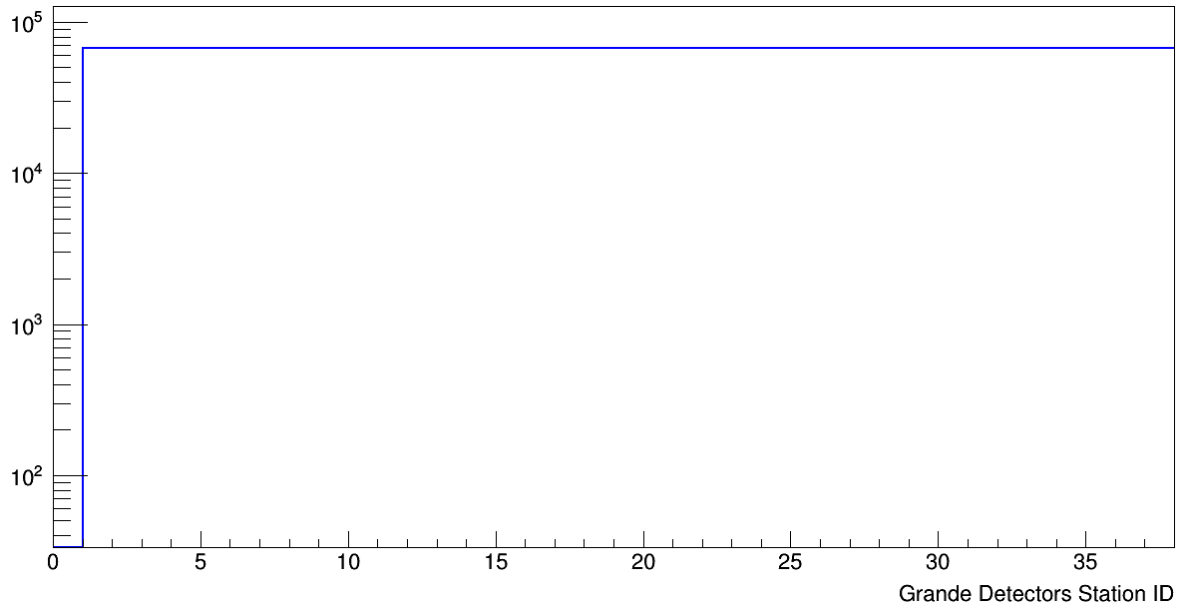


Fig. 5.1.3 *Distribution of station IDs for e/γ-detector stations*

5.1.5 EXAMPLE

As an example for energy deposits in the GRANDE array the **GDeposit** distribution of two events is shown in fig. 5.1.4. The warmer the color the higher the deposited energy in the 37 GRANDE detector stations.

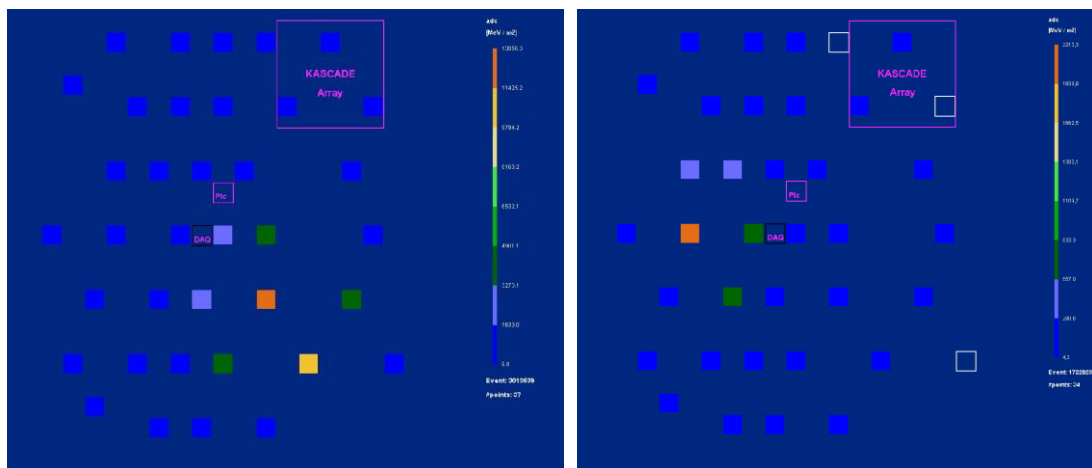


fig. 5.1.4 *Two examples of energy deposits in the GRANDE array*

5.2 ARRIVAL TIMES

In the measurement the '**Grande Arrival Times**' of each GRANDE array station represents the first time stamp of each station that has been hit by a charged particle corrected for cable delays and electronic effects. Basically the same applies in simulations but no further corrections are necessary. The first signals of each station represent the shower front and are used to determine the shower direction.

The quantity '**GRANDE Arrival Time**' offers the possibility to reconstruct the shower disc and the arrival direction of the extensive air shower that hit GRANDE.

A detector station, which did not provide any time information, was treated as 'silent station'. Only arrival times and station IDs for non-silent stations are included in the data sets.

Handling the '**GArrival**' quantity mostly requires some additional information either on the absolute coordinates of the detector station or on the distance to the reconstructed shower core. Therefore the quantity **GArrivals** is always supplied with the times values. Furthermore, the number of detector stations with valid arrival time information (**GArrivalN**) is provided as well.

Note: in chapter 7.2 are examples on how to handle the quantity 'Grande Arrival Times'

Thus, you will always be supplied with the following data sets:

GArrivalN	number of GRANDE detector stations with arrival times [1 ... 37]
GArrival	Arrival time in [ns] bins
GArrivals	detector station ID [1...37]

5.2.1 NUMBER OF GRANDE DETECTOR STATIONS WITH VALID ARRIVAL TIMES (GARRIVALN)

The distribution of **GArrivalN** is shown in fig. 5.2.1.

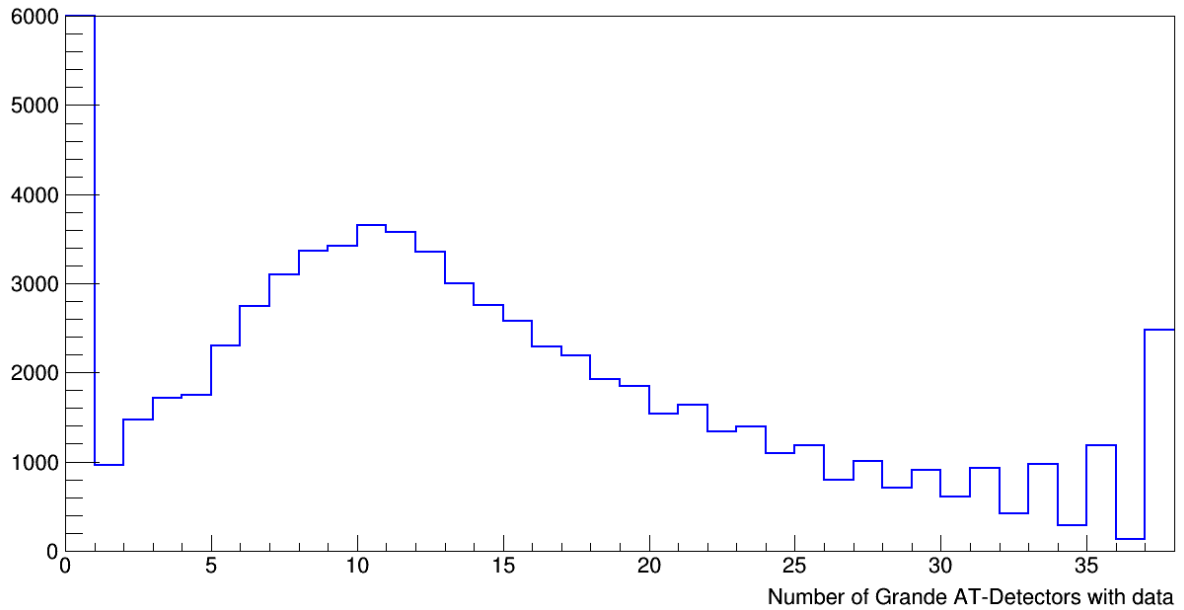


Fig. 5.2.1. *Distribution of the number of GRANDE detector stations with reconstructed 'Arrival Times' information*

5.2.2 ARRIVAL TIMES PER GRANDE STATION (GARRIVAL)

The '**GRANDE Arrival Times**' are given with a resolution of 1ns/bin. Fig 5.2.2 shows the 'Grande Arrival Time' distribution.

In the measurements, the values of the '**GArrival**' can cannot be negative due to the fact that the delay for trigger coincidence is rather high because of the long distances between the Grande detectors. In simulations, negative values are possible for GRANDE because the event time is taken from the first 7/7- coincidence and earlier time stamps in the stations within the respective trigger hexagon are possible.

This effect is illustrated by the red curve where only showers with a reconstructed zenith angle below 15° are plotted while the green curve denotes showers with zenith angles above 20° .

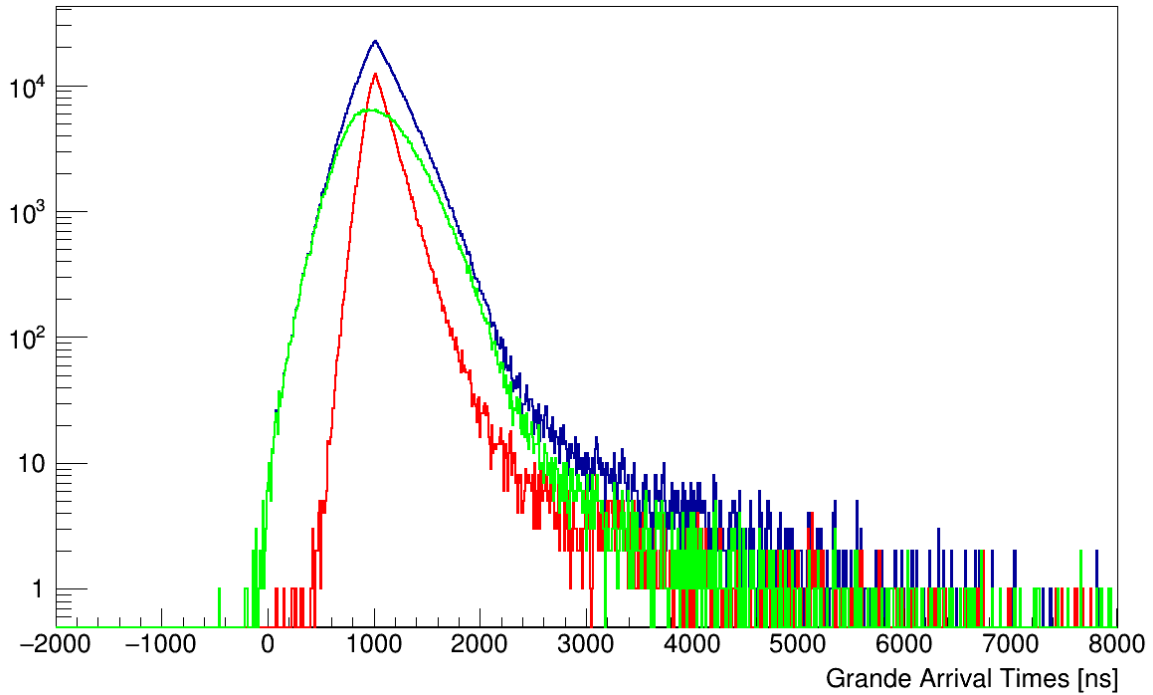


Fig. 5.2.2 *GRANDE Arrival time distribution; no cuts (blue); $Z_e < 15^\circ$ (red); $Z_e > 20^\circ$ (green):*

5.2.3 GRANDE STATION ID (GARRIVALS)

The GRAND station ID (same as 5.1.4) holds the information of the location of the respective detector station. The transformation from the station ID to the GRANDE coordinates of the respective Grande detector station is in detail described in chapter 7.4 and Appendix B. Fig 5.2.3 shows the distribution of station IDs of the GRANDE detector stations with AT information. The structure is mostly caused by the area cut for the effective area in the core position of the GRANDE showers.

Note: This value is always shipped with the 'GRANDE Arrival Times' in the root files.

Reconstruction of Simulated GRANDE Data in KCDC

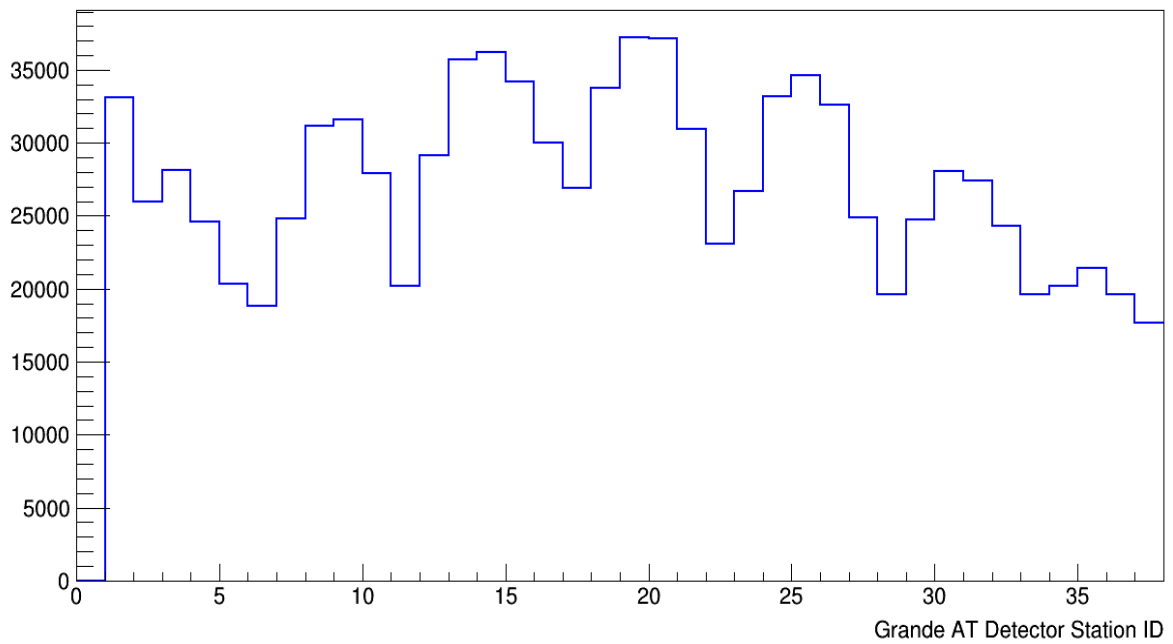


Fig. 5.2.3 *Distribution of station IDs for GRANDE detector stations with valid arrival times*

5.2.4 EXAMPLE

As an example for the arrival times in GRANDE the **GArrival** distribution of two events is shown in fig. 5.2.4. The warmer the color the bigger the time difference which usually corresponds to larger zenith angles.

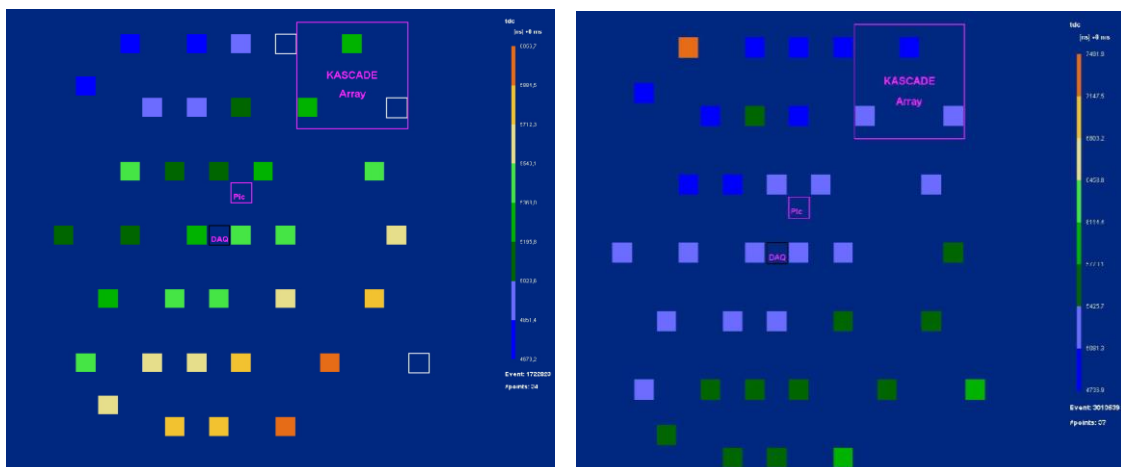


Fig. 5.2.4 *Two examples of arrival time distributions in GRANDE*

6 SIMULATION DATA IN KCDC

The CORSIKA simulation package offers a variety of information describing the real shower development and the secondary particles at observation level. Some of these data like the primary particle initiating the shower or its energy are passed through the analysis steps of event simulation (CORSIKA), detector simulation (CRES) and data reconstruction (KRETA) and stored in the respective ROOT trees.

From all available observables taken directly from the simulations we choose 10 to be published in KCDC called ‘Monte Carlo Information’.

All these numbers are true only for the observation level, latitude and longitude of KASCADE.

Monte Carlo Information			
True Energy	True Primary Energy inducing the shower	<i>eV</i>	<i>TrEP</i>
True Particle ID	True Primary Particle ID inducing the shower		<i>TrPP</i>
True X Core Position	True location of the simulated shower core x-position	<i>m</i>	<i>TrXc</i>
True Y Core Position	True location of the simulated shower core y-position	<i>m</i>	<i>TrYc</i>
True Zenith Angle	True simulated zenith angle with respect to the vertical	<i>° (degree)</i>	<i>TrZe</i>
True Azimuth Angle	True simulated azimuth angle with respect to north	<i>° (degree)</i>	<i>TrAz</i>
True Number of Electrons	True simulated number of electrons at observation level	<i>(number of)</i>	<i>TrNe</i>
True Number of Muons	True simulated number of Muons at observation level	<i>(number of)</i>	<i>TrNm</i>
True Number of Photons	True simulated number of Photons at observation level	<i>(number of)</i>	<i>TrNg</i>
True Number of Hadrons	True simulated number of Hadrons at observation level	<i>(number of)</i>	<i>TrNh</i>

The plots shown in this chapter are only examples, mostly based on a subsample of the simulated data sets and only for one simulation model (QGSjet-II-04). So, applying user cuts in your own analysis can change these spectra drastically.

6.1 TRUE PRIMARY ENERGY (TREP)

The energy of the particle inducing the air shower is an input for the CORSIKA air shower simulation code. In our case, we simulated showers with a primary energy following a power law spectrum with a slope of '-2':

$$dN/dE_0 \propto E_0^{-2}$$

As the real spectral index is about '-2.7', the spectral index of '-2' is a compromise. Simulating with the correct spectral index requires many simulated showers at low energies to get enough statistics at highest energies, which is in our case 10^{18} eV, with the advantage that nearly no corrections would be necessary. On the other hand the spectral index of '-2' reduces the simulation time and the disk spaces required at the expense of complex corrections being applied during data analysis.

Fig. 6.1.1 shows the input energy spectrum for a standard simulation set of the showers reconstructed by KRETA for the COMBINED detector (red) together with the respective input spectrum from CORSIKA without any cuts (black). The difference is caused by the quality cuts applied. The deviation from linearity starts around $5 \cdot 10^{15}$ eV (red curve) which denotes that the reconstruction algorithm is not fully efficient below that energy.

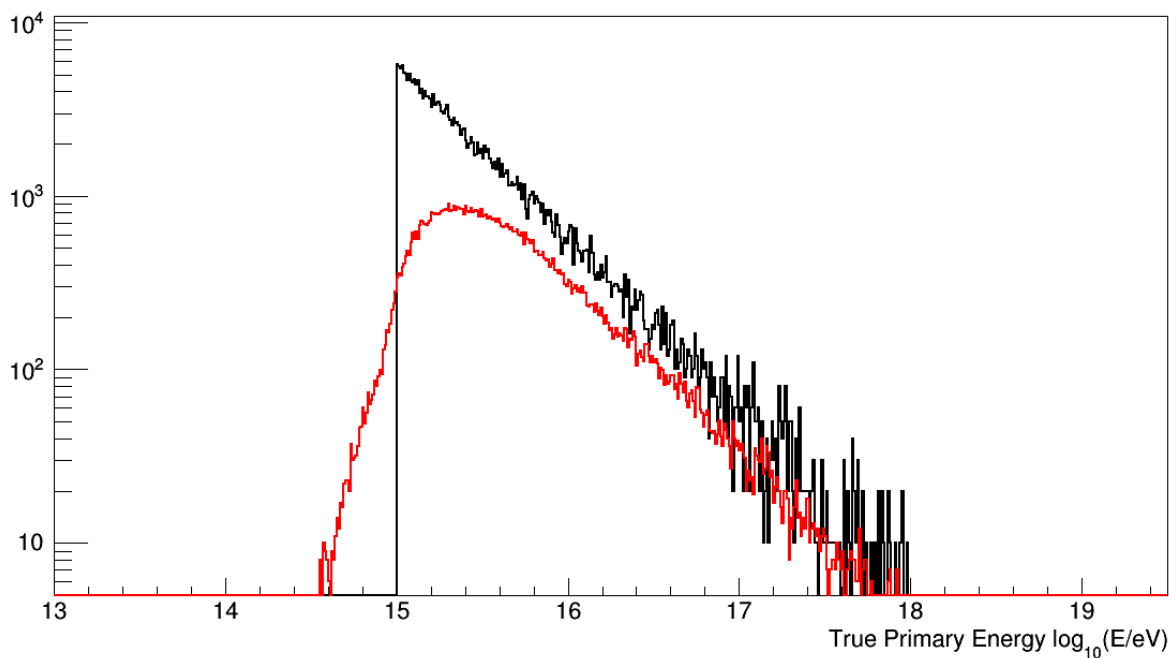


Fig. 6.1.1 *Spectrum of the true energy of incident particles in $[\log_{10}]$ eV simulated for COMBINED : red: ; simulations without cuts: black*

6.2 TRUE PRIMARY PARTICLE ID (TRPP)

The ID of the particle inducing the air shower is an input for the CORSIKA air shower simulation code. We simulated 5 primaries representing 5 different mass groups and photons. These primaries and their respective IDs are:

proton	ID= 14	representing the lightest mass
helium	ID= 402	representing a light mass group
carbon	ID= 1206	representing the CNO-group
silicon	ID= 2814	representing a medium heavy mass group
iron	ID= 5626	representing the heaviest mass
gamma	ID= 1	representing the photons

6.3 TRUE SHOWER DIRECTION (TRZE, TRAZ)

The zenith angle and the azimuth angle of the incident particles are input parameters for the CORSIKA air shower simulation code. The zenith angle spectrum reaches from 0° to 42° in simulation with the shape shown in fig. 6.3.1. The zenith angle is selected at random in this interval to match equal particle fluxes from all solid angle elements of the sky and a registration by a horizontal flat detector arrangement.

As we use the same reconstruction algorithm for simulations and for measured data where the fit parameters are only fine-tuned up to about 30°, the zenith angle range is limited in simulations too.

Fig. 6.3.1 shows the zenith angle spectrum for a standard simulation set of the showers reconstructed by KRETA for the COMBINED detector (red) together with the input spectrum from CORSIKA (black). The differences are caused by the quality cuts applied.

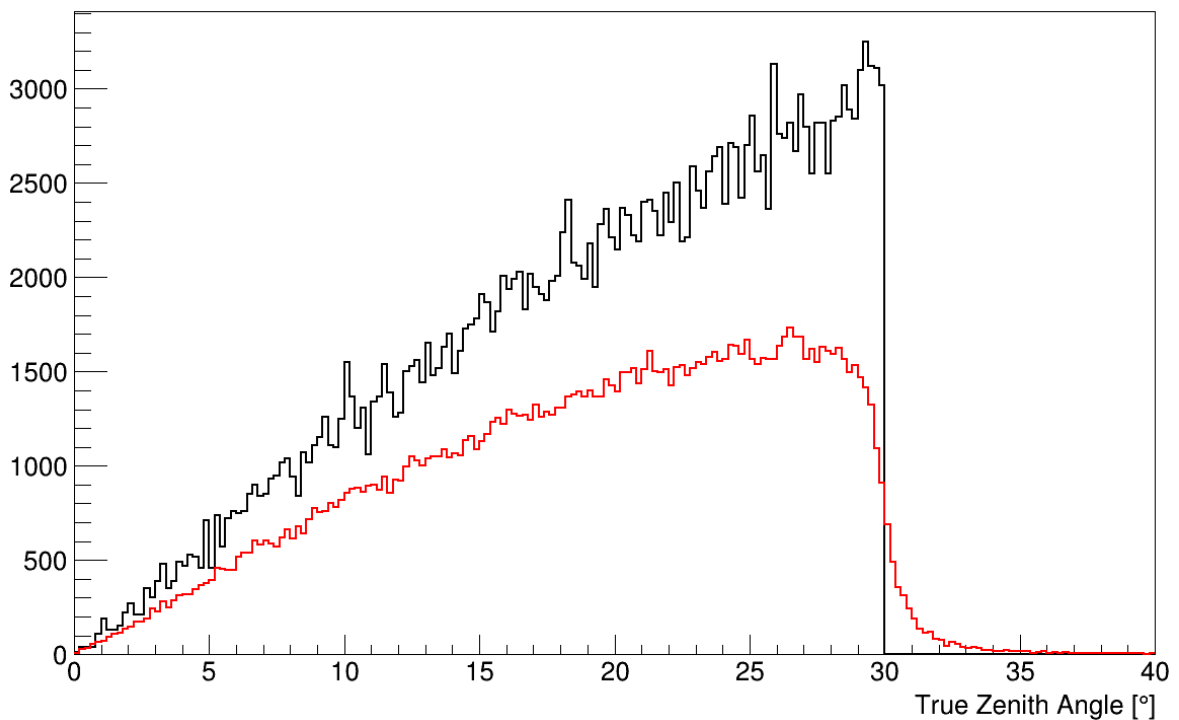


Fig. 6.3.1 *Spectrum of the true zenith angle of the incident particles in [°] simulated for COMBINED: red; ; simulations without standard quality cuts: black*

The azimuth angle is always simulated between 0° and 360° where for $\Phi = 0^\circ$ the shower axis points to the North, $\Phi = 90^\circ$ it points to the East. Fig. 6.3.2 shows the azimuth angle spectrum for a standard simulation set of the showers reconstructed by KRETA for the detector component COMBINED (red) and the input spectrum from CORSIKA (black). The differences are caused by the quality cuts applied.

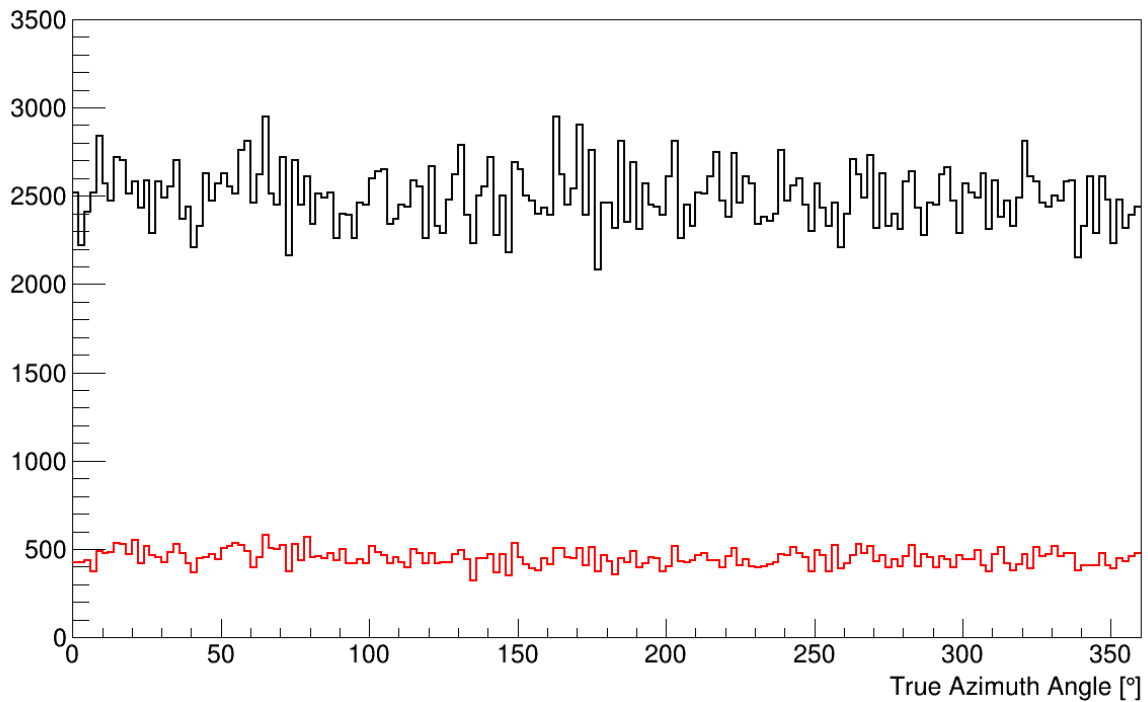


Fig. 6.3.2 *Spectrum of the true azimuth angle of the incident particles in [°] simulated for COMBINED: red; ; simulations without standard quality cuts: black*

6.4 TRUE NUMBERS OF ELECTRONS (TRNE)

The **true number of electrons** is derived from the CORSIKA output as the number of electrons at the observation level of KASCADE at 110 m asl. Only electrons above 3 MeV low energy cut-off are taken into account.

Fig 6.4.1 shows the N_e spectra for the 5 different mass groups simulated, proton (blue), helium (purple), carbon (black), silicon (green), iron (red) and for photons (light blue).

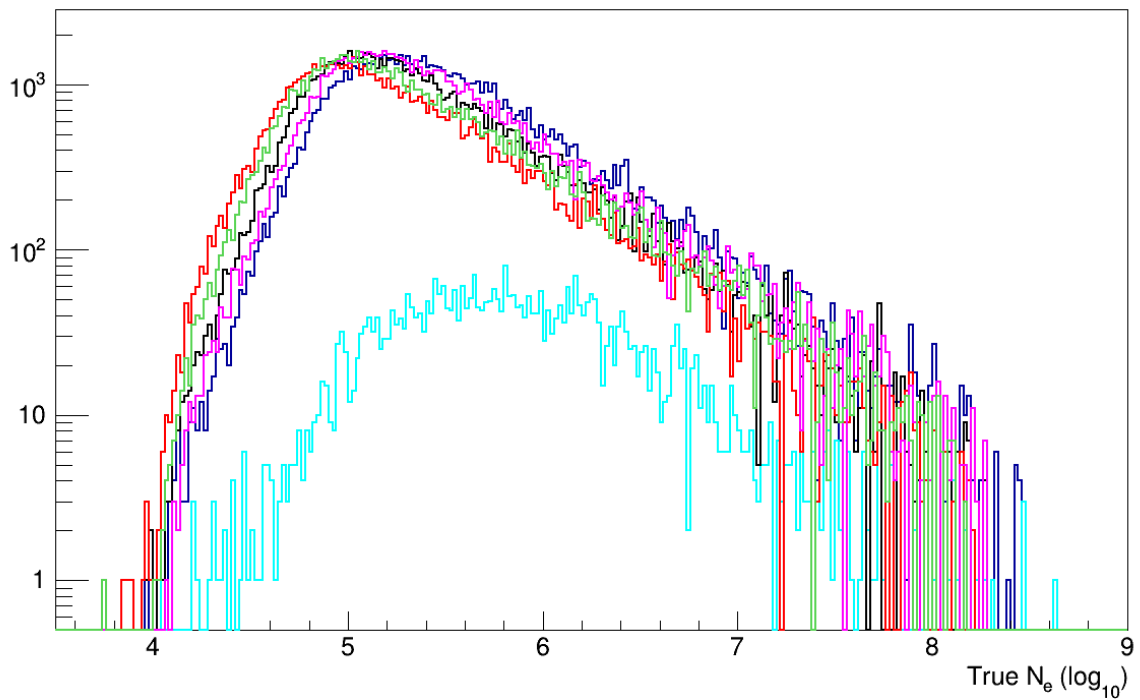


Fig. 6.4.1 *Spectrum of the number of electrons at observation level of KASCADE; simulated are: proton (blue), helium (purple), carbon (black), silicon (green), iron (red) and photons (light blue).*

6.5 TRUE NUMBERS OF MUONS (TRNM)

The **true number of muons** is derived from the CORSIKA output as the number of muons at the observation level of KASCADE at 110 m asl. Only muons above 100 MeV low energy cut-off are taken into account.

Fig 6.5.1 shows the N_μ spectra for the 5 different mass groups simulated, proton (blue), helium (purple), carbon (black), silicon (green), iron (red) and for photons (light blue).

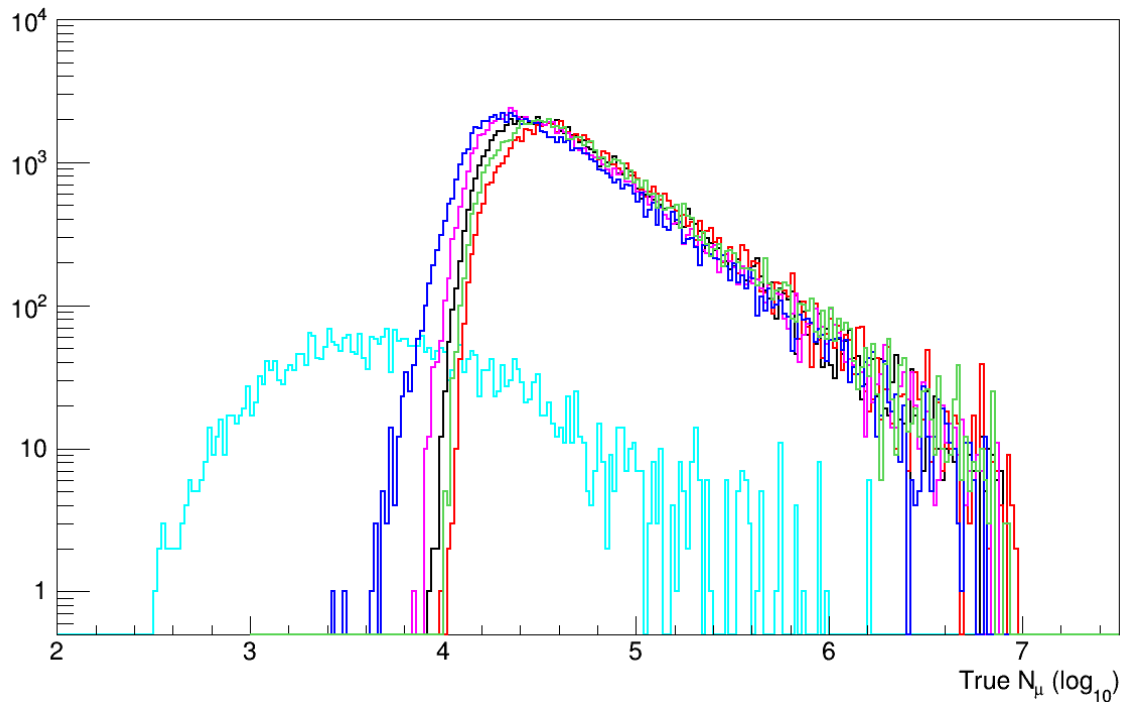


Fig. 6.5.1 *Spectrum of the number of muons at observation level of KASCADE; simulated are: proton (blue), helium (purple), carbon (black), silicon (green), iron (red) and photons (light blue).*

6.6 TRUE NUMBERS OF PHOTONS (TRNP)

The **true number of photons** is derived from the CORSIKA output as the number of photons and π^0 at the observation level of KASCADE at 110 m asl. Only photons and π^0 above 3 MeV low energy cut-off are taken into account.

Fig 6.6.1 shows the $\gamma + \pi^0$ spectra for the 5 different mass groups simulated, proton (blue), helium (purple), carbon (black), silicon (green), iron (red) and photons (light blue).

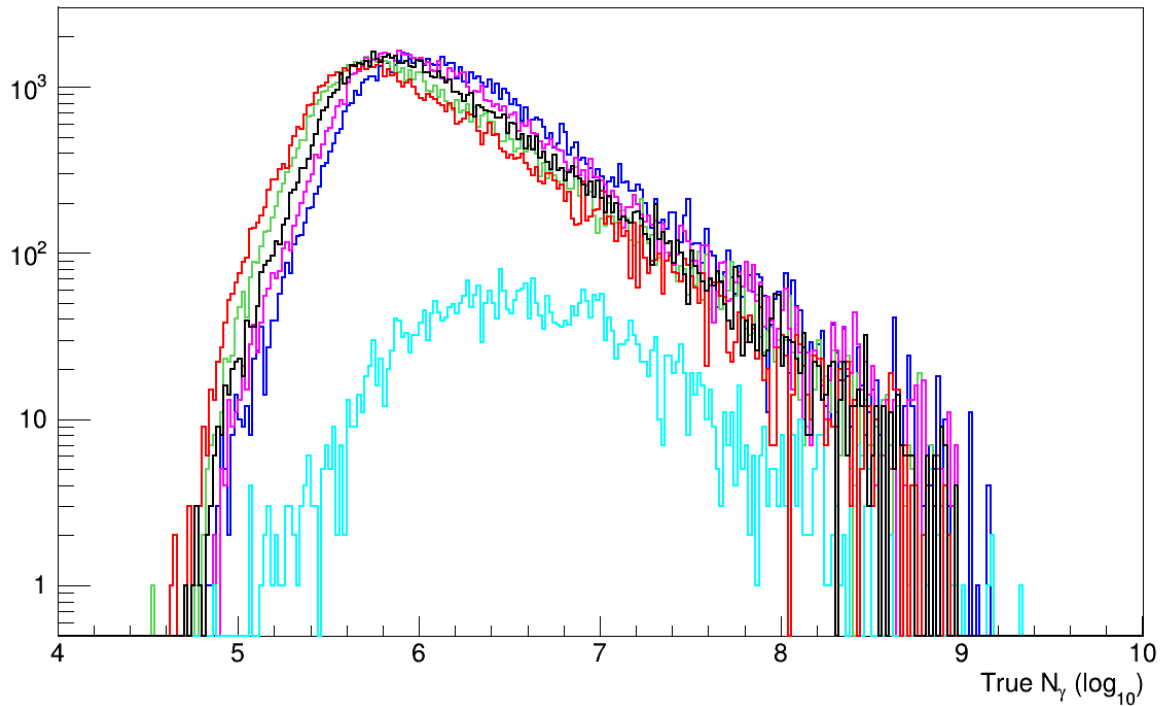


Fig. 6.6.1 *Spectrum of the number of γ and π^0 at observation level of KASCADE; simulated are: proton (blue), helium (purple), carbon (black), silicon (green), iron (red), and photons (light blue).*

6.7 TRUE NUMBERS OF HADRONS (TRNH)

The **true number of hadrons** is derived from the CORSIKA output as the number of hadrons at the observation level of KASCADE at 110 m asl. Only hadrons above 100 MeV low energy cut-off are taken into account.

Fig 6.7.1 shows the hadron spectra for the 5 different mass groups simulated, proton (blue), helium (purple), carbon (black), silicon (green), iron (red) and photons (light blue).

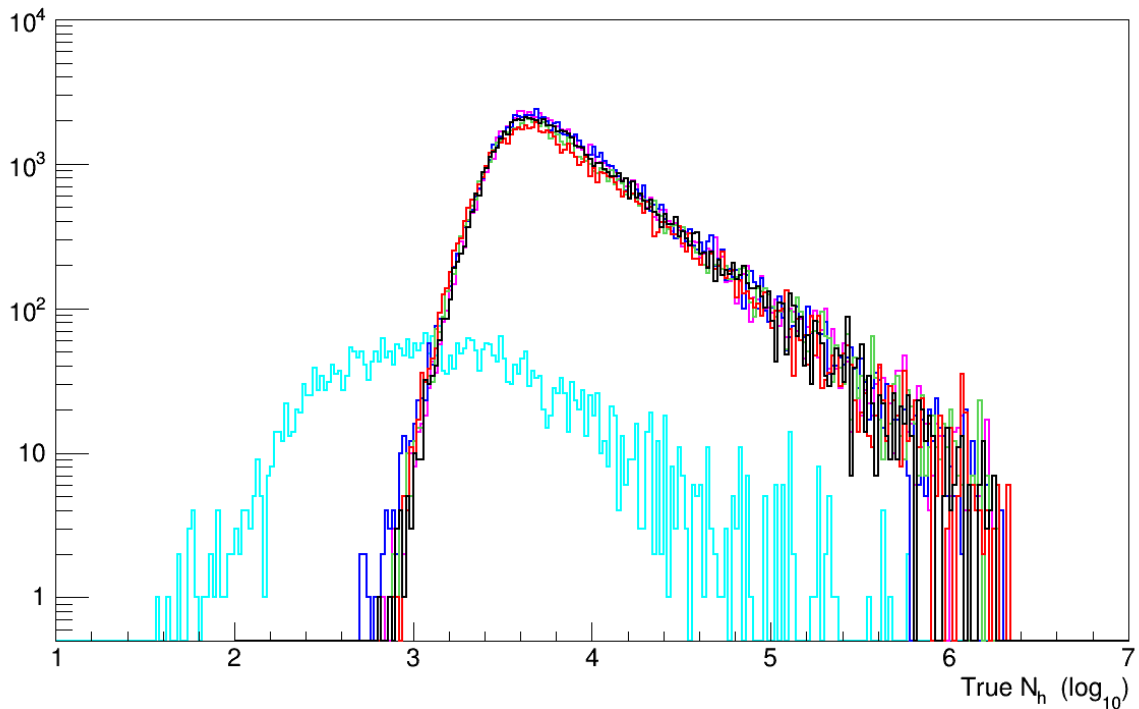


Fig. 6.7.1 *Spectrum of the number of hadrons at observation level of KASCADE; simulated are: proton (blue), helium (purple), carbon (black), silicon (green), iron (red), and photons (light blue).*

6.8 TRUE SHOWER CORE POSITION (TRXC, TRYC)

The **true shower core position** is derived from the detector simulation (CRES) output, defined as the position within the detector area where the shower centre is located. In the detector simulations, this centre can be chosen when initialising the detector simulation routine. The core positions are uniformly distributed over the whole detector area, even beyond the border, without any fiducial area cuts applied.

Figs. 6.8.1 shows the true shower core distributions if the reconstructed shower core lies within the active area of the COMBINED detector component (all cuts applied).

Extensive air showers with a core position outside the detector area have a great probability for being incorrectly reconstructed. Therefore, only showers with a maximum core distance less than 91 m radius from the centre of the KASCADE detector area and a well defined and understood GRANDE area are taken into account. Within the KASCADE area (91m radius cut) are more showers reconstructed mainly because of the lower N_e cut applied. From North-West

to South-East of the GRANDE array the number of reconstructed shower cores is decreasing. With increasing distance of the shower core to the centre of the KASCADE array the number of muons decreases and thus the probability for a successful analysis reduces.

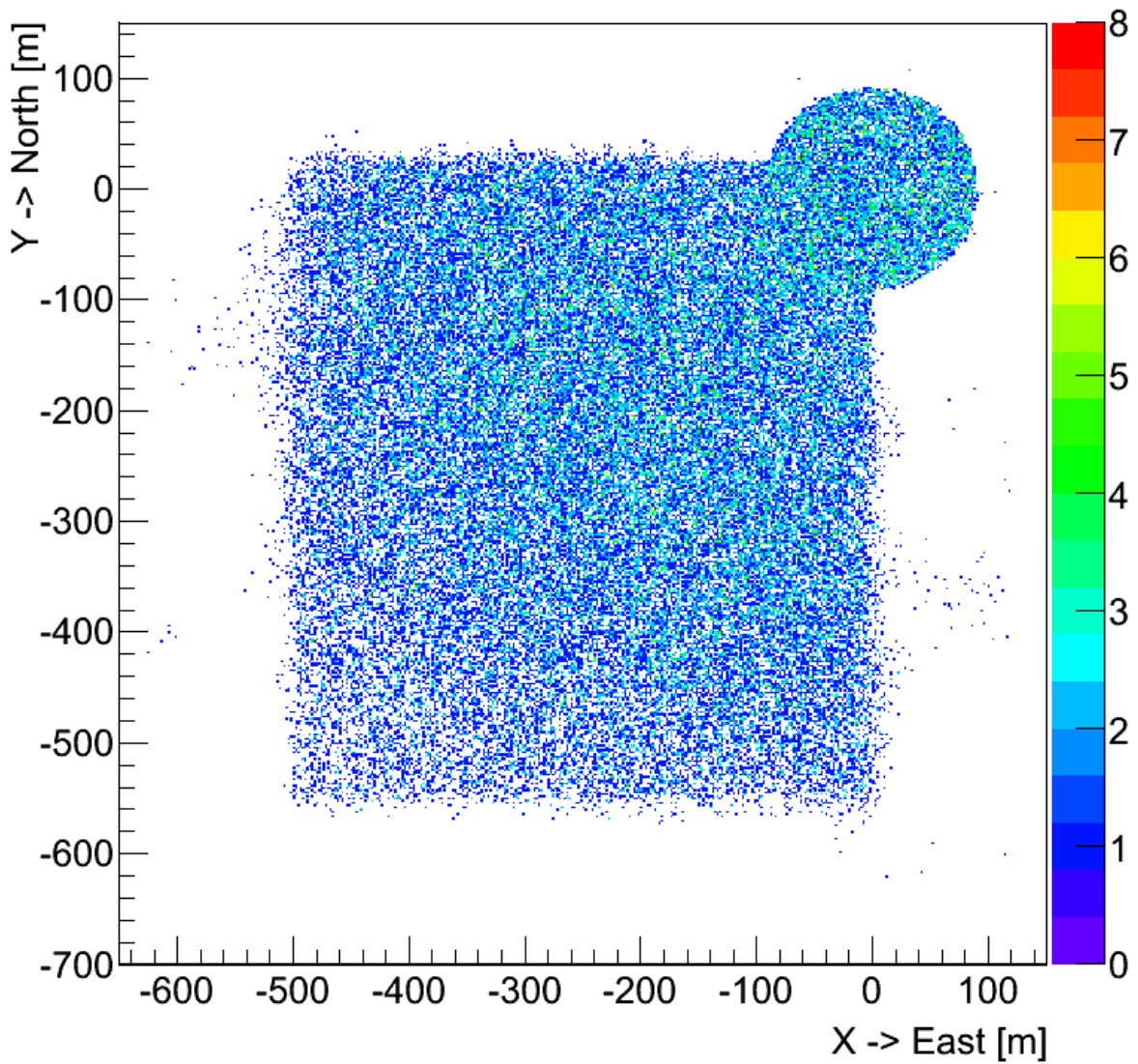


Fig. 6.8.1

Shower core distributions for simulated particles reconstructed with KRETA for COMBINED

7 SIMULATION DATA ANALYSIS HELPS

This chapter provides some valuable information on how to deal with the simulated COMBINED data, based on the experience of several years of data analysis.

7.1 CUTS

Concerning applied cuts we usually distinguish between ‘**Data Selection Cuts**’ and ‘**Advised Cuts**’. For this simulation, all cuts turned out to be necessary to guarantee high quality data sets.

7.1.1 QUALITY CUTS FOR SIMULATED COMBINED SHOWERS

The ‘**Data Selection Cuts COMBINED**’ have been applied while generating the simulation ROOT files. The cuts that were used here are mostly the same as those used for the measured data analyzed with COMBINED. They were determined through intensive tests as part of a doctoral thesis (see reference list: S.Schoo)

These Cuts are:

- **the shower reconstruction in the KASCADE and in the GRANDE Array Processors were successful;**
all reconstruction steps have been performed without failure;
- **area cuts;**
the reconstructed shower core is within the KASCADE array (91m radius) or in the fiducial area of the GRANDE array (see chapter 3.). This cut is applied to get rid of so called ‘border effects’ which occur when a shower is reconstructed close to the border and one cannot distinguish if the shower core is inside or outside the respective array. In this case the lateral density fit function is meaningless;
- **AGE cut**
COMBINED uses a modified NKG-function to fit the lateral shower shape. Within this function, the age parameter values are limited theoretically to a range from 0.1 to 1.48. The age cut values depend on the location of the reconstructed shower core:

core within KASCADE:	0.20 < age < 1.48
core within GRANDE:	0.15 < age < 1.48;

- **zenith angle $ZE < 30^\circ$;**
the KASCADE experiment was designed to record events with a zenith angle well below 60° . For the COMBINED analysis the upper zenith angle limit is set to 30° for both simulations and measurement;
- **$\lg(N_e)$ cut;**
this cut is just applied to remove the non-physical rubbish. The N_e cut values depend on the location of the reconstructed shower core

core within KASCADE:	$3.2 < \lg(N_e) < 9.0$
core within GRANDE:	$4.8 < \lg(N_e) < 9.0$;
- **$\lg(N_\mu)$ cut**
this cut is just applied to remove the non-physical rubbish
 $3.0 < \lg(N_\mu) < 9.0$;
- **N_μ / N_e cut;**
the N_μ / N_e relation cut is applied to remove the non-physical rubbish.
 $N_\mu / N_e > 0.001$
- **ndtg cut**
the number of GRANDE stations used for time fit if the shower core is within the GRANDE array.
ndtg > 11;
- **shower core fluctuation**
the core position between analysis iteration levels may not exceed 70m.
dist (level3-level1) =< 70m;

The data published do not contain events which did not survive ALL 'Data Selection Cuts COMBINED' listed above.

There are some more complex cuts applied to remove rare non-physical artefacts.

7.2 EXPERT'S ADVICES

Here are some advices that we think are helpful for people doing analysis with the KCDC data.

- **be careful applying cuts on the quantity 'energy';**
the quantity energy is a rough estimation based on the measured numbers of electrons (N_e) and the number of muons (N_μ) by means of an "Energy Estimator" whose parameters are deduced with help of a Monte-Carlo Simulation sets optimized for the zenith angle range 0° to 17° (see chapter 3.1). It would be advisable to cut on N_e or/and N_μ instead;

- **how to handle the quantities ‘Energy Deposit’ and ‘Arrival Times’;**

the deposit value ‘0’ denotes a station, which was working but is not a part of the present event. If you are interested in the station coordinates please refer to chapter 7.3 and appendix-A. (chapter 7.4 and appendix-B for GRANDE respectively).

Basically, the same applies for the quantity ‘Arrival Times’. But here only stations marked as active detectors with valid time information are taken into account.

- **the ‘row_mapping’ file**

must always be used to match events from different detector components like ‘general’ and ‘combined’. When a detector component is missing in the respective event the row_mapping entry is set to ‘-1’;

C++ code examples how to deal with the row-mapping file can be downloaded.

For KCDC COMBINED data:

https://kcdc.iap.kit.edu/static/txt/KCDC_analyze_COMBINED_example.C.gz ,

for simulation:

https://kcdc.iap.kit.edu/static/txt/KCDC_analyze_COMBINED_simulations_example.C.gz .

7.3 CALCULATION OF KASCADE DETECTOR STATION LOCATIONS FROM ID

For the ‘e/γ-Energy Deposits’, the ‘μ-Energy Deposits’ and the ‘Arrival Times’ in KASCADE, the position of the detector stations is given in so called ‘Station IDs’ which is a number between 1 and 252 for e/γ-detectors and for μ-detectors for KASCADE. The allocation table and the python-code fragment to calculate the real position of the KASCADE stations in KASCADE coordinates are given in [appendix ‘A’](#).

7.4 CALCULATION OF GRANDE DETECTOR STATION LOCATIONS FROM ID

For the ‘GRANDE Energy Deposits’ and the ‘GRANDE Arrival Times’ the position of the detectors is given in so called ‘Station IDs’ which is a number between 1 and 37. The allocation table to calculate the real position of the respective GRANDE station in KASCADE coordinates is given in [appendix ‘B’](#).

8 SIMULATION DATA SETS

With KCDC we offer 42 root files with simulated data for direct download for the COMBINED detector component. The simulation data sets cover the same energy ranges as the reconstructed data. The cuts applied to the simulations are the same as for the data provided in DataShop.

Three High Energy Interaction Models have been simulated under the same conditions, which are:

Parameter	Range
Energy range (Standard Set)	$10^{15} < E_0 < 10^{18}$ eV
Energy range (High Energy Extension)	$5.62 \cdot 10^{17} < E_0 < 3.16 \cdot 10^{18}$ eV
Spectral index (slope)	-2.00
Zenith angle (pr,he,co,si,fe)	0.0° - 30.0°
Zenith angle (γ)	0.0° - 30.0°
Azimuth angle	0.0° - 360.0°
Observation level	110 m asl
Transition energy	200 GeV (E_{lab}) ¹⁾
Energy cutoff hadrons	100 MeV
Energy cutoff electrons	3 MeV
Energy cutoff muons	100 MeV
Energy cutoff photons/pions	3 MeV
Magnetic Field (horizontal component)	20.0 μ T
Magnetic Field (vertical component)	43.2 μ T

¹⁾ transition energy (E_{lab} in GeV) between high and low-energy hadronic interaction models

In the following sections, the available simulation sets are listed.

- col 1 primary particle initiating the shower
- col 2 number of showers simulated with the parameters listed in in table above times the factor of reuses
- col 3 number of showers surviving all quality cuts for the respective detector component i.e. the number of showers in the download root files
- col 4 root file size (the file size of the zipped download file is a factor of two smaller)
- col 5 root download file name

8.1 COMBINED SIMULATION DATA SETS

8.1.1 QGSJET-II-04 & FLUKA 2012.2.14_32

QGSjet-II-04 & FLUKA 2012.2.14_32 (standard set)				
Primary Particle	Events		File Size [MB]	Download File Name
	simulated	reconstruct		
proton	963,555 * 10	173,590	223	COMBINED_Sim_qgs-4_pr1.root
helium	963,555 * 10	172,920	220	COMBINED_Sim_qgs-4_he1.root
carbon	963,555 * 10	165,029	219	COMBINED_Sim_qgs-4_co1.root
silicon	963,555 * 10	157,642	201	COMBINED_Sim_qgs-4_si1.root
iron	963,555 * 10	148,413	190	COMBINED_Sim_qgs-4_fe1.root
all 5 prim's	4,817,776 * 10	817,594	1,045	COMBINED_Sim_qgs-4_5prim1.root
gamma	41,096 * 10	7,464	8.5	COMBINED_Sim_qgs-4_gm1.root

QGSjet-II-04 & FLUKA 2012.2.14_32 (High Energy Extension)				
Primary Particle	Events		File Size [kB]	Download File Name
	simulated	reconstruct		
proton	90 * 10	217	551	COMBINED_Sim_qgs-4_HE_pr1.root
helium	90 * 10	242	614	COMBINED_Sim_qgs-4_HE_he1.root
carbon	90 * 10	228	578	COMBINED_Sim_qgs-4_HE_co1.root
silicon	90 * 10	289	725	COMBINED_Sim_qgs-4_HE_si1.root
iron	90 * 10	255	643	COMBINED_Sim_qgs-4_HE_fe1.root
all 5 prim's	450 * 10	1,231	3,055	COMBINED_Sim_qgs-4_HE_5prim1.root
gamma	69 * 10	24	74	COMBINED_Sim_qgs-4_HE_gm1.root

Note the download file size is a factor of about 2 smaller than the values given in column 4 because we offer only zipped files for download.

8.1.2 EPOS LHC & FLUKA 2011.2b.4_32

EPOS LHC & FLUKA 2011.2b.4_32 (standard set)				
Primary Particle	Events		File Size [MB]	Download File Name
	simulated	reconstruct		
proton	449,561 * 10	84,588	109	COMBINED_Sim_epos-LHC_pr.root
helium	449,561 * 10	83,725	107	COMBINED_Sim_epos-LHC_he.root
carbon	449,561 * 10	78,932	101	COMBINED_Sim_epos-LHC_co.root
silicon	449,561 * 10	75,783	97	COMBINED_Sim_epos-LHC_si.root
iron	449,561 * 10	70,753	91	COMBINED_Sim_epos-LHC_fe.root
all 5 prim's	2,247,805 * 10	393,781	506	COMBINED_Sim_epos-LHC_5prim.root
gamma	513,896 * 10	3,992	5	COMBINED_Sim_epos-LHC_gm.root

EPOS LHC & FLUKA 2011.2b.4_32 (High Energy Extension)				
Primary Particle	Events		File Size [kB]	Download File Name
	simulated	reconstruct		
proton	60 * 10	187	476	COMBINED_Sim_epos-LHC_HE_pr.root
helium	60 * 10	172	440	COMBINED_Sim_epos-LHC_HE_he.root
carbon	60 * 10	179	454	COMBINED_Sim_epos-LHC_HE_co.root
silicon	60 * 10	144	371	COMBINED_Sim_epos-LHC_HE_si.root
iron	60 * 10	158	401	COMBINED_Sim_epos-LHC_HE_fe.root
all 5 prim's	300 * 10	840	2087	COMBINED_Sim_epos-LHC_HE_5prim.root
gamma	46 * 10	39	110	COMBINED_Sim_epos-LHC_HE_gm.root

Note the download file size is a factor of about 2 smaller than the values given in column 4 because we offer only zipped files for download.

8.1.3 SIBYLL 2.3c & FLUKA 2011.2c.3_64

SIBYLL 2.3c & FLUKA 2011.2c.3_64 (standard set)				
Primary Particle	Events		File Size [MB]	Download File Name
	simulated	reconstruct		
proton	452,740 * 10	85,411	110	COMBINED_Sim_sibyll-23c_pr.root
helium	452,740 * 10	84,192	108	COMBINED_Sim_sibyll-23c_he.root
carbon	452,740 * 10	81,403	104	COMBINED_Sim_sibyll-23c_co.root
silicon	452,740 * 10	75,989	98	COMBINED_Sim_sibyll-23c_si.root
iron	452,740 * 10	72,644	94	COMBINED_Sim_sibyll-23c_fe.root
all 5 prim's	2,236,700 * 10	399,639	514	COMBINED_Sim_sibyll-23c_5prim.root
gamma	411,184 * 10	3,968	4.6	COMBINED_Sim_sibyll-23c_gm.root

SIBYLL 2.3c & FLUKA 2011.2c.3_64 (High Energy Extension)				
Primary Particle	Events		File Size [kB]	Download File Name
	simulated	reconstruct		
proton	60 * 10	170	438	COMBINED_Sim_sibyll-23c_HE_pr.root
helium	60 * 10	156	399	COMBINED_Sim_sibyll-23c_HE_he.root
carbon	60 * 10	167	423	COMBINED_Sim_sibyll-23c_HE_co.root
silicon	60 * 10	139	358	COMBINED_Sim_sibyll-23c_HE_si.root
iron	60 * 10	168	429	COMBINED_Sim_sibyll-23c_HE_fe.root
all 5 prim's	300 * 10	800	800	COMBINED_Sim_sibyll-23c_HE_5prim.root
gamma	46 * 10	19	63	COMBINED_Sim_sibyll-23c_HE_gm.root

Note the download file size is a factor of about 2 smaller than the values given in column 4 because we offer only zipped files for download.

8.1.4 SIBYLL 2.3D & FLUKA 2011.2x4-64

SIBYLL 2.3d & Fluka 2011.2x4-64 (standard set)				
Primary Particle	Events		File Size [MB]	Download File Name
	simulated	reconstruct		
proton	456,848 * 10	86,552	112	COMBINED_Sim_sibyll-23d_pr.root
helium	456,848 * 10	84,990	109	COMBINED_Sim_sibyll-23d_he.root
carbon	456,848 * 10	81,432	104	COMBINED_Sim_sibyll-23d_co.root
silicon	456,848 * 10	77,222	99	COMBINED_Sim_sibyll-23d_si.root
iron	456,848 * 10	74,107	95	COMBINED_Sim_sibyll-23d_fe.root
all 5 prim's	2,284,240 * 10	404,303	519	COMBINED_Sim_sibyll-23d_5prim.root
gamma	411,920 * 10	4,059	4.6	COMBINED_Sim_sibyll-23d_gm.root

SIBYLL 2.3d & Fluka 2011.2x4-64 (High Energy Extension)				
Primary Particle	Events		File Size [kB]	Download File Name
	simulated	reconstruct		
proton	60 * 10	156	402	COMBINED_Sim_sibyll-23d_HE_pr.root
helium	60 * 10	193	485	COMBINED_Sim_sibyll-23d_HE_he.root
carbon	60 * 10	167	425	COMBINED_Sim_sibyll-23d_HE_co.root
silicon	60 * 10	139	360	COMBINED_Sim_sibyll-23d_HE_si.root
iron	60 * 10	157	402	COMBINED_Sim_sibyll-23d_HE_fe.root
all 5 prim's	300 * 10	812	2019	COMBINED_Sim_sibyll-23d_HE_5prim.root
gamma	46 * 10	19	62	COMBINED_Sim_sibyll-23d_HE_gm.root

Note the download file size is a factor of about 2 smaller than the values given in column 4 because we offer only zipped files for download.

8.2 GET ROOT SIMULATIONS

From the 'KCDC' – 'Simulations' page registered users can download data sets directly just by clicking the respective download button (see fig 8.2.2.). Users that are not yet registered have access to the 'General Info' page where some information around the subject of simulations for KASCADE and how to register are provided.

Furthermore, the 'General Info' page contains general information on how the provided data records were created and which quantities are published. Simulations for the two DataShops KASCADE and COMBINED are currently available invoked via the respective menu items.

The screenshot shows the KCDC website interface. At the top, there is a navigation bar with links for 'KIT', 'IAP', 'HOME', 'Data Privacy', 'Impressum', 'admin', and 'logout'. The main header features the KIT logo, the text 'KASCADE Cosmic Ray Data Centre (KCDC) / Open β ', and the KCDC logo. A left sidebar contains a menu with categories like 'Information', 'Announcements', 'User Account', 'Data Shops', 'Simulations', 'Spectra', 'Materials', 'Publications', 'Report a Bug', 'Education/Lehre', and 'KCDC Partners'. The main content area is titled 'Event Simulations for COMBINED data analysis'. It contains a paragraph of introductory text, a bulleted list of links for general information, a section titled 'Some general information concerning the COMBINED data analysis simulations published', another paragraph of text, a bulleted list of simulation models (QGSjet-II-04, EPOS-LHC, SIBYLL 2.3c & SIBYLL 2.3d, and FLUKA), and a paragraph explaining the simulation availability. Below this is a table with two columns: 'ROOT tree' and 'description'. The table lists four types of ROOT trees: 'general', 'combined', 'trmc', and 'row_map'. At the bottom of the main content area, there is a section titled 'Table of simulations available for COMBINED data analysis' with a table listing simulation models under three columns: QGSjet, EPOS, and SIBYLL. The table lists 'QGSjet-II-04 Comb', 'EPOS LHC Comb', 'SIBYLL 2.3c Comb', and 'SIBYLL 2.3d Comb'. A note below the table says 'Click on the model to get to download pages'. At the very bottom of the page, there is a footer: 'KCDC OPEN - BETA - VERSION SKARAGAN 2.0 BASED ON: KAOS (2.0.0)'.

Fig. 8.2.1. *COMBINED 'Simulations' for direct download*

[[Juergen]] | KIT | IKP | HOME | Impressum | admin | logout

KIT
Karlsruhe Institute of Technology

KASCADE Cosmic Ray Data Centre (KCDC) / Open β

KCDC

- KCDC Homepage
- KCDC Motivation
- KCDC Regulations
- Information
- Announcements
- FAQs
- User Account
- Data Shops
- Simulations
- Spectra
- Materials
- Publications
- Report a Bug
- Education/Lehre

Air Shower Simulations with QGSjet-II-04 and FLUKA for COMBINED Data Analysis

Technical data for QGSjet-II-04 COMBINED simulations

High energy model QGSjet-II-04 ($E_{\text{lab}} > 200\text{GeV}$)
 Low energy model FLUKA 2012.2.14_32 ($E_{\text{lab}} < 200\text{GeV}$)
 Energy range COMBINED $1.0 \times 10^{15} < E_0 < 1.0 \times 10^{18} \text{ eV}$ (HE: $< 3.16 \times 10^{18} \text{ eV}$)

Detector component	Primary particle	Events simul*reused	Events processed	download size	root files
COMBINED	proton	44.926 * 10	81.134	104 MB	download
	helium	44.926 * 10	80.581	103 MB	download
	carbon	44.926 * 10	76.879	98 MB	download
	silicon	44.926 * 10	73.174	94 MB	download
	iron	44.926 * 10	68.812	88 MB	download
	gamma	41.096 * 10	3933	4,5 MB	download

High Energy Extension (5.62×10^{17} to $3.16 \times 10^{18} \text{ eV}$)

Detector component	Primary particle	Events simul*reused	Events processed	download size	root files
COMBINED	proton	60 * 10	145	373 kB	download
	helium	60 * 10	148	382 kB	download
	carbon	60 * 10	170	434 kB	download
	silicon	60 * 10	172	437 kB	download
	iron	60 * 10	183	464 kB	download
	gamma	46 * 10	17	57 kB	download

Information concerning the COMBINED simulation download page

- col 1 simulated detector component. We have used the same shower with the core position randomly distributed over a pre-defined detector area.
- col 2 the five primaries simulated are representing five different mass groups. Additionally gammas have been simulated for special studies.
- col 3 number of simulated showers per primary particle and how often the same shower has been thrown on a randomly chosen location inside a pre-defined detector area.
- col 4 number of showers provided the user in the respective ROOT file per primary particle after all quality cuts applied.
- col 5 size of ROOT the data file. The download size of the zipped file is smaller by a factor of two. Additionally the 'End User License Agreement' (EULA) and the 'Simulation Manual' are shipped with every download.
- col 6 download buttons for the five primaries plus gamma. We offer only ROOT files for download but we can produce HDF5 files on request.
- col 7 download_ALL button to get all five primaries of one detector component at once (gammas are not included). The size of the download file corresponds roughly to the sum of the sizes of the five primaries.

HE ext The HighEnergy extension to the standard data set provides only a few showers at highest energies ($5.62 \times 10^{17} < E_0 < 3.16 \times 10^{18} \text{ eV}$).

QGSjet-II-04 COMBINED Information

Events simul * reused denotes the number of events simulated and how often they have been reused, while Events processed specifies the number of events surviving all quality cuts which are included in the respective root file. Clicking on the respective primary download link will open a dialog box to start the ftp download. download ALL will download the simulations of all 5 primaries in one zipped file. Gamma induced shower data are not included. For a more detailed description of the simulation sets, applied cuts and download procedure check the [KCDC-Combined Simulations Manual](#)

KCDC OPEN - BETA - VERSION PENTARUS 1.0 BASED ON: KAOS (1.1.0)

Fig. 8.2.2.

example download page for the QGSjet-II-04 simulation model

9 SIMULATION DATA FORMAT

Concerning the simulation data sets we offer at present only ROOT files for download via the KCDC web pages. ROOT is an object-oriented framework developed by CERN aimed at solving the data analysis challenges of high-energy physics.

9.1 ROOT FILES

Like the COMBINED data measured with the KASCADE-Grande detectors provided for download via the KCDC DataShop, the COMBINED simulation ROOT files are organised in trees. The files contain four trees, one for the COMBINED detector component, one tree for the ‘general’ information where all data arrays are included, one tree for the true Monte Carlo information ‘trmc’ and a tree to map the entries for each event called ‘row_map’ (see table below and fig. 9.1.1.).

ROOT tree	description
general	all data arrays; run- & event-number
comb	all reconstructed COMBINED quantities (E, Xc,Yc,Ze,Az,Ne,Nmu,Age)
trmc	all MC information from CORSIKA and CRES (TrEP,TRPP,TrXc,TrYc, TrZe, TrAz,TrNe,TrNg,TrNm,TrNh)
row_map	information to synchronise the trees

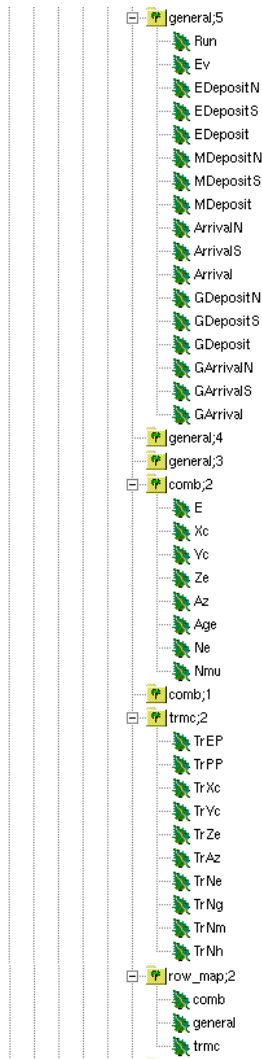


Fig. 9.1.1. *ROOT-trees example for simulations with all quantities published*

9.2 PROBLEMS WHILE HANDLING THE DATA FILES

9.2.1 WARNING WHEN OPENING ROOT FILES

The root files are created using the 'ROOT 6' version. If you open the *events.root* file with a different version you might get some warnings as outlined below which can be ignored.

root [1] Warning in <TStreamerInfo::BuildCheck>:
 The StreamerInfo of class TTree read from file events.root
 has the same version (=19) as the active class but a different checksum.
 You should update the version to ClassDef(TTree,20).
 Do not try to write objects with the current class definition,
 the files will not be readable.

Simulation Data Format

Warning in <TStreamerInfo::CompareContent>: The following data member of the on-file layout version 19 of class 'TTree' differs from the in-memory layout version 19:

```
double fWeight; //  
:  
:
```

9.2.2 32-BIT LINUX SYSTEMS

As the files transmitted can be rather large, we strongly recommend using a 64-bit system. There is p.e. a 2GB file-size limit in LINUX. This limit is deeply embedded in the versions of Linux for 32-bit CPUs so there is no workaround for this situation.

10 REFERENCE LIST

10.1 KCDC

The KASCADE Cosmic-ray Data Centre KCDC: Granting Open Access to Astroparticle Physics Research Data

The European Physical Journal C (2018) → **publication to be cited**

A new release of the KASCADE Cosmic Ray Data Centre (KCDC)

35th International Cosmic Ray Conference (ICRC)

Bexco, Busan, Korea; 12. - 20.7.2017

The KASCADE Cosmic-ray Data Centre (KCDC)

34th International Cosmic Ray Conference (ICRC)

The Hague, Netherlands; 30.7. - 6.8.2015

The KASCADE Cosmic-ray Data Centre (KCDC)

24th European Cosmic Ray Symposium (ECRS)

Kiel, Germany; 1. - 5.9.2014

The KASCADE Cosmic ray Data Center - providing open access to astroparticle physics research data

Helmholtz Open Access Webinars on Research Data Webinar

15; 8. - 12.11.2013

KCDC - publishing research data from the KASCADE experiment

Helmholtz Open Access Workshop

DESY, Hamburg; 11.6.2013

10.2 KASCADE

The Cosmic-Ray Experiment – KASCADE

Nuclear Instruments and Methods; A513 (2003) p490-510

A Warm-liquid Calorimeter for Cosmic-ray Hadrons

Nuclear Instruments and Methods; A427 (1999) 528-542

10.3 KASCADE-GRANDE

The KASCADE-Grande experiment

Nuclear Instruments and Methods; A620 (2009) p202-216

10.4 COMBINED

Energy Spectrum and Mass Composition of Cosmic Rays and How to Publish Air-Shower Data

PhD Thesis Sven Schoo 2016

https://web.iap.kit.edu/KASCADE/publication/PhD_Theses/ThesisSvenSchoo.pdf

10.5 WEB –LINKS

For more information on KASCADE/KASCADE see:

<https://web.iap.kit.edu/KASCADE/>

For more information on KCDC see:

<https://kcdc.iap.kit.edu/>

10.6 SIMULATIONS

GEANT: CERN report Brun R. et al., GEANT3 User Guide, CERN/DD/EE/84-1 (1987)

CORSIKA:

https://web.iap.kit.edu/corsika/physics_description/corsika_phys.pdf

<https://web.iap.kit.edu/corsika/usersguide/usersguide.pdf>

11 GLOSSARY

COMBINED We use the name **COMBINED** as a synonym for combined data analysis of the KASCADE and the GRANDE detector systems of the KASCADE-Grande experiment. The combined analysis merges the advantages of the formerly separated KASCADE and GRANDE analyses and leads to a consistent spectrum in the energy range 10^{15} to 10^{18} eV. The aim of the combined analysis was to utilize this improved reconstruction to get one single, consistent energy spectrum.

CORSIKA **CORSIKA** (**CO**smic **R**ay **S**imulations for **KA**scade) is a program package for detailed simulation of extensive air showers initiated by high-energy cosmic ray particles. Protons, light nuclei up to iron, photons, and many other particles may be treated as primaries.

The particles are tracked through the atmosphere until they undergo reactions with the air nuclei or - in the case of instable secondaries – decay.

CRES **CRES** (**C**osmic **R**ay **E**vent **S**imulation) is code package for the simulation of the signals / energy deposits in all detector components of KASCADE/KASCADE-Grande as response to an extensive air shower as simulated with **CORSIKA**.

KAOS **KAOS** is the acronym for **K**arlsruhe **A**stroparticle physics **O**pen data **S**oftware. It has been written in the context of the KASCADE Cosmic Ray Data Centre ([KCDC](#)), a web portal designed for the publication of scientific data recorded with the [KASCADE experiment](#). **KAOS** is implemented using a plugin-based design with a focus on easy extensibility and modifiability in order to work also outside the context of KCDC.

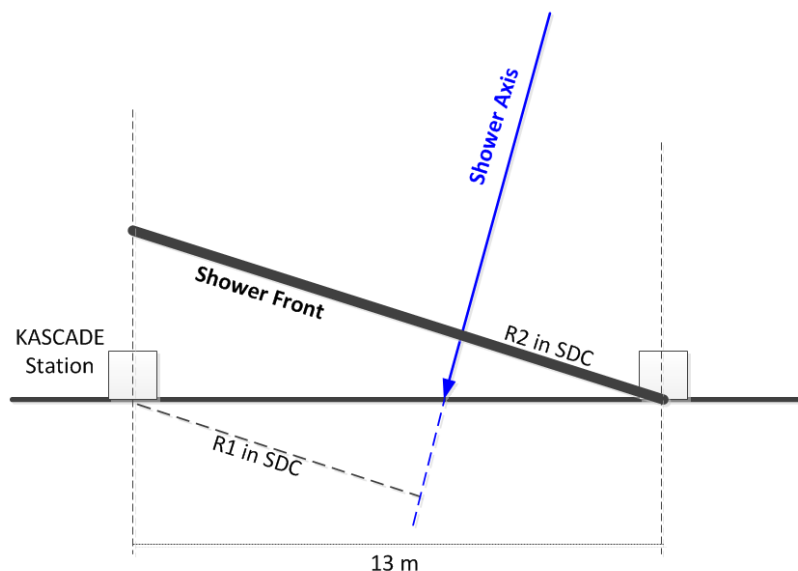
Glossary

KRETA (**K**ascade **R**econstruction of **E**xtensive **A**ir showers) is the main data analysis engine of the KASCADE/KASCADE-Grande Experiment. KRETA is written in Fortran77 and makes extensive use of the CERN library and its various software packages.

MIP **Minimum ionizing particles (MIPs)** are charged particles, which embody the minimum ionizing losses in substances. This situation occurs when the kinetic energy of particles is at least twice larger than their rest mass. For example, electrons (or protons) can be considered as minimum ionizing particles when their kinetic energy is greater than 1 MeV (or 2 GeV). Since the ionization losses of these particles are only weakly dependent on their momentum, it is generally accepted that minimum ionizing particles produce an even distribution of free charge carriers along their paths. Muons for example suffer an energy loss of roughly 1.5 MeV/cm when passing through a plastic scintillator.

Quantity The KASCADE variables published in the KCDC web portal are called quantities

SDC **Shower Disc Coordinates**. The sketch below illustrates how the radii R1 and R2 are calculated in SDC.



Glossary

ZEBRA **ZEBRA** is a memory management system and part of the CERN library. ZEBRA allows a dynamic creation of data structures at execution time as well as the manipulation of those structures.

12 APPENDIX

12.1 APPENDIX A – KASCADE STATION COORDINATES

Correlation between station ID as given in the data arrays and the x- and y-positions in KASCADE coordinates. The positions are given in [m]. The column ‘Detect’ shows the detectors installed (number of e/γ and μ detectors). The red numbers indicate that the station is dislocated from the regular grid. Four stations in the centre of the KASCADE array are missing, their positions are blocked by the central calorimeter. The scheme of the nomenclature is illustrated in fig. A.1.

St-ID	X- Y-Position [m]	Detect	St-ID	X- Y-Position [m]	Detect	St-ID	X- Y-Position [m]	Detect
1	-97.5 / -97.5	2 e/γ & 4 μ	85	-19.5 / -45.5	4 e/γ	169	6.5 / 32.5	4 e/γ
2	-84.5 / -97.5	2 e/γ & 4 μ	86	-6.5 / -45.5	4 e/γ	170	19.5 / 32.5	4 e/γ
3	-84.5 / -84.5	2 e/γ & 4 μ	87	-6.5 / -32.5	4 e/γ	171	19.5 / 45.5	4 e/γ
4	-97.5 / -84.5	2 e/γ & 4 μ	88	-19.5 / -32.5	4 e/γ	172	6.5 / 45.5	4 e/γ
5	-71.5 / -97.5	2 e/γ & 4 μ	89	-19.5 / -19.5	4 e/γ	173	58.5 / 6.5	2 e/γ & 4 μ
6	-58.5 / -97.5	2 e/γ & 4 μ	90	-6.3 / -18.5	4 e/γ	174	71.5 / 6.5	2 e/γ & 4 μ
7	-58.5 / -84.5	2 e/γ & 4 μ	91	-19.5 / -6.5	4 e/γ	175	71.5 / 19.5	2 e/γ & 4 μ
8	-71.5 / -84.5	2 e/γ & 4 μ	92	-45.5 / -19.5	4 e/γ	176	58.5 / 19.5	2 e/γ & 4 μ
9	-71.5 / -71.5	2 e/γ & 4 μ	93	-32.5 / -19.5	4 e/γ	177	84.5 / 6.5	2 e/γ & 4 μ
10	-58.5 / -71.5	2 e/γ & 4 μ	94	-32.5 / -6.5	4 e/γ	178	97.5 / 6.5	2 e/γ & 4 μ
11	-58.5 / -58.5	2 e/γ & 4 μ	95	-45.5 / -6.5	4 e/γ	179	97.5 / 19.5	2 e/γ & 4 μ
12	-71.5 / -58.5	2 e/γ & 4 μ	96	6.5 / -45.5	4 e/γ	180	84.5 / 19.5	2 e/γ & 4 μ
13	-97.5 / -71.5	2 e/γ & 4 μ	97	19.5 / -45.5	4 e/γ	181	84.5 / 32.5	2 e/γ & 4 μ
14	-84.5 / -71.5	2 e/γ & 4 μ	98	19.5 / -32.5	4 e/γ	182	97.5 / 32.5	2 e/γ & 4 μ
15	-84.5 / -58.5	2 e/γ & 4 μ	99	6.5 / -32.5	4 e/γ	183	97.5 / 45.5	2 e/γ & 4 μ
16	-97.5 / -58.5	2 e/γ & 4 μ	100	32.5 / -45.5	4 e/γ	184	84.5 / 45.5	2 e/γ & 4 μ
17	-45.5 / -97.5	2 e/γ & 4 μ	101	45.5 / -45.5	4 e/γ	185	58.5 / 32.5	2 e/γ & 4 μ
18	-32.5 / -97.5	2 e/γ & 4 μ	102	45.5 / -32.5	4 e/γ	186	71.5 / 32.5	2 e/γ & 4 μ
19	-32.5 / -84.5	2 e/γ & 4 μ	103	32.5 / -32.5	4 e/γ	187	71.5 / 45.5	2 e/γ & 4 μ
20	-45.5 / -84.5	2 e/γ & 4 μ	104	32.5 / -19.5	4 e/γ	188	58.5 / 45.5	2 e/γ & 4 μ
21	-19.5 / -97.5	2 e/γ & 4 μ	105	45.5 / -19.5	4 e/γ	189	-97.5 / 58.5	2 e/γ & 4 μ
22	-6.5 / -97.5	2 e/γ & 4 μ	106	45.5 / -6.5	4 e/γ	190	-84.5 / 58.5	2 e/γ & 4 μ
23	-6.5 / -84.5	2 e/γ & 4 μ	107	32.5 / -6.5	4 e/γ	191	-84.5 / 71.5	2 e/γ & 4 μ
24	-19.5 / -84.5	2 e/γ & 4 μ	108	7.5 / -19.5	4 e/γ	192	-97.5 / 71.5	2 e/γ & 4 μ
25	-19.5 / -71.5	2 e/γ & 4 μ	109	19.5 / -19.5	4 e/γ	193	-71.5 / 58.5	2 e/γ & 4 μ
26	-6.5 / -71.5	2 e/γ & 4 μ	110	19.5 / -6.5	4 e/γ	194	-58.5 / 58.5	2 e/γ & 4 μ

Appendix

St-ID	X- Y-Position [m]	Detect	St-ID	X- Y-Position [m]	Detect	St-ID	X- Y-Position [m]	Detect
27	-6.5 / -58.5	2 e/ γ & 4 μ	111	58.5 / -45.5	2 e/ γ & 4 μ	195	-58.5 / 71.5	2 e/ γ & 4 μ
28	-19.5 / -58.5	2 e/ γ & 4 μ	112	71.5 / -45.5	2 e/ γ & 4 μ	196	-71.5 / 71.5	2 e/ γ & 4 μ
29	-45.5 / -71.5	2 e/ γ & 4 μ	113	71.5 / -32.5	2 e/ γ & 4 μ	197	-71.5 / 84.5	2 e/ γ & 4 μ
30	-32.5 / -71.5	2 e/ γ & 4 μ	114	58.5 / -32.5	2 e/ γ & 4 μ	198	-58.5 / 84.5	2 e/ γ & 4 μ
31	-32.5 / -58.5	2 e/ γ & 4 μ	115	84.5 / -45.5	2 e/ γ & 4 μ	199	-58.5 / 97.5	2 e/ γ & 4 μ
32	-45.5 / -58.5	2 e/ γ & 4 μ	116	97.5 / -45.5	2 e/ γ & 4 μ	200	-71.5 / 97.5	2 e/ γ & 4 μ
33	6.5 / -97.5	2 e/ γ & 4 μ	117	97.5 / -32.5	2 e/ γ & 4 μ	201	-97.5 / 84.5	2 e/ γ & 4 μ
34	19.5 / -97.5	2 e/ γ & 4 μ	118	84.5 / -32.5	2 e/ γ & 4 μ	202	-84.5 / 84.5	2 e/ γ & 4 μ
35	19.5 / -84.5	2 e/ γ & 4 μ	119	84.5 / -19.5	2 e/ γ & 4 μ	203	-84.5 / 97.5	2 e/ γ & 4 μ
36	6.5 / -84.5	2 e/ γ & 4 μ	120	97.5 / -19.5	2 e/ γ & 4 μ	204	-97.5 / 97.5	2 e/ γ & 4 μ
37	32.5 / -97.5	2 e/ γ & 4 μ	121	97.5 / -6.5	2 e/ γ & 4 μ	205	-45.5 / 58.5	2 e/ γ & 4 μ
38	45.5 / -97.5	2 e/ γ & 4 μ	122	84.5 / -6.5	2 e/ γ & 4 μ	206	-32.5 / 58.5	2 e/ γ & 4 μ
39	45.5 / -84.5	2 e/ γ & 4 μ	123	58.5 / -19.5	2 e/ γ & 4 μ	207	-32.5 / 71.5	2 e/ γ & 4 μ
40	32.5 / -84.5	2 e/ γ & 4 μ	124	71.5 / -19.5	2 e/ γ & 4 μ	208	-45.5 / 71.5	2 e/ γ & 4 μ
41	32.5 / -71.5	2 e/ γ & 4 μ	125	71.5 / -6.5	2 e/ γ & 4 μ	209	-19.5 / 58.5	2 e/ γ & 4 μ
42	45.5 / -71.5	2 e/ γ & 4 μ	126	58.5 / -6.5	2 e/ γ & 4 μ	210	-6.5 / 58.5	2 e/ γ & 4 μ
43	45.5 / -58.5	2 e/ γ & 4 μ	127	-97.5 / 6.5	2 e/ γ & 4 μ	211	-6.5 / 71.5	2 e/ γ & 4 μ
44	32.5 / -58.5	2 e/ γ & 4 μ	128	-84.5 / 6.5	2 e/ γ & 4 μ	212	-19.5 / 71.5	2 e/ γ & 4 μ
45	6.5 / -71.5	2 e/ γ & 4 μ	129	-84.5 / 19.5	2 e/ γ & 4 μ	213	-19.5 / 84.5	2 e/ γ & 4 μ
46	19.5 / -71.5	2 e/ γ & 4 μ	130	-97.5 / 19.5	2 e/ γ & 4 μ	214	-6.5 / 84.5	2 e/ γ & 4 μ
47	19.5 / -58.5	2 e/ γ & 4 μ	131	-71.5 / 6.5	2 e/ γ & 4 μ	215	-6.5 / 97.5	2 e/ γ & 4 μ
48	6.5 / -58.5	2 e/ γ & 4 μ	132	-58.5 / 6.5	2 e/ γ & 4 μ	216	-19.5 / 97.5	2 e/ γ & 4 μ
49	58.5 / -97.5	2 e/ γ & 4 μ	133	-58.5 / 19.5	2 e/ γ & 4 μ	217	-45.5 / 84.5	2 e/ γ & 4 μ
50	71.5 / -97.5	2 e/ γ & 4 μ	134	-71.5 / 19.5	2 e/ γ & 4 μ	218	-32.5 / 84.5	2 e/ γ & 4 μ
51	71.5 / -84.5	2 e/ γ & 4 μ	135	-71.5 / 32.5	2 e/ γ & 4 μ	219	-32.5 / 97.5	2 e/ γ & 4 μ
52	58.5 / -84.5	2 e/ γ & 4 μ	136	-58.5 / 32.5	2 e/ γ & 4 μ	220	-45.5 / 97.5	2 e/ γ & 4 μ
53	84.5 / -97.5	2 e/ γ & 4 μ	137	-58.5 / 45.5	2 e/ γ & 4 μ	221	6.5 / 58.5	2 e/ γ & 4 μ
54	97.5 / -97.5	2 e/ γ & 4 μ	138	-71.5 / 45.5	2 e/ γ & 4 μ	222	19.5 / 58.5	2 e/ γ & 4 μ
55	97.5 / -84.5	2 e/ γ & 4 μ	139	-97.5 / 32.5	2 e/ γ & 4 μ	223	19.5 / 71.5	2 e/ γ & 4 μ
56	84.5 / -84.5	2 e/ γ & 4 μ	140	-84.5 / 32.5	2 e/ γ & 4 μ	224	6.5 / 71.5	2 e/ γ & 4 μ
57	84.5 / -71.5	2 e/ γ & 4 μ	141	-84.5 / 45.5	2 e/ γ & 4 μ	225	32.5 / 58.5	2 e/ γ & 4 μ
58	97.5 / -71.5	2 e/ γ & 4 μ	142	-97.5 / 45.5	2 e/ γ & 4 μ	226	45.5 / 58.5	2 e/ γ & 4 μ
59	97.5 / -58.5	2 e/ γ & 4 μ	143	-45.5 / 6.5	4 e/ γ	227	45.5 / 71.5	2 e/ γ & 4 μ
60	84.5 / -58.5	2 e/ γ & 4 μ	144	-32.5 / 6.5	4 e/ γ	228	32.5 / 71.5	2 e/ γ & 4 μ
61	58.5 / -71.5	2 e/ γ & 4 μ	145	-32.5 / 19.5	4 e/ γ	229	32.5 / 84.5	2 e/ γ & 4 μ
62	71.5 / -71.5	2 e/ γ & 4 μ	146	-45.5 / 19.5	4 e/ γ	230	45.5 / 84.5	2 e/ γ & 4 μ
63	71.5 / -58.5	2 e/ γ & 4 μ	147	-19.5 / 6.5	4 e/ γ	231	45.5 / 97.5	2 e/ γ & 4 μ
64	58.5 / -58.5	2 e/ γ & 4 μ	148	-6.3 / 24.5	4 e/ γ	232	32.5 / 97.5	2 e/ γ & 4 μ
65	-97.5 / -45.5	2 e/ γ & 4 μ	149	-19.5 / 19.5	4 e/ γ	233	6.5 / 84.5	2 e/ γ & 4 μ

Appendix

St-ID	X- Y-Position [m]	Detect	St-ID	X- Y-Position [m]	Detect	St-ID	X- Y-Position [m]	Detect
66	-84.5 / -45.5	2 e/ γ & 4 μ	150	-19.5 / 32.5	4 e/ γ	234	19.5 / 84.5	2 e/ γ & 4 μ
67	-84.5 / -32.5	2 e/ γ & 4 μ	151	-6.5 / 32.5	4 e/ γ	235	19.5 / 97.5	2 e/ γ & 4 μ
68	-97.5 / -32.5	2 e/ ν & 4 μ	152	-6.5 / 45.5	4 e/ γ	236	6.5 / 97.5	2 e/ γ & 4 μ
69	-71.5 / -45.5	2 e/ γ & 4 μ	153	-19.5 / 45.5	4 e/ γ	237	58.5 / 58.5	2 e/ γ & 4 μ
70	-58.5 / -45.5	2 e/ ν & 4 μ	154	-45.5 / 32.5	4 e/ γ	238	71.5 / 58.5	2 e/ γ & 4 μ
71	-58.5 / -32.5	2 e/ γ & 4 μ	155	-32.5 / 32.5	4 e/ γ	239	71.5 / 71.5	2 e/ γ & 4 μ
72	-71.5 / -32.5	2 e/ γ & 4 μ	156	-32.5 / 45.5	4 e/ γ	240	58.5 / 71.5	2 e/ γ & 4 μ
73	-71.5 / -19.5	2 e/ γ & 4 μ	157	-45.5 / 45.5	4 e/ γ	241	84.5 / 58.5	2 e/ γ & 4 μ
74	-58.5 / -19.5	2 e/ γ & 4 μ	158	19.5 / 6.5	4 e/ γ	242	97.5 / 58.5	2 e/ γ & 4 μ
75	-58.5 / -6.5	2 e/ γ & 4 μ	159	19.5 / 19.5	4 e/ γ	243	97.5 / 71.5	2 e/ γ & 4 μ
76	-71.5 / -6.5	2 e/ γ & 4 μ	160	10.2 / 24.1	4 e/ γ	244	84.5 / 71.5	2 e/ γ & 4 μ
77	-97.5 / -19.5	2 e/ ν & 4 μ	161	32.5 / 6.5	4 e/ γ	245	84.5 / 84.5	2 e/ γ & 4 μ
78	-84.5 / -19.5	2 e/ γ & 4 μ	162	45.5 / 6.5	4 e/ γ	246	97.5 / 84.5	2 e/ γ & 4 μ
79	-84.5 / -6.5	2 e/ γ & 4 μ	163	45.5 / 19.5	4 e/ γ	247	97.5 / 97.5	2 e/ γ & 4 μ
80	-97.5 / -6.5	2 e/ γ & 4 μ	164	32.5 / 19.5	4 e/ γ	248	84.5 / 97.5	2 e/ γ & 4 μ
81	-45.5 / -45.5	4 e/ γ	165	32.5 / 32.5	4 e/ γ	249	58.5 / 84.5	2 e/ γ & 4 μ
82	-32.5 / -45.5	4 e/ γ	166	45.5 / 32.5	4 e/ γ	250	71.5 / 84.5	2 e/ γ & 4 μ
83	-32.5 / -32.5	4 e/ γ	167	45.5 / 45.5	4 e/ γ	251	71.5 / 97.5	2 e/ γ & 4 μ
84	-45.5 / -32.5	4 e/ γ	168	32.5 / 45.5	4 e/ γ	252	58.5 / 97.5	2 e/ γ & 4 μ

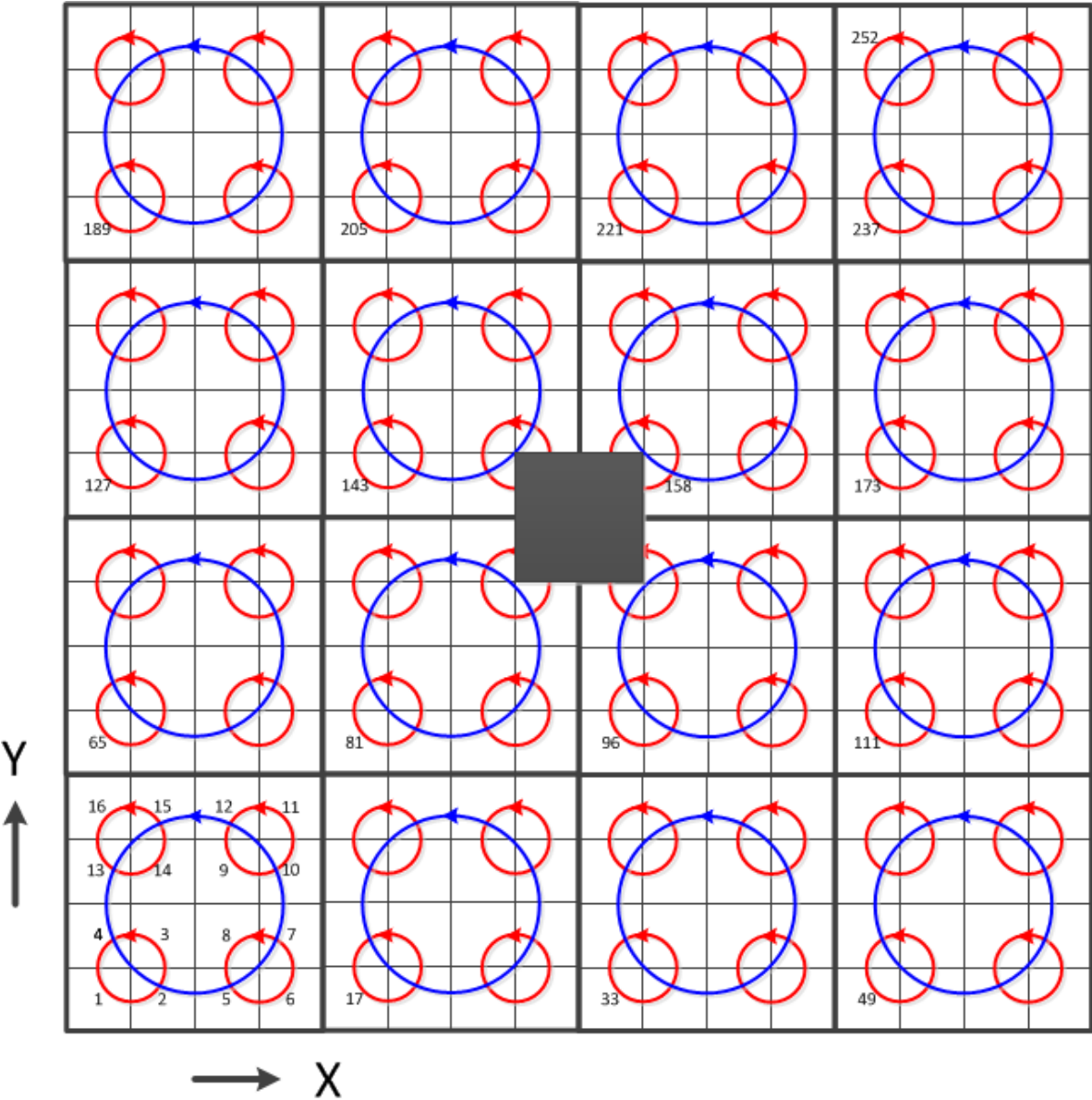


Fig. A.1 *The scheme of the counting of the array station IDs (1 ... 252)*

Appendix

Python-code to calculate x- and y-positions from the station IDs

```
def get_station_locs():
    dstcl = 5200.           // width of array cluster [cm]
    dstqa = 2600.          // width of one sub-cluster [cm]
    dstas = 1300.          // distance between stations [cm]
    sddy = [-1., -1., 1., 1.] // count matrix X
    sddx = [-1., 1., 1., -1.] // count matrix Y
    iasn = 0
    real_iasn = 0
    stations = {}

    for icl in range(1, 17):
        ycl = (float(floor((icl-1)/4))-1.5)*dstcl
        xcl = (float(fmod(icl-1, 4))-1.5)*dstcl

        for j in range(0,4):
            yqa = ycl + 0.5 * dstqa*sddy[j]
            xqa = xcl + 0.5 * dstqa*sddx[j]
            for k in range(0,4):
                yas = yqa + 0.5 * dstas*sddy[k]
                xas = xqa + 0.5 * dstas*sddx[k]
                iasn += 1

            if yas < -dstas or yas > dstas or xas < -dstas or xas > dstas:
                real_iasn += 1
                icdd = icl * 100 + fmod(iasn-1, 16) + 1

    # stations dislocated from the regular grid
    if icdd == 610:           # ID 90
        xas += 23.0
        yas += 100.
    elif icdd == 713:       # ID 108
        xas += 100.
    elif icdd == 1007:     # ID 148
        xas += 20.
        yas += 495.9
    elif icdd == 1104:     # ID 160
        xas += 366.5
        yas += 461.0

    stations[str(real_iasn)] = [xas/100., yas/100.]
    return stations
```

12.2 APPENDIX B – GRANDE STATION COORDINATES

Correlation between the GRANDE station ID as given in the Grande data arrays and the x- and y-positions in KASCADE coordinates. The positions are given in [m] in reference to the KASCADE array centre. The red numbers indicate that the station has been moved during the lifetime of Grande.

Date of validity for the positions given in the table below is 20.12.2003 – 5.11.2012

St-ID	X- Y- Z-Position [m]	St-ID	X- Y- Z-Position [m]	St-ID	X- Y- Z-Position [m]
1	-0.14 / 65.33 / 2.47	14	-260.09 / -136.2 / 1.52	27	-533.7 / -409.1 / 0.87
2	-131.3 / 70.87 / 2.05	15	-377.5 / -145.0 / 1.67	28	101.2 / -507.6 / 1.74
3	-257.0 / 101.7 / 1.96	16	-481.5 / -155.5 / 1.83	29	-24.72 / -507.6 / 1.90
4	-384.8 / 96.12 / 0.84	17	44.09 / -276.6 / 1.65	30	-196.5 / -504.1 / 1.81
5	-499.6 / 95.51 / 1.81	18	-95.83 / -276.0 / 1.29	31	-317.9 / -529.2 / 1.84
6	64.48 / -42.03 / 1.15	19	-195.4 / -272.6 / 1.63	32	-443.3 / -525.9 / 1.95
7	-64.99 / -41.42 / 1.11	20	-319.8 / -267.6 / 1.92	33	-566.5 / -526.4 / 0.63
8	-211.2 / -40.54 / 1.47	21	-481.5 / -234.9 / 1.59	34	-111.9 / -654.9 / 1.90
9	-329.0 / -49.29 / 1.86	22	-608.3 / -281.8 / 0.94	35	-275.0 / -645.4 / 1.71
10	-426.1 / -7.66 / 1.46	23	24.79 / -391.3 / 1.32	36	-389.1 / -653.3 / 1.71
11	-569.8 / 46.42 / 1.90	24	-112.9 / -383.6 / 1.66	37	-517.9 / -620.8 / 1.96
12	24.21 / -156.6 / 1.31	25	-249.8 / -392.0 / 1.48		
13	-140.1 / -143.8 / 1.53	26	-386.5 / -382.1 / 1.84		

Stations 8 and 30 had to be moved from their original locations by several meters. Their positions and the matching *dates of validity* are outlined in the table below.

St-ID	X- Y- Z-Position [m]	valid from	valid until
8	-211.2 / -40.54 / 1.47	20.12.2003 00:00	23.09.2005 12:00
8	-224.4 / -33.68 / 2.03	23.09.2005 12:00	5.11.2012 23:59
30	-196.5 / -504.1 / 1.81	20.12.2003 00:00	11.05.2011 00:00
30	-193.9 / -525.0 / 1.81	11.05.2011 00:00	5.11.2012 23:59